Nature, Origin, and Evolution of the Pyrenean-Cantabrian Junction

R. Lescoutre, G. Manatschal, J. Muñoz

AGU ADVANCING EARTH AND SPACE SCIENCE

Tectonics

RESEARCH ARTICLE
10.1029/2020TC006134

Key Points:

- The orogenic architecture of the Pyrenean-Cantabrian junction results from decoupled thin-skinned and thick-skinned modes of deformation
- The Aptian-Cenomanian rift segments spatially overlapped north and south of the Basque massifs
- The Aptian-Cenomanian rift architecture argues against a major Pamplona transfer fault

Supporting Information:

Supporting Information may be found in the online version of this article.

Correspondence to:

R. Lescoutre,
rodolphe.lescoutre@gmail.com

Citation:

Lescoutre, R., Manatschal, G., & Muñoz, J. A. (2021). Nature, origin, and evolution of the Pyrenean-Cantabrian junction. *Tectonics*, *40*, e2020TC006134. https://doi.org/10.1029/2020TC006134

Received 12 FEB 2020
Accepted 22 APR 2021

Nature, Origin, and Evolution of the Pyrenean-Cantabrian Junction

R. Lescoutre[1,3], G. Manatschal[1], and J. A. Muñoz[2]

[1]IPGS, EOST-CNRS, Université de Strasbourg, Strasbourg, France, [2]Grup de Geodinàmica i Anàlisi de Conques, Institut GEOMODELS, Departament de Dinàmica de la Terra i de l'Oceà, Facultat de Geologia, Universitat de Barcelona, Barcelona, Spain, [3]Department of Earth Sciences, Uppsala University, Uppsala, Sweden

Abstract We investigate the present-day orogenic architecture of the Pyrenean-Cantabrian junction corresponding to a boundary between inverted rift segments using seismic interpretation, field data, and borehole information. This junction was formerly attributed to a major NNE-SSW striking Pamplona transfer fault segmenting the Basque-Cantabrian and Mauléon basins during both rifting and convergence. Our study shows that the orogenic architecture results from a strong decoupling between the thick-skinned (basement-involved) and the thin-skinned (detached in the Upper Triassic evaporites) modes of deformation. The evaporites decoupling horizon was responsible for the transport and allochthony of the former rift basins over large distances on top of the Basque massifs and the Ebro and Aquitaine foreland basins. A crustal-scale cross-section depicts the allochthony of the Basque massifs forming a crustal wedge over the crusts of Iberian, Ebro, and Eurasian affinity. Three-dimensional analysis of the present-day architecture suggests that two phases of rifting and related basins can be recognized: the Late Jurassic-Barremian and the Aptian-Cenomanian basins. Furthermore, we show that during the Aptian-Cenomanian, the Mauléon and Basque-Cantabrian rift segments spatially overlapped north and south of the Basque massifs and were controlled by WNW-ESE striking extensional faults. These results discard the existence of a major Pamplona transfer fault and argue for NNE-SSW direction of extension during the mid-Cretaceous. This study emphasizes the role of inheritance during rifting and reactivation and provides a new syn-rift template, which controlled the Alpine reactivation. Finally, these results have major implications for the Iberia-Eurasia plate boundary and the kinematics of the North Pyrenean basins.

1. Introduction

The Pyrenean-Cantabrian orogenic system (Figure 1a) resulted from the inversion of a hyperextended rift system that developed during the Late Jurassic-Late Cretaceous all along the Iberian, Ebro, and European plate boundaries (Teixell et al., 2018; Tugend et al., 2014). Before this extensional event, Triassic rifting, Stephano-Permian to late Variscan tectonics involving strike-slip and extensional deformation, and Variscan and pre-Variscan tectono-metamorphic events also affected the Pyrenean-Cantabrian domain (e.g., Burg et al., 1994).

The structural style of the Pyrenean-Cantabrian orogen and the related tectono-sedimentary evolution change significantly along-strike. These changes are mainly expressed by differences in width, asymmetry of the double-wedge, thrust kinematics, involvement of basement, and topography. Differences in basement involvement and topography are so strong that different geological and physiographic units formed, receiving distinct names such as Cantabrian and Pyrenean Ranges. The main factors controlling the orogenic structural style, and as a result of the along strike differences, are the inversion of the inherited Mesozoic rift template and the distribution of the Triassic salt (Beaumont et al., 2000; Jammes et al., 2014; Teixell et al., 2018). Other factors, such as the weakness of the inherited Variscan crust and the lithospheric thermal state, have also contributed to the structural evolution and the observed longitudinal changes (Clerc & Lagabrielle, 2014; Jammes et al., 2014). These longitudinal changes are so strong that Souquet et al. (1977) proposed to subdivide the Pyrenean-Cantabrian orogenic system into three main segments, bounded by two major crustal-scale transverse structures: the Segre and Pamplona faults. This interpretation was in opposition to the most accepted structural subdivision into strike-parallel zones (Choukroune & Mattauer, 1978; Mattauer, 1968; Séguret, 1972). However, in the transition between the eastern and central Pyrenees, it has

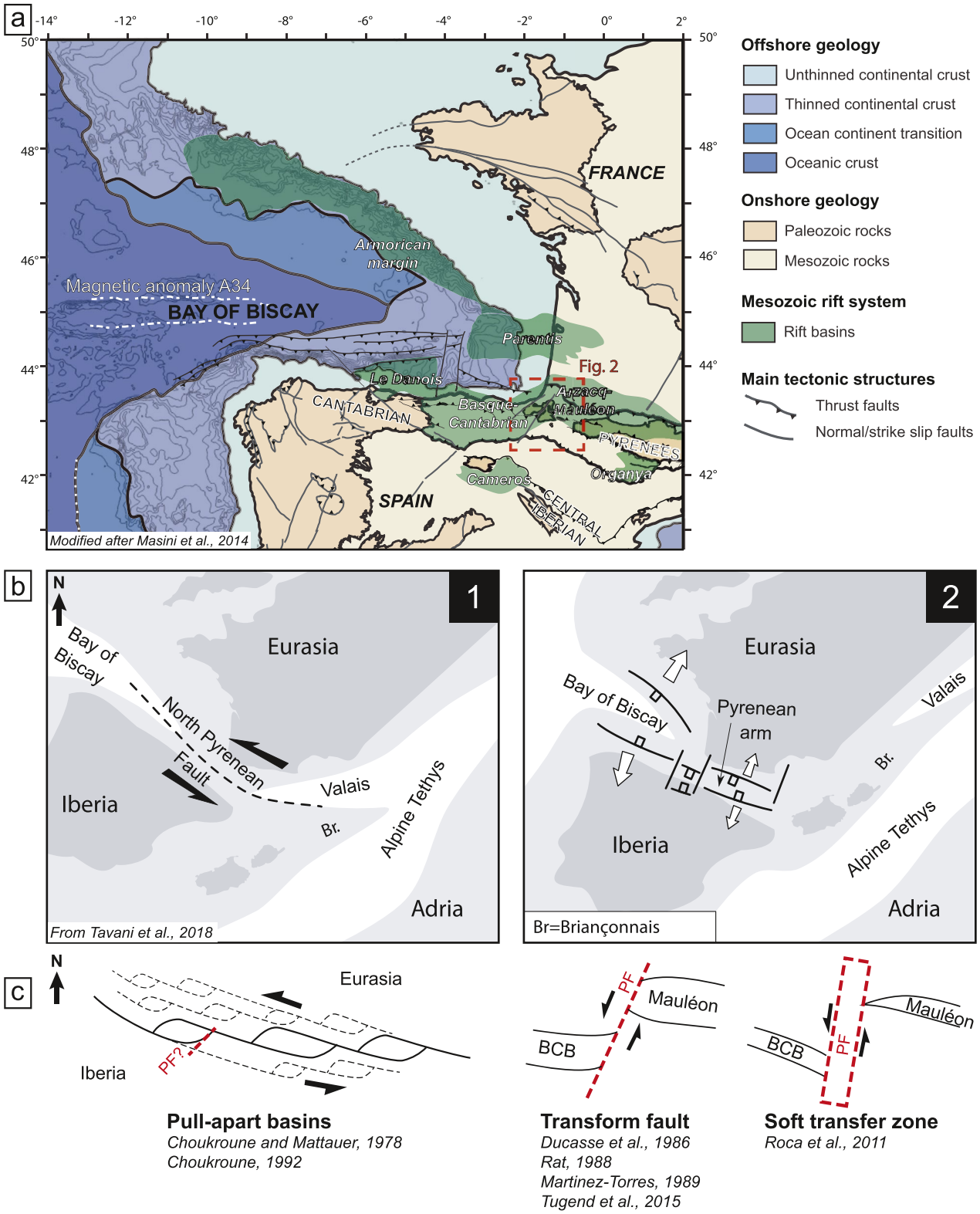

Figure 1. (a) Map of the Mesozoic rift basins between France and Spain. Location of the study area (Basque Pyrenees) is indicated by the red square. Modified after Masini et al. (2014). (b) Eurasia–Iberia kinematic scenarios at mid-Cretaceous time. Strike-slip scenario (1) after Stampfli & Borel (2002) and orthogonal rifting scenario (2) after Manatschal and Müntener (2009). Br.: Briançonnais. Modified after Tavani et al. (2018). (c) Models for the Pyrenean-Cantabrian junction during Aptian to Cenomanian. BCB, Basque-Cantabrian basin; PF, Pamplona fault.

been demonstrated that the prominent oblique NE-SW structures do not correspond with a crustal-scale transfer fault ("the Segre fault"). Instead, they represent oblique thrusts and related folds that developed by progressive rotation during the development of a major thrust salient in the central Pyrenees (Muñoz et al., 2013; Sussman et al., 2004; Vergés, 2003). The other major transfer fault at the western edge of the western Pyrenees, the Pamplona fault, is still considered a major structural element of the chain, regardless the difficulties to recognize a prominent fault in the field (DeFelipe et al., 2017; Ducoux et al., 2019; Saspiturry, Cochelin, et al., 2019).

The transition from the western Pyrenees to the eastern part of the Cantabrian segment, herein referred to as the Pyrenean-Cantabrian junction (Figure 1a) represents a key area for the understanding of the contractional reactivation of the Pyrenean-Cantabrian rift system as it delimits two distinct reactivated rift segments. In the western Pyrenees, the Mauléon basin represents a hyperextended domain (Masini et al., 2014; Saspiturry, Razin, et al., 2019; Tugend et al., 2014). This domain is shifted to the south further west at the eastern edge of the Basque-Cantabrian Basin (BCB; Figures 1a and 2). These basins formed during the Late Jurassic to Late Cretaceous rifting, in relation to relative displacements between the Iberia-Ebro-European plates and were associated with local mantle exhumation (DeFelipe et al., 2017; Jammes et al., 2009; Lagabrielle et al., 2010) and High-Temperature/Low-Pressure (HT/LP) metamorphism of the sedimentary cover (Albarède & Michard-Vitrac, 1978; Clerc et al., 2015; Cuevas & Tubía, 1999; DeFelipe et al, 2017, 2018; Ducoux et al., 2019; Golberg & Leyreloup, 1990; Mendia & Ibarguchi, 1991; Montigny et al., 1986). Subsequent shortening due to the northward displacement of Iberia/Ebro lead to the inversion of these basins and their incorporation into the Pyrenean double-wedging orogen (see review in Teixell et al., 2018). The present trend of the orogen is strongly controlled by the axis of the inherited rift system and shows significant left-stepped shifts along a poorly characterized NNE-SSW striking lineament/zone defining the so-called Pamplona fault in the Basque Pyrenees (Figures 1a and 1c).

Former publications generally proposed, or suggested, the existence of this fault as a major, sharp lithospheric transfer fault responsible for the transfer of deformation between the two segments (Figure 1c; Rat, 1988; Razin, 1989; Richard, 1986). The occurrence of a major transfer fault at the Pyrenean-Cantabrian junction suggests a decoupling of these two realms during Mesozoic rifting and Cenozoic convergence, and raises questions about where and how major structural units terminate laterally (e.g., rift basins, orogenic slab). It also questions the general kinematics and/or location of the Iberia-Ebro-Europe plate boundaries (Figure 1b; e.g., Angrand et al., 2020; Nirrengarten et al., 2018; Tavani et al., 2018; Tugend et al., 2015). These recent geodynamic models involving a continental block (Ebro) in between the classical Iberia-Europe plate boundary have been proposed to solve some of the geometric and kinematic issues involved by the counter-clockwise rotation and the lateral displacement of the Iberian plate along a single, localized plate boundary. In these three plate models, part of the sinistral strike-slip deformation is distributed between the North Pyrenean Zone and the Central Iberian Chain (Figure 1). However, none of these models have discussed how such a kinematic evolution relates to the occurrence of a supposed major NNE-SSW striking Pamplona fault extending from the Ebro to the European plates.

The kinematics of the Iberian plate during the Late Jurassic to Late Cretaceous is heavily debated due to the lack of reliable constraints and the poorly defined pre-chron 34 restoration of the southern North Atlantic (Barnett-Moore et al., 2016; Nirrengarten et al., 2018). Indeed, during the Late Jurassic to Campanian/Santonian (chron 34), two extreme kinematic scenarios (see Nirrengarten et al., 2018 for details) have been proposed to account for the formation of basins along the Iberia-Ebro-Europe plate boundaries (Figure 1c). One model involves a pure E-W strike-slip displacement, of up to 400 km, leading to the formation of pull-apart basins (Figures 1b and 1c, left inserts; Canérot, 2017; Choukroune & Mattauer, 1978; Choukroune, 1992; Oliva-Urcia et al., 2010), suggesting that the NE-SW striking structures such as the Pamplona fault might correspond to basin-bounding faults. The opposite model proposes orthogonal, N-S extension from Late Aptian onwards that post-date a yet poorly defined Late Jurassic-Early Cretaceous transtensional phase (Angrand et al., 2020; Tugend et al., 2015). In this scenario, the Pamplona fault would correspond to either a sharp (e.g., Rat, 1988; Tugend et al., 2015) or soft (Roca et al., 2011) transfer zone, segmenting and transferring the deformation between the Mauléon and the Basque-Cantabrian basins (Figures 1b and 1c, right inserts). The absence of strong criteria from onshore geology makes it difficult to arbitrate between

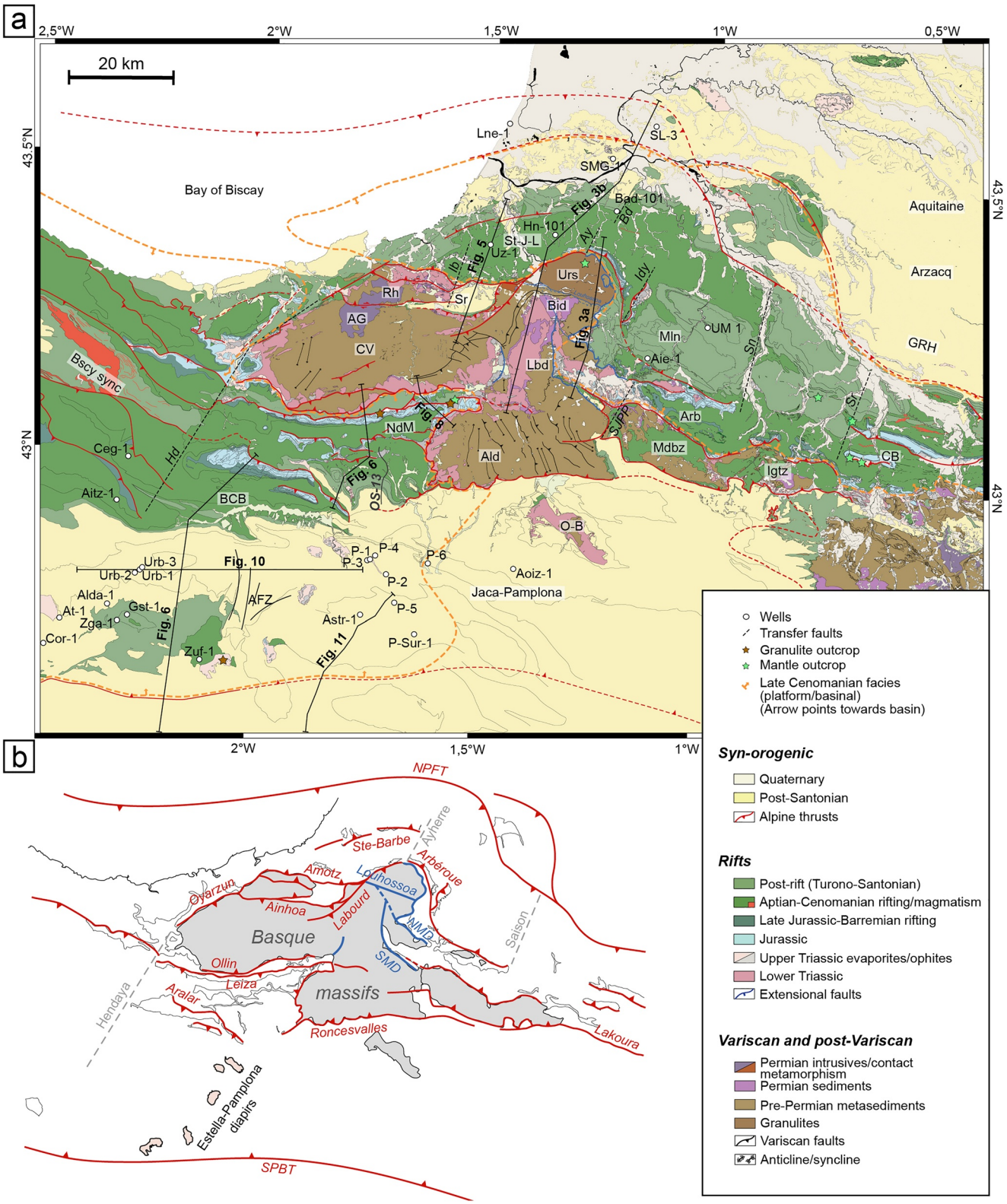
a
2,5°W
2°W
1,5°W
1°W
0,5°W
43,5°N
43°N
20 km
Bay of Biscay
Aquitaine
Arzacq
GRH
Lne-1
SL-3
SMG-1
Bad-101
Hn-101
St-J-L
Uz-1
Urs
Rh
Sr
Bid
AG
CV
Lbd
Mln
UM 1
Aie-1
Arb
Mdbz
Igtz
CB
Ald
NdM
Ceg-1
Aitz-1
BCB
O-B
Aoiz-1
Jaca-Pamplona
Urb-3
Urb-2
Urb-1
P-1
P-3
P-4
P-6
P-2
P-5
P-Sur-1
Alda-1
At-1
Gst-1
Zga-1
Cor-1
Zuf-1
AFZ
Astr-1
Bscy sync
Hd
OS-13
Fig. 3b
Fig. 5
Fig. 3a
Fig. 8
Fig. 6
Fig. 10
Fig. 11
SJPP
Sl
b
NPFT
Ste-Barbe
Ayherre
Arbéroue
Amotz
Louhossoa
Ovarzun
Ainhoa
Labourd
Basque
NMD
SMD
massifs
Saison
Ollin
Leiza
Aralar
Hendaya
Roncesvalles
Lakoura
Estella-Pamplona diapirs
SPBT
Wells
Transfer faults
Granulite outcrop
Mantle outcrop
Late Cenomanian facies (platform/basinal) (Arrow points towards basin)
Syn-orogenic
Quaternary
Post-Santonian
Alpine thrusts
Rifts
Post-rift (Turono-Santonian)
Aptian-Cenomanian rifting/magmatism
Late Jurassic-Barremian rifting
Jurassic
Upper Triassic evaporites/ophites
Lower Triassic
Extensional faults
Variscan and post-Variscan
Permian intrusives/contact metamorphism
Permian sediments
Pre-Permian metasediments
Granulites
Variscan faults
Anticline/syncline

the different models and to constrain the timing of deformation between the different plates (e.g., Tavani et al., 2018; Teixell et al., 2018).

Yet, the existence of this so-called Pamplona transfer fault (sometimes also referred to as a transform fault, e.g., Razin, 1989) is speculative as it is based only on indirect observations or on local, second-order structures. As a consequence, its age, length, and depth remain evasive and unconstrained (e.g., Chevrot et al., 2014; Jammes, Tiberi, et al., 2010). Moreover, recent studies about segmentation in rift and orogenic systems have revealed the variety and the complexity of such domains (e.g., Allken et al., 2012; Bubeck et al., 2017; Granado et al., 2017; Péron-Pinvidic et al., 2017; Zwann et al., 2016), far away from the simple model involving a major strike-slip fault. In particular for rift systems, it appears that they depict more transitional domains accommodating the segmentation via transfer (complex sets of oblique, strike-slip faults) or accommodation zones (overlapping rift basins potentially associated with block rotations; e.g., Zwaan et al., 2016), sometimes at the tips of V-shaped basins.

Our in-depth study of the regional geology and of existing models points out the need of a careful analysis of the architecture of the Pyrenean-Cantabrian junction to evaluate the mode of deformation in the Basque Pyrenees. At present no models integrating small and large-scale observations, involving the role of inheritance and describing the timing, nature, and kinematics of this segmented system have been proposed. As such, a better determination of the present-day architecture is necessary to decipher the type of boundary (sharp/soft transfer zone, accommodation zone) and the kinematics between the Pyrenean and the Cantabrian rift segments during Mesozoic rifting (Figure 1c).

In our study we address the following questions:

- How do the Pyrenean and Cantabrian segments connect in the Basque Pyrenees? Do they interfere through time or do they evolve independently?
- How is the deformation partitioned across the junction during both extensional and compressional events?
- How can the rift template be defined and what was its role during reactivation?

In this study, new and existing N-S and E-W striking cross-sections and a geological map integrating new and existing field data are presented to characterize the deformation affecting the Basque Pyrenees and to discuss the nature, origin, and evolution of the junction between the Cantabrian and Pyrenean segments. We describe the present-day architecture and define the role of inheritance in controlling the present-day architecture. Finally, we discuss the implications for the location and kinematics of the Iberia-Ebro-Eurasia plate boundaries.

2. Geological Setting

2.1. Evolution of the Cantabrian and Pyrenean Segments in the Pyrenean-Cantabrian System

2.1.1. Variscan and Late to Post Variscan Phase

The Pyrenean-Cantabrian orogenic system has been superimposed on the former Variscan orogen. In the study area, it involved the Variscan foreland (Ballèvre et al., 2014; Delvolvé et al., 1998), where Carboniferous flysch sediments ("Culm" facies) were deposited coeval with granitic magmatism and HT/MP-LP

Figure 2. (a) Geological map of the Western Pyrenean-Eastern Cantabrian system. Location of boreholes, cross-sections, and seismic interpretations presented in this study are shown on the map. Details on the distribution of the Late Cenomanian basinal versus platform facies are provided in supporting information (Figure S1) based on geological maps, wells, and publications (e.g., Bodego & Agirrezabala, 2017; Daguin, 1948). (b) Simplified map representing the main structures and units. Massifs/basins: Ald, Aldudes massif; Arb, Arbailles massif; AG: Aya granite; BCB: Basque-Cantabrian basin; Bid: Bidarray Permian basin; Bscy sync: Biscay synclinorium; CB: Chaînons Béarnais; CV: Cinco Villas massif; GRH: Grand Rieu High; Igtz: Igountze massif; Lbd: Labourd massif; Mdbz: Mendibelza massif; Mln: Mauléon basin; NdM: Nappe des Marbres; O–B: Oroz-Betelu massif; Rh: La Rhune massif; Sr: Sare basin; St-J-L: St-Jean-de-Luz basin; Urs: Ursuya massif. Thrusts: NPFT: North Pyrenean Frontal Thrust; SPBT: South Pyrenean Basal Thrust. Extensional faults: NMD: North Mauléon Detachment; SMD: South Mauléon Detachment. Transfer/transverse faults: AFZ: Andia Fault Zone; Ay: Ayherre; Bd: Bardos; Ib: Ibarron; Idy: Iholdy; SJPP: St-Jean-Pied-de-Port; Sn: Saison; Sr: Saraillé; Hd: Hendaya. Boreholes: Aie-1: Ainhice-1; Aitz-1: Aitzgorry-1; Astr-1: Astrain-1; At-1: Atauri-1; Bad-101: Bardos-101; Ceg-1: Cegama-1; Cor-1: Corres-1; Gst-1: Gastiain-1; HN-101: Hasparren-101; Lne-1: Labenne-1; P-1/2/3/4/5/6: Pamplona-1/2/3/4/5/6; P-Sur-1: Pamplona Sur-1; SL-3: St-Lon-3; SMG-1: Ste-Marie-de-Gosse-1; UM-1: Uhart-Mixe-1; Urb-1/2/3: Urbasa-1/2/3; UZ-1: Ustaritz-1; Zuf-1: Zufia-1; Zga-1: Zuñiga-1.

metamorphism in the hinterland (330–295 Ma) (Cochelin, 2016; Martínez Catalán et al., 2007). The Variscan belt involved the collision between Gondwana and Laurussia (Aguilar et al., 2013; Arthaud & Matte, 1975; Cochelin, 2016) from Devonian to Permian. At latest Carboniferous-earliest Permian times the belt developed an orocline formed by the present-day Ibero-Armorican arc (Ballèvre et al., 2014; Martínez Catalán et al., 2007). This Late Variscan stage is related to N-S to NW-SE compression (in present-day coordinates) associated with dextral strike-slip displacement and dome formation (Aguilar et al., 2015; Arthaud & Matte, 1975; Cochelin, 2016). At this stage, metamorphism evolved from medium to low pressure and granulite facies metamorphism affected the lower structural levels (Ribeiro et al., 2019). This event is compatible with local extensional exhumation of the deep structural levels, coeval with a dextral strike-slip tectonic setting, and the onset of extensional collapse of the Variscan orogen. It was also contemporaneous to or followed by calc-alkaline granitic magmatism and volcanism (Aguilar et al., 2013; Bixel & Lucas, 1987; Denèle et al., 2011; Lago et al., 2004). Afterward, a significant change in magmatism occurred at Late Permian times: alkaline magmatism announced the onset of the extensional break-up of Pangea and the onset of a new tectonic cycle (Denèle et al., 2011; Lago et al., 2004).

In the Variscan basement caught up in the Basque massifs (Figure 2), various generations of Variscan folds and a major NE-SW trending thrust dipping toward the east between the Cinco Villas and Labourd massifs have been described (Campos, 1979; Heddebaut, 1973; Mohr & Pilger, 1965; Muller & Roger, 1977). In the Aldudes and Oroz-Betelu massifs, Variscan folds and thrusts are mostly striking NW-SE to N-S (Campos, 1979). Note that E-W structures formerly attributed to the Variscan have been described in the Aldudes massif as well (e.g., Muller & Roger, 1977), however, they most probably correspond to Alpine-related structures as they seem to deform the Lower Triassic unit (Figure 2a). N-S to NE-SW and NW-SE trending folds deform the detritic flysch of the "Culm" facies of mid-Carboniferous age, which composes the major part of the Cinco Villas massif (Campos, 1979). The Aya granite pluton, emplaced at 267 Ma within Devonian metasediments, is cropping out in the Cinco Villas massif together with its contact metamorphism (e.g., Denèle et al., 2011). Late to post-Variscan granulites are at present exposed within the Ursuya unit or as smaller blocks within the Cretaceous basins. On the Labourd massif, the N°20E-trending Bidarray basin, filled by Permian and Triassic red beds, has been attributed to the Permian transtensional event (Bixel & Lucas, 1987; Saspiturry, Cochelin, et al., 2019).

However, little is known about the crustal position of the Ursuya granulites before onset of the Cretaceous rifting. While some studies (Cochelin, 2016; Ducasse et al., 1986; Guitard et al., 1996; Saspiturry, Cochelin, et al., 2019; Vissers, 1992) propose a scenario in which the granulites were exhumed during Late Variscan to Permian, other studies propose a mid-Cretaceous age for the exhumation (Hart et al., 2016, 2017; Jammes et al., 2009; Masini et al., 2014). The lack of clasts of granulite rocks within the Permian and Lower Triassic clastics (Hart et al., 2016; Saspiturry, Cochelin, et al., 2019) together with field observations (for details, see Jammes et al., 2009; Masini et al., 2014) suggest a post-Triassic exhumation and denudation of the granulites, as supported by thermochronological data (Hart et al., 2016, 2017). However, based on combined field observations, the orientation of the syn-kinematic high-grade deformation (Vielzeuf, 1984) and on the existing thermochronological data set, Saspiturry, Cochelin, et al. (2019) proposed that the granulites were exhumed during the Permian in relation with the formation of a metamorphic core complex in an E-W oriented transtensional regime. Note that both scenarios have been recognized in the eastern Pyrenees where a Late Variscan and a mid-Cretaceous ages have been determined in the granulites of the Roc de Frausa massif (Axial Zone) and in the Agly massif, respectively (Aguilar et al., 2015; Odlum & Stockli, 2019), highlighting the complexity to identify a unique solution for the exhumation history of the granulites in the Pyrenean realm.

The post-Variscan, Late Permian-Triassic episode corresponds to an isostatically equilibrated lithosphere on which widespread Lower Triassic fluviatile sandstones followed by Jurassic shallow marine sediments were deposited without showing evidence for major aggradation. Moreover, the control of Variscan structures on the Mesozoic evolution of the Basque Pyrenees was suggested by Arthaud and Matte (1975), García-Mondéjar et al. (1996), Muller and Roger (1977) or recently Saspiturry, Cochelin, et al. (2019) based on their orientation. However, no clear reactivation of Variscan structures has been evidenced so far.

2.1.2. Rifting Episodes

The large-scale kinematics of the Iberian plate is poorly defined during Late Jurassic and Early Cretaceous rifting due to the lack of well-defined magnetic anomalies and pin points (Figure 1). After a poorly constrained Triassic transtensional event (e.g., Angrand et al., 2020; Soto et al., 2017; Soula et al., 1979), the opening of the southern North Atlantic initiating in Late Jurassic involved a sinistral displacement of Iberia with respect to Eurasia. Choukroune and Mattauer (1978) and Choukroune (1992) proposed a sinistral strike-slip deformation between the Iberian and Eurasian plates resulting in the formation of pull-apart basins belonging to a Late Jurassic to Late Cretaceous single rift event based on the kinematic scenario of Olivet (1996). In contrast, other studies (Jammes et al., 2009; Tugend et al., 2015) proposed a main Early to Late Cretaceous north-south extensional event that followed the first phase of transtensional deformation that may be responsible for the formation of Late Jurassic to Early Cretaceous basins. In this study, we will describe the different rifting events and discuss their kinematic evolution based on the description of the Basque Pyrenees (Figures 1 and 2).

2.1.2.1. Triassic Rifting

The Early to Middle Triassic is represented by the deposition of Lower Triassic continental detritic sandstones that are overlain by marine limestones belonging to the Muschelkalk Fm. This evolution can be observed throughout the Eurasian and Iberian plates. It is followed by the deposition of claystones and evaporites of the Keuper Fm (Stevaux & Winnock, 1974). in confined basins. This rifting event, which remains poorly constrained, is proposed to have formed along E-W to NW-SE directed transtensional systems related to the opening of the Neotethys and/or the Central and/or northern North Atlantic (Boess & Hoppe, 1986; Doré et al., 1999; Scotese & Schettino, 2017).

In the Pyrenean-Cantabrian system, these basins were controlled by N°50–60E, N°80E and N°110E to N°140E normal faults in the Aquitaine basin (Curnelle, 1983; Muller & Roger, 1977; Peybernès & Souquet, 1984; Puigdefàbregas & Souquet, 1986; Rat, 1988; Soula et al., 1979) and NW-SE to W-E faults in the Cantabrian system (García-Mondéjar et al., 1986; López-Gómez et al., 2019) that may have been used as pathways for the Late Triassic alkaline magmatism (ophites). The significant amount of ophites in the NE corner of the Nappe des Marbres (Figure 2a), as well as the presence of breccias at the bottom of the Jurassic succession in the hanging wall of the Leiza fault (Figure 2b) would account for the last stages of this rift event (Gallego et al., 1994).

The Lower Triassic sandstones and the Upper Triassic evaporites are widespread in the Cantabrian and Pyrenean domains. However, the extent and importance of this extensional event, and hence the original thickness of the Keuper evaporites, remain poorly constrained as part of the Late Triassic evaporites have been remobilized during subsequent tectonic events (e.g., Labaume & Teixell, 2020). Subsequently, the widespread transgressional carbonate platform of the Jurassic from the NW marks the transition to an open sea shelf environment during a period with little tectonic activity (Biteau et al., 2006; Gallego et al., 1994).

2.1.2.2. Late Jurassic to Barremian Rifting

This tectonic phase, which roughly takes place at the initiation of rifting along the western margin of the Iberian plate (Barnett-Moore et al., 2016; Nirrengarten et al., 2018), corresponds to the deposition of the Purbeck-Weald shallow marine to continental deposits occurring in various locations of Western Europe and especially in Spain and France (e.g., BCB: Ábalos, 2016, Ábalos et al., 2008; Tavani et al., 2013; Cameros: Casas Sainz, 1993; Parentis: Ferrer et al., 2012; Pyrenees: Peybernès, 1982).

In the study area, Late Jurassic to Barremian basins have been described in the BCB (e.g., Amiot, 1982; Cámara, 2020; Campos, 1979; Del Pozo, 1971; Lamare, 1936; Llanos, 1980; Pujalte, 1977; Soler, 1971) and in the Central and Western Pyrenees (e.g., Canérot et al., 1978; Combes et al., 1998; Delfaud, 1970; Lenoble, 1992; Peybernes, 1978). In the Western Pyrenees, they appear as disconnected small basins (e.g., Delfaud, 1970) associated with the formation of bauxites on the Jurassic limestones at the southern margin of the basin (Chaînons Béarnais), followed by the formation of lignite and deposition of Wealdian carbonates (Canérot et al, 1978, 1999; Combes et al., 1998; Peybernes, 1978). A broader basin (central BCB) with marine deposits has been described in the BCB together with smaller basins (east of the Hendaya fault) (e.g., Amiot, 1982; Soler, 1971). The depositional environment shows a high variability with marine to lagoonal or lacustrine

deposits going from limestones to shale, anhydrite, and sandstones (Campos, 1979; Delfaud, 1970; Peybernes, 1978; Soler, 1971). In the Nappe des Marbres (north-east BCB), Late Jurassic (late Oxfordian-Kimmeridgian) clastic wedges interlayered with ramp carbonates were sourced from the N-NW, attesting for an emerged area (Aurell et al., 2003; Bádenas, 1996) that would correspond to the Basque massifs. In the Arzacq and Mauléon basins, authors (Delfaud, 1970; Puigdefàbregas & Souquet, 1986; Richard, 1986) suggest that these basins were related to basement subsidence accommodated along N°10E to N°50E and N°110E structures. In the BCB, Salomon et al. (1982) showed similar orientations and geometries associated with variations in depocenter thicknesses that they related to subsiding rotational blocks.

Because the kinematics and structures governing these marine to continental basins are poorly constrained, their importance for the subsequent tectonic events is difficult to estimate. Yet, their sparse distribution in Western Europe seems to reveal a complex pre-Aptian diffuse Iberia-Ebro-Europe plate boundary that needs, in detail, to be defined.

2.1.2.3. Aptian to Cenomanian Rifting

This period corresponds to accretion of oceanic crust in the Bay of Biscay and to the formation of deep E-W striking hyperextended basins within the Cantabrian and Pyrenean systems. This hyperextension event leads locally to mantle exhumation (DeFelipe et al., 2017; Lagabrielle et al., 2010), alkaline magmatism (Azambre & Rossy, 1976; Montigny et al., 1986), and HT/LP metamorphism of the sedimentary cover (Albarède & Michard-Vitrac, 1978; Clerc et al., 2015; Cuevas & Tubía, 1999; Ducoux et al., 2019; Golberg & Leyreloup, 1990; Martínez-Torres, 1992; Mendia & Ibarguchi, 1991; Montigny et al., 1986). The increase of accommodation space in the North Pyrenean Zone and in the BCB is expressed in the sedimentation by the transition from Aptian carbonate platform and marls to thick Albian turbidite sequences, referred to as the "Flysch Noir" (Rat, 1959; Souquet et al., 1985).

In the study area (Figure 2), this hyperextension is controlled by WNW-ESE striking extensional faults such as the South and the North Mauléon Detachment faults (SMD and NMD, respectively) (Masini et al., 2014) or the reactivated SPBT/Barbarin and Leiza faults at the bottom of the eastern BCB (DeFelipe et al., 2017, 2018; Ducoux et al., 2019; Larrasoaña, Parés, Millán, et al., 2003). Note that an alternative structural architecture has been proposed by Saspiturry, Razin, et al. (2019) for the Mauléon basin, refuting the existence of the SMD and NMD as major detachment faults and proposing that the Occabe normal fault (SMD equivalent) and the North Arbailles fault (NMD equivalent) represent antithetic structures related to a south-dipping St-Palais detachment. Kinematic indicators and lateral ramps argue for an NNE-SSW displacement along these structures (Jammes et al., 2009; Masini et al., 2014). Several studies proposed that most of the present-day compressional structures (e.g., Amotz, Leiza, Sainte-Barbe, Lakoura thrust faults) reactivated former extensional faults during the Cenozoic convergence (e.g., DeFelipe, 2017; Ducoux et al., 2019; Labaume & Teixell, 2020; Razin, 1989; Saspiturry, Razin, et al., 2019; Teixell, 1993; Teixell et al., 2018). Moreover, N-S to NNE-SSW transfer faults (TF) have been recognized in both basins. In the Mauléon basin, they control the progressive westward opening toward the late Albian to Cenomanian St-Jean-de-Luz basin (e.g., St-Jean-Pied-de-Port, Ayherre, and Ibarron TF) (Claude, 1990; Razin, 1989, Figure 2b). In the BCB, the Hendaya and Pamplona faults (Figure 2b) are considered to represent transfer faults, even though their role during Aptian to Cenomanian rifting is still poorly understood (e.g., Aller & Zeyen, 1996; Jammes, Tiberi, et al., 2010). The Pamplona fault is usually considered as the eastern termination of the BCB basin (e.g., Cuevas & Tubía, 1999; Frankovic et al., 2016; García-Mondéjar et al., 1996; Pedreira et al., 2003). The location of the former rift axis is given by the occurrence of the granulite and mantle rocks such as observed along the E-W Chaînons Béarnais and Leiza (or Leitza) fault (e.g., Azambre & Monchoux, 1998; DeFelipe, 2017; DeFelipe et al., 2017; Lagabrielle et al., 2010; Lamare, 1936; Llanos, 1980; Mendia & Ibarguchi, 1991). This is supported by the HT/LP metamorphism of the Late Triassic to Albian rocks of the Nappe des Marbres (Ducoux et al., 2019; Lamare, 1936; Martínez-Torres, 1992) and Chaînons Béarnais (Corre et al., 2018). In the St-Jean-de-Luz basin, an enigmatic block of marmorized and scapolite-bearing Jurassic limestones is cropping out to the south of Biarritz (BRGM, 1963) suggesting that the mid-Cretaceous metamorphism could extent north of the Cinco Villas massif. In both systems, the late Cenomanian could represent the end of fault-controlled subsidence and the transition to post-rift thermal subsidence (e.g., Teixell et al., 2018). This is suggested by the formation of carbonate platforms ("calcaire des Cañons") on the margins of the Mauléon–St-Jean-de-Luz basins (e.g., Cuvillier et al., 1964; Floquet

et al., 1988; Puigdefàbregas & Souquet, 1986; Razin, 1989) and on the southern margin of the BCB (e.g., Feuillée & Rat, 1971; Floquet, 1998; Gräfe, 1999) while deep water turbidites or marls are deposited above hyperextended domains (e.g., Puigdefàbregas & Souquet, 1986, Figure 2 and supporting information). During this time, the Basque massifs were considered to form a basement high with episodes of emersion (Floquet et al., 1988; Mathey, 1986; Razin, 1989; Vacherat et al., 2017). However, a recent publication from DeFelipe et al. (2019) suggests, based on temperatures determined by inverse modeling of low-temperature thermometry data, that the Cinco Villas massif was covered by several kilometers of sediments during the Late Cretaceous. These authors propose that a large part of the sedimentary pile was composed of syn-rift sediments deposited over the massif in the hanging wall of the Ollin fault.

In contrast to the Late Jurassic—Barremian rift event, the Aptian—Cenomanian depositional environment is mostly deep marine and the distribution of the basins follows a roughly continuous E-W trend. The Aptian—Cenomanian rift event argues for a north-south extension direction as indicated by the existing kinematic data such as N°20E transfer faults (Razin, 1989; Roca et al., 2011; Tavani et al., 2018), N°110E detachments faults (DeFelipe et al., 2017; Jammes et al., 2009; Masini et al., 2014; Saspiturry, Razin, et al., 2019), and the continuous E-W stripe of HT/LP metamorphic rocks along the North Pyrenean Metamorphic Zone (e.g., Clerc et al., 2015). However, Late Jurassic-Barremian deformation is difficult to assess due to the lack of recognition of any pre-Aptian structures and to the significant amount of salt sealing basement faults. As such, the role of any Late Jurassic-Barremian structures on the evolution of the hyperextended rift event is unknown and likely underestimated. Moreover, the eastern termination of the BCB and the western termination of the Mauléon basin, although considered in studies to correspond to the Pamplona fault, have not been characterized due to the lack of exposure.

2.1.2.4. Convergence and Collision

The convergence between the Iberian, Ebro, and Eurasian plates initiated at 83.5 Ma (latest Santonian) due to the northward migration of the Africa plate with respect to Europe (e.g., Macchiavelli et al., 2017; McClay et al., 2004; Thinon et al., 2001). This led to the northward underthrusting of lithospheric material below the Eurasian crust in the Pyrenean segment (e.g., Chevrot et al., 2018 and references therein). This compressional event is associated with syn-orogenic flysch sedimentation that initiated during Santonian in the external part of the orogen (e.g., Boillot & Capdevila, 1977; Capote et al., 2002). Main crustal thickening occurred from Eocene onward resulting in a double asymmetric wedge-type crustal architecture (Ábalos, 2016; Cámara, 1997; Mouthereau et al., 2014; Muñoz, 1992; Seguret, 1972; Teixell, 1990; Teixell et al., 2016, 2018). In most parts of the Pyrenean and Cantabrian systems, tectonic inversion led to the inversion of hyperextended basins and reactivation of WNW-ESE rift structures such as the North Pyrenean Frontal Thrust (NPFT) and the South Pyrenean Basal Thrust (SPBT) (e.g., Lagabrielle et al., 2010; Mouthereau et al., 2014; Roca et al., 2011; Teixell et al., 2016, 2018; Tugend et al., 2014; Vacherat et al., 2017).

Across the Pyrenean-Cantabrian junction, the westward continuation of the north-directed Pyrenean subduction was debated (Ducasse et al., 1986; Turner, 1996) but was recently confirmed by active and passive seismic imaging (Díaz et al., 2012; Pedreira et al., 2003). Reactivation of WNW-ESE rift structures and closure of hyperextended domains has been proposed in the Mauléon, BCB, and St-Jean-de-Luz basins (e.g., DeFelipe et al., 2017; Ducoux et al., 2019; Johnson & Hall, 1989; Lagabrielle et al., 2010; Larrasoaña, Parés, Millán, et al., 2003; Razin, 1989; Saspiturry, Razin, et al., 2019; Teixell, 1993; Tugend et al., 2014). However, the timing of initiation of tectonic inversion in this area remains poorly constrained. In these basins, shortening was partially accommodated by thin-skinned deformation (deformation of the Upper Triassic evaporites and its sedimentary cover) occurring along the Triassic Keuper evaporite decollement level (e.g., Cámara, 2020; Carola et al., 2013; Claude, 1990; Larrasoaña, Parés, Millán, et al., 2003; Le Pochat, 1982; Razin, 1989) eventually rooting on thick-skinned (deformation of the Lower Triassic sandstones and below) crustal thrusts such as the Labourd thrust, the NPFT and the SPBT (e.g., Cámara, 1997; Richard, 1986; Teixell, 1998; Teixell et al., 2018).

Despite the recognition of reactivated normal faults, the timing of reactivation and the role of thin-versus thick-skinned deformation is unrevealed in the Basque Pyrenees. In particular, little is known about the role of both Late Jurassic—Barremian and Aptian—Cenomanian structures controlling the reactivation.

This geological setting highlights the remaining questions about the evolution of the Basque Pyrenees. The complex tectonic events and the occurrence of a decoupling salt level at the base of the Mesozoic sediments make it difficult to decipher the structural framework of the Pyrenean-Cantabrian junction. As such, authors often refer to a NE-SW striking crustal fault, referred to as the Pamplona fault, to accommodate the deformation between both systems.

2.2. The Pamplona Fault: Previous Interpretations and Kinematic Implications

The Pamplona fault (PF) has been initially defined as a N°20E structure located south of the Basque massifs by (1) the alignment of salt diapirs between the Jaca-Pamplona basin and the BCB, (2) the eastern termination of the Nappe des Marbres against the Aldudes massif, and (3) the opposite transport direction of the main thrusts on each side of the PF (Feuillée & Rat, 1971; Rat, 1988; Richard, 1986). The salt diapirs are usually referred to as the Estella-Elizondo diapirs (Feuillée & Rat, 1971) or "diapirs Navarrais" (Richard, 1986) and define a lineament that runs from Estella to the Basque massifs (Brinkmann & Logters, 1968). In this study, and to avoid overinterpretation, we will solely refer to the aligned, well-defined rounded-shape diapirs observed on the map as the Estella-Pamplona diapirs (Figure 2). García-Mondéjar et al. (1996) proposed that the diapirs originated on an inherited NNE-SSW Variscan structure. In this area, the proposed PF separates a western domain (BCB) composed of Jurassic to Turonian sediments from an eastern domain (Jaca-Pamplona basin) where Upper Jurassic to Lower Cretaceous sediments are either reduced or absent (eroded or never deposited) (Larrasoaña, Parés, Millán, et al., 2003; Richard, 1986). Note that Pueyo-Anchuela et al. (2007), based on well stratigraphy and gravimetric data, proposed the existence of the Early Cretaceous Oroz-Betelu-Unzué fault, parallel to the PF and located near the Oroz-Betelu massif (Figure 2). To the north of the Basque massifs, Razin (1989) and Claude (1990) described a change of the deformation mode across the Bardos (and Ayherre) fault due to the absence of indurated Jurassic to Lower Cretaceous sediments on the western side of this fault (Figure 2). As such, and because of its NE-SW trend, this fault is sometimes considered as the northward continuation of the PF (Claude, 1990; Razin, 1989), even though some authors are shifting its trace east of the Labourd massif (e.g., Jammes et al., 2009; Larrasoaña, Parés, Millán, et al., 2003; Martínez-Torres, 1992). An east to west jump of the Moho from 40 to 30 km across the Basque massifs has been described by Daignieres et al. (1982) from a seismic refraction profile, although a lack of data in this area has been pointed out by the authors. However, a more recent and longer E-W refraction profile from Pedreira et al. (2003) did not confirm this Moho jump beneath the Basque massifs, but only a diffuse E-W crustal velocity change at ~15–20 km depth. At shallow depth, a deepening of the top basement toward the west (i.e., from the Jaca-Pamplona basin to the BCB) has been identified in the eastern BCB from seismic reflection and well data (e.g., Vergés, 2003; Pueyo-Anchuela et al., 2007). Díaz et al. (2012) proposed, based on three largely offset N-S receiver function analysis, that the European Moho is offset across the Pamplona fault. South of the Basque massifs, Ruiz, Gallart, et al. (2006); see also Ruiz, Díaz, et al. (2006) attributed a ~20 km wide cluster of earthquakes to a segment of the Pamplona fault, among which they reported a strike-slip component (both sinistral and dextral) for three of them based on their focal mechanisms. Note however that these three focal mechanisms concern only very shallow earthquakes (0.37, 0.40, and 5.98 km deep) most probably related to the Estella-Pamplona salt diapirs and in particular to the salt-related Andia fault zone (Larrasoaña, Parés, Millán, et al., 2003). On the other hand, gravity anomaly maps highlight a shift of a shallow high-density anomaly from the Mauléon basin toward the south-east in the Basque Pyrenees (Casas et al., 1997), and Chevrot, Villaseñor, et al. (2014) identified a P-wave velocity contrast at >50 km depth in the Basque Pyrenees.

Because the orientation of the PF (N°20E) is similar to Variscan and Triassic structures and to the trend of the Bidarray Permian basin (see Section 2.1.1), authors proposed a Variscan to Triassic and/or Jurassic age for this structure (e.g., Curnelle, 1983; García-Mondéjar et al., 1996; Martínez-Torres, 1992; Muller & Roger, 1977; Rat, 1988). However, the role of this structure in the Pyrenean evolution and kinematics is controversial and different authors proposed different scenarios depending on the position, age, and extent of the PF. In summary, two competing models have been proposed for the Mesozoic (Figure 1): (1) Normal fault in a pull-apart setting due to E-W transtension (suggested by Choukroune & Mattauer, 1978; Choukroune, 1992; Larrasoaña, Parés, del Valle, et al., 2003); and (2) N°20E transfer fault (Rat, 1988; Roca et al., 2011; Saspiturry, Cochelin, et al., 2019; Tugend et al., 2015) segmenting the Mauléon basin and BCB. In the latter interpretation, the PF was either interpreted as a hard or a soft transfer zone.

(1) Based on a kinematic restoration between the Iberian and Eurasian plates and on the triangular shape of the Cretaceous rift basins north of the North Pyrenean Fault (NPF) (e.g., Debroas, 1987), Choukroune and Mattauer (1978) proposed a model of pull-apart basins (Figures 1b and 1c). These basins developed across the actual Cantabrian and Pyrenean mountain chains due to the supposed eastward displacement and rotation of the Iberian plate relative to the Eurasian plate. SE-NW directed kinematics has been suggested from interpretation of AMS data within Albian sediments of the Mauléon basin (Oliva-Urcia et al., 2010). In this model, the eastward displacement occurred along the NPF, defined as a Variscan to Alpine strike-skip fault defining the Iberia-Eurasia plate boundary. In the Eastern and Central Pyrenees, the NPF corresponds to a jump in the Moho topography (Arthaud & Matte, 1975; Choukroune et al., 1973; Choukroune & Mattauer, 1978; Daignieres, 1978; Roure et al., 1989). Note that the western continuation of the NPF (as a major E-W steep fault) in the Western Pyrenees remains debated, so is the location of the Iberia-Eurasia plate boundary (e.g., Engeser & Schwentke, 1986; Larrasoaña, Parés, del Valle, et al., 2003; Peybernès & Souquet, 1984; Rat, 1988; Schott & Peres, 1988). As such, studies attempted to define the Iberian or Eurasian affinity of the different Palaeozoic Basque massifs. Some studies suggest a plate boundary in the western prolongation of the Nappe des Marbres, that is, the Aldudes massif would belong to the Iberian plate and the Labourd/Cinco Villas massifs to the Eurasian plate. These studies are based either on the location of the HT/LP metamorphic rocks (Engeser & Schwentke, 1986; Peybernès & Souquet, 1984), on the Hercynian structural orientation (Martínez-Torres, 1992), or on the paleomagnetic orientation of the Triassic red beds (see Larrasoaña, Parés, del Valle, et al., 2003 and references therein). In contrast, Rat (1988) suggested that the structural pattern and the presence of the N-S Pamplona fault make it difficult to involve displacement within the Basque massifs, and proposed that they all belong to the Eurasian plate. A similar proposition (excluding the Oroz-Betelu massif, of Iberian affinity) is made by Schott and Peres (1988) based on paleomagnetic data from the Basque massifs.

(2) Alternative interpretations involve a N-S to N°30E sinistral (or dextral, see review in Larrasoaña, Parés, Millán, et al., 2003) Pamplona strike-slip fault in the Basque Pyrenees that follows Late Variscan structural trends (Arthaud & Matte, 1975; García-Mondéjar et al., 1996; Mattauer, 1968; Muller & Roger, 1977). A transfer fault was used to explain the transfer of deformation from the Western Pyrenees to the eastern Basque-Cantabrian system during both Cretaceous extension and Cenozoic inversion (e.g., Roca et al., 2011; Saspiturry, Cochelin, et al., 2019; Tugend et al., 2015). These interpretations are based on geological and geophysical interpretations and the present-day observed offset of the mid-Cretaceous rift axis (BCB to Mauléon rift systems) (Figures 1b and 1c).

It has to be noticed that all previous studies either describe the PF from a large-scale point of view (e.g., Richard, 1986) while seismic (Cámara, 2020) or field (Larrasoaña, Parés, Millán, et al., 2003) studies focused either on the eastern termination of the BCB or the western termination of the Mauléon basin (Claude, 1990; Razin, 1989; Saspiturry, Cochelin, et al., 2019). In this study, we focus on the evolution of both the BCB and Mauléon basin and their relationship with inherited structures using large-scale seismic data and field observations.

2.3. Map Description of the Cantabrian-Pyrenean Junction

We have compiled a geological map of the Basque Pyrenees based on previous geological maps, publications and our own observations (Figure 2). As such, the French part of the map is modified after the 50,000 harmonized geological map of the BRGM (Genna, 2007) and the Spanish part from the geological maps of IGME (Gabaldón, Hernández Samaniego, Ramírez del Pozo, Ramírez del Pozo, et al., 1984; Gabaldón, Merino, et al., 1984; Gabaldón, Hernández Samaniego, Ramírez del Pozo, Carbaya Olivares, et al., 1984; Campos et al., 1972b, 1972a; Campos & García-Dueñas, 1972; Carbayo et al., 1972, 1977; Del Valle, 1972; Del Valle, Villalobos, et al., 1973, 1972; Gabaldón et al., 1985; Juch et al., 1972; Knausse et al., 1972; Merino et al., 1984; Puigdefábregas et al., 1976; Ramírez et al., 1986) and Ábalos (2016). The St-Jean-de-Luz and Sare basins are modified after the work of Razin (1989) and the south-west region of the Mauléon basin is from Masini et al. (2014). The Oroz-Betelu massif area is constrained from Ciry et al. (1963) and the Variscan structures of the Basque massifs are taken from Heddebaut (1973), Mohr and Pilger (1965) and Campos (1979, and references therein).

On a map view, the Palaeozoic rocks of the Basque massifs show Variscan deformation mainly characterized by NE-SW to NW-SE faults and folds. This north-trending attitude contrasts with the main WNW-ESE Variscan structural trend in the western part of the Axial Zone (i.e., the south-easternmost part of Figure 2a), although there more N-S trending structures are also observed (Matte, 2002; Ternet et al., 2004). The Variscan structures are rather continuous throughout the massifs (e.g., the main Variscan thrust; Schoeffler, 1982) and are truncated by the N°20E Permian structures of the Bidarray Permian basin (part of the Labourd massif) and by the Aya magmatic intrusion within the Cinco Villas massif.

The Lower Triassic sandstones seal the Variscan and Permian structures, but they never crop out on top of the Ursuya granulitic unit. At the scale of the Basque massifs, the Lower Triassic sandstones form a continuous and only slightly deformed rim that marks the tectonic or stratigraphic contact with the post-Lower Triassic sedimentary cover. Lower Triassic red beds are absent along the eastern edges of the Labourd and Aldudes massifs, either as a result of structural omission by Early Cretaceous extensional faults (SMD and NMD detachments) or by erosion in the uplifted footwall (SE corner of the Aldudes massif; Figure 2).

The Upper Triassic evaporites are well represented throughout the study area, where they mostly appear along compressional structures (e.g., Chaînons Béarnais, Nappe des Marbres, Figure 2a) and along N°20E structures (e.g., Saison or Iholdy transfer faults in the Mauléon basin, Figure 2b). They contain blocks and fragments of Palaeozoic and Mesozoic rocks as well as granulites and mantle rocks (e.g., Leiza faults and Chaînons Béarnais). In the eastern BCB, the Upper Triassic evaporites crop out in diapirs (Estella-Pamplona diapirs; Figure 2b) containing blocks of Mesozoic and Palaeozoic rocks. Moreover, garnet-biotite-sillimanite bearing paragneisses, which are typical for granulite facies metamorphism, and scapolite-bearing Jurassic blocks have been reported in the Estella diapir (Cincunegui et al., 1943; Pflug & Schöll, 1976).

The supra-evaporite sequence appears on a map view as tilted and folded by E-W to WNW-ESE trending structures within the BCB and Mauléon basin. The Jurassic rocks are very often associated with Triassic evaporites and Alpine thrusts (Figure 2a). Interestingly, on the south-western part of the Aldudes massif, the Jurassic limestones and marls are missing and Aptian to Albian conglomerates and calcareous sandstones are overlaying directly Upper Triassic ophites, Middle Triassic limestones, and Lower Triassic sandstones (Figure 2a). No Jurassic rocks are observed within the Jaca-Pamplona basin and very few within the St-Jean-de-Luz basin.

Upper Jurassic to Barremian rocks corresponding to the Purbeck-Weald facies are observed in the Mauléon basin and BCB and behave similar to the Jurassic limestones in the present-day architecture. However, they are reduced or absent in both the Nappe des Marbres, the St-Jean-de-Luz basin, and the Jaca-Pamplona basin.

The Aptian to Santonian syn-to post-hyperextension sequences roughly follow a WNW-ESE trend at regional scale and depict a sigmoid shape around the Palaeozoic Basque massifs (Figure 2a). WNW-ESE (N°110E) rift structures such as the SMD and NMD are well preserved in the southwest of the Mauléon Basin (Figure 2b; Masini et al., 2014) and display a rotation toward the north when approaching the Labourd massif and especially the Bidarray Permian basin. In the St-Jean-de-Luz basin, the rift-inherited Amotz fault (Richard, 1986) shows a similar WNW-ESE orientation, while the reactivated Ste-Barbe back-thrust (Razin, 1989) shows a roughly WSW-ENE orientation. In Figure 2 (and supporting information), we depict the limit between Late Cenomanian shelf and basinal facies deposits, corresponding to the sediments deposited at the end of rifting and at the beginning of thermal subsidence. The axis of rift basins, where the crust was significantly thinned, displays basinal facies characterized by marls or deep water turbidite deposits while the surrounding domains show shelf environment characterized by carbonate platform deposits, often onlapping onto the Palaeozoic basement.

The post-Santonian (syn-convergence) rocks crop out mainly north of the NPFT and south of SPBT (also to the north of the SPBT in the Jaca-Pamplona basin) where they have been deformed along WNW-ESE-oriented folds. Compressional structures show mainly an E-W to WNW-ESE orientation (e.g., NPFT, SPBT, Aralar, and Amotz faults) except around the Basque massifs where various thrust fault orientations are observed (e.g., NNE-SSW Labourd thrust, WSW-ENE Roncesvalles thrust, Figure 2b).

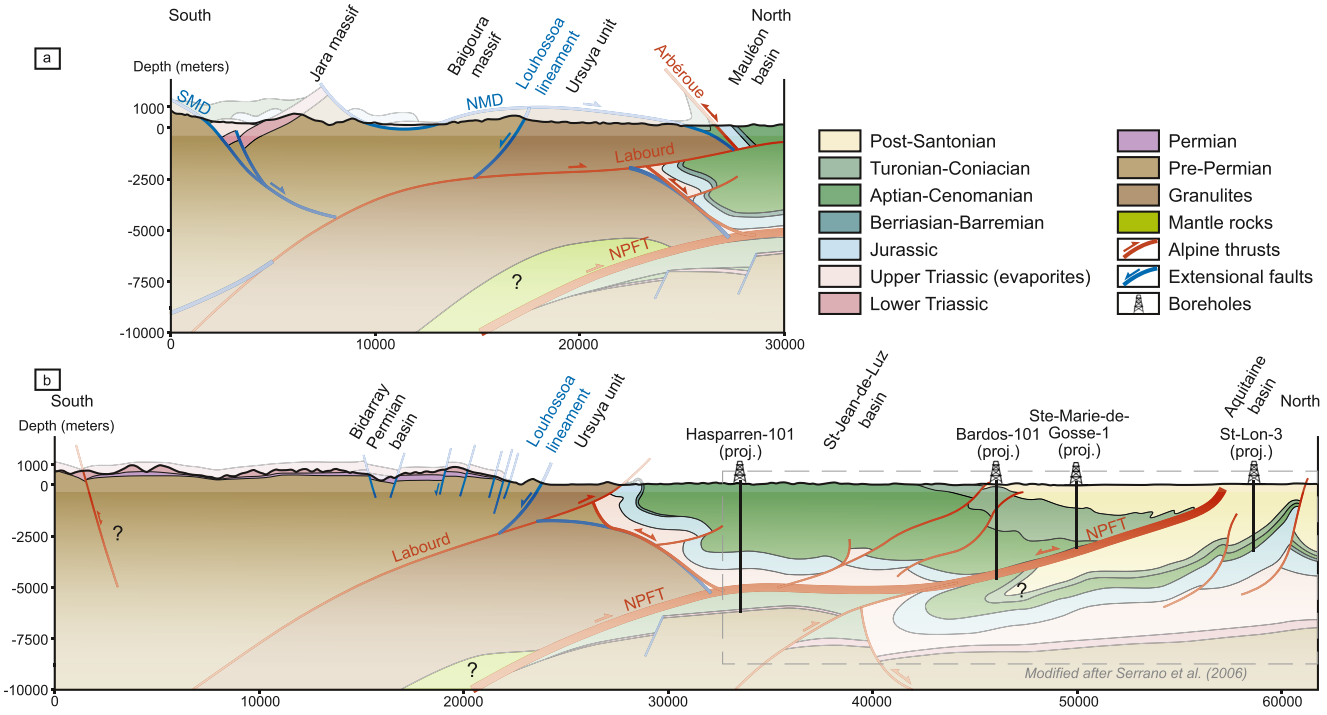

Figure 3. N-S cross-sections across the eastern (a) and western (b) Labourd massif. Note the allochthony of the Labourd massif on the Aquitaine platform and the preservation of pre-Alpine structures on top of the Labourd basement. Location in Figure 2. Description of the figure is provided in the text.

3. Cross-Sections and Seismic Interpretations Across the Pyrenean-Cantabrian Junction

In the following, we describe cross-sections and seismic interpretations that correspond to key areas to describe the architecture of the studied area. These cross-sections cover an N-S zone that follows the hypothetic trace of the Pamplona fault between the Mauléon–St-Jean-de-Luz basins, Labourd-Cinco Villas massifs, and BCB-Jaca-Pamplona basins (see Figure 2). The seismic profiles (only available in PDF format), which have been shot between 1968 and 1983 by Repsol oil company, and the borehole information displayed in the following are available on demand on the IGME website (info.igme.es/sigeof/). To project boreholes (at depth) on the seismic lines (in time) and to juxtapose geological cross-sections (in depth) next to the interpreted seismic sections, we manually apply a simple time-depth conversion of 4.5 s (TWT) corresponding to 10,000 m by vertical stretching of the seismic sections. Such simple time-depth conversions are justified by the results of conversions based on well logs in equivalent settings further to the east, where a similar conversion rule was deduced (Fernández et al., 2012).

3.1. Western Mauléon Basin-Labourd Massif

Figures 3a and 3b are N-S cross-sections across the Aldudes, Labourd and Ursuya massifs (Figure 2a). Cross-section 3a runs in the eastern part of the Labourd massif, from the Aldudes massif to the Mauléon basin. The cross-section 3b runs in the western part of the Labourd massif, from the Aldudes massif to the Aquitaine platform via the St-Jean-de-Luz basin. The St-Jean-de-Luz basin and southern Aquitaine platform section are modified after the seismic interpretation of Serrano et al. (2006). The subsurface data are constrained by own field measurements (Figure 4) and observations and the BRGM geological maps (Genna, 2007). The assumption on the location of mantle (or high density) rocks at very shallow depth on our cross-sections is based on the results from Wang et al. (2016).

The southern part of cross-section 3a shows the Palaeozoic rocks of the Aldudes massif and the Albian SMD (Hart et al., 2017; Masini et al., 2014). To the north, in the hanging wall of the SMD, the Lower Triassic sandstones of the Jara massif are tilted toward the south. They are overlain by Late Triassic evaporites,

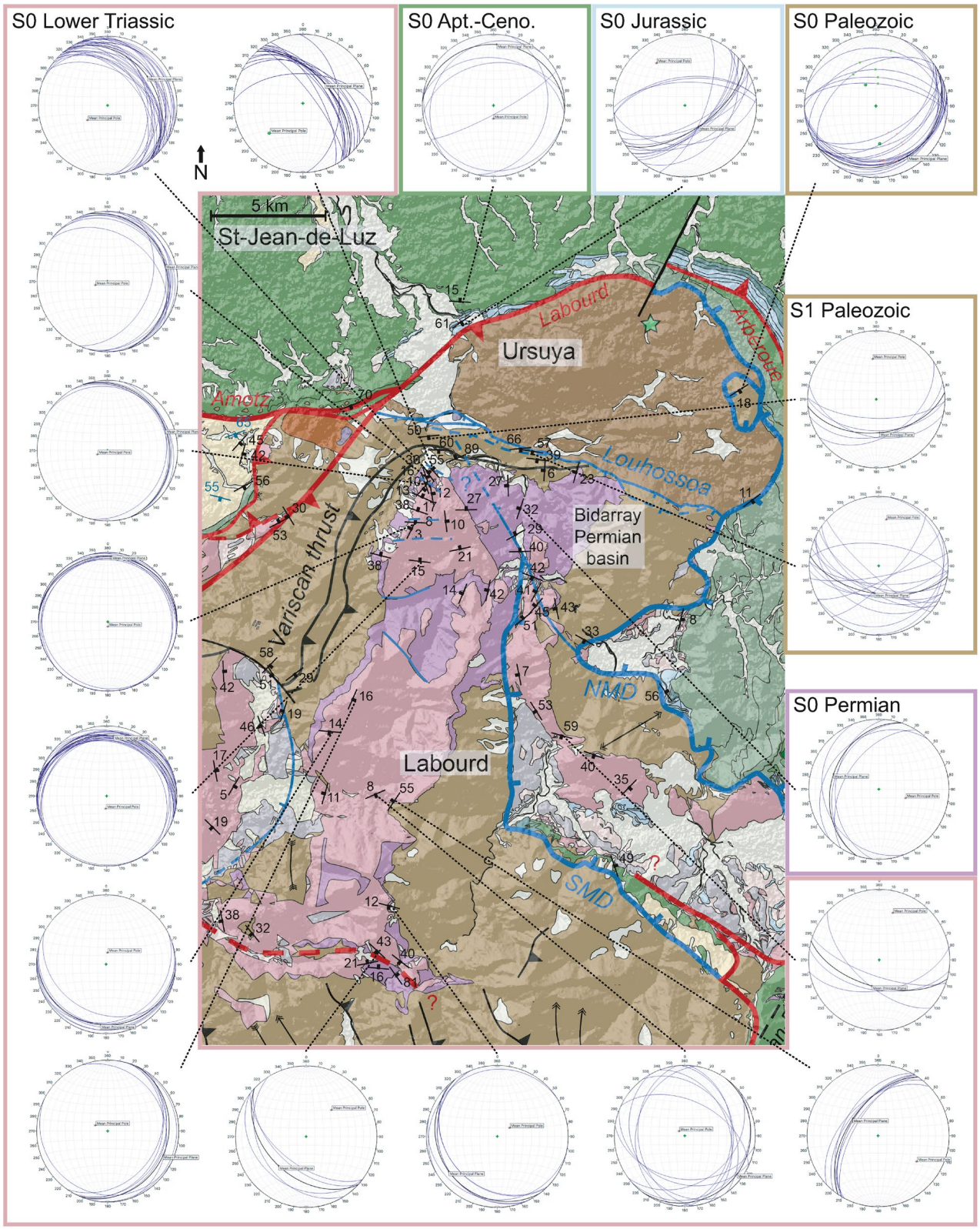

Figure 4. Geological map of the Labourd–Ursuya area with structural data. For caption, see Figure 2.

Jurassic limestones, and Albo-Cenomanian breccias and shales (Masini et al., 2014). The NMD and the allochthonous Mesozoic cover compose the northern face of the Jara massif. Further to the north, the NMD truncates the south-dipping Louhossoa lineament (Figure 2b) which juxtaposes the granulite facies metamorphic rocks of the Ursuya unit to the north, to the low to medium grade Palaeozoic rocks of the Baigoura massif to the south. This structural relationship has been described by Jammes et al. (2009), which defined the Louhossoa lineament as a mid-crustal shear zone eventually exhumed and titled by the NMD during the Late Cretaceous rifting phase. Note that an alternative scenario from Saspiturry, Cochelin, et al. (2019) considers the Louhossoa structure to be Late Variscan in age, related to the exhumation of the granulite, and as such refutes the existence of the NMD. However, the latter study does not provide information on how crustal extension was accommodated in this area during the mid-Cretaceous rifting. The northern tip of the Ursuya unit is capped by an overturned syncline composed of Albian to Turonian deposits and the tectono-sedimentary breccias of the Bonloc through (Jammes et al., 2009; Richard, 1986). The Late Triassic to mid-Cretaceous rocks of the Arbéroue Croissant (Figure 2b) are tilted toward the north along a south-vergent thrust and display about 200 m of Neocomian deposits unconformably laying on Middle Jurassic sediments (Upper Jurassic eroded) (Richard, 1986).

Cross-section 3b is located to the west of the previous section, however, in this western section, no sedimentary cover is preserved on the Ursuya unit and the Labourd thrust is cropping out. Moreover, to the north, the Hasparren 101, Bardos 101 and Ste-Marie-de-Gosse 1 boreholes and the seismic interpretation (modified after Serrano et al. [2006]) show that the Mesozoic cover is thrust on top of Late Cretaceous calcareous flysch and the Aquitaine platform along the NPFT, detached into the Upper Triassic salt. In the hanging wall of the NPFT, Upper Jurassic (only Oxfordian) to mid-Albian sediments were not drilled by the Hasparren 101 and Bardos 101 boreholes (Figure 3b). To the south of the section, the Lower Triassic sandstones seal the Bidarray Permian basin and display a remarkably flat bedding that extends to the Aldudes massif, which depicts a large anticlinorium up to the Roncesvalles fault where Lower Triassic rocks crop out again (Figure 2a). Near the Ursuya unit, the Lower Triassic sandstone beds are affected by several south-vergent low offset normal faults and are abruptly dipping toward the NE in the proximity of the Louhossoa lineament (Figures 3b and 4), suggesting a post-Triassic age for the Louhossoa shear zone.

At depth, the occurrence of the autochthonous Aquitaine basement has been attested by the Hasparren 101 borehole, which highlights the stratigraphic contact of the Turono-Senonian calcareous turbidites onto the Lower Triassic sandstones at 6,212 m. To restore the allochthonous mid-Cretaceous Mauléon and St-Jean-de-Luz basins between the Labourd massif and the thick Aquitaine crust, Razin (1989) proposed a major thrust ("Chevauchement Pyrénéen," or NPFT) that transported the Labourd and Cinco Villas massifs on top of the Aquitaine basement during Pyrenean convergence. Such important thrust sheet loading is likely responsible for the general southward tilt of the Aquitaine basement observed on seismic sections (e.g., Serrano et al., 2006). Beneath the St-Jean-de-Luz basin on Figure 3b, we suggest the reactivation and the rotation of a former north-dipping extensional fault that bounded the Aquitaine basin (where the entire Mesozoic sequence in preserved) from the paleo-high drilled by the Hasparren 101 borehole to the south (corresponding to the western continuation of the Grand Rieu high? See Le Rouat borehole further east in Lescoutre et al., 2019). A thrust fault subsequently formed within the basement high and merged upward with the NPFT beneath which the roll-over syncline of the Mesozoic cover from the Aquitaine basin was overturned and eventually scraped off. On both sections, we display the north-vergent Labourd thrust (Hall & Johnson, 1986; Razin, 1989; Zolnaï, 1971), which has been suggested based on map relationships showing the Jurassic rocks of the St-Jean-de-Luz–Mauléon basins being overlain by the Ursuya unit on its north-western part, and by the large-scale folding of the Alpine structures in the basins that mimics the shape of the Labourd massif to the north. The location of the mantle at depth is extrapolated from the tomographic cross-section of Wang et al. (2016) that reveals a fast anomaly from about 10 km depth below the eastern Labourd massif. Note that, in addition to the large-scale interpretations of Wang et al. (2016) or Saspiturry, Razin, et al. (2019) involving a dome-shaped mantle body, our interpretation suggests that mantle slices might have been emplaced within the crust in the hanging wall of orogenic thrusts. The occurrence of such mantle bodies associated with crustal rocks at very shallow depth is further supported by the occurrence of serpentinized mantle rocks in the Ursuya massif (locality of Sohano; Figure 4).

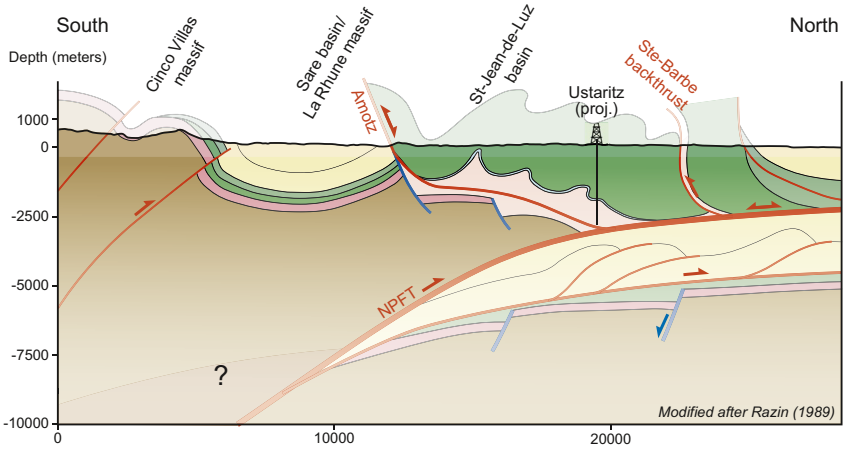

Figure 5. N-S cross-section across the St-Jean-de-Luz basin. Modified after Razin (1989). Location in Figure 2. See caption in Figure 3. Description of the figure is provided in the text.

These cross-sections highlight the allochthony of both the Labourd massif (southern margin of the mid-Cretaceous basins) and the Mesozoic sediments that composed the Mauléon and St-Jean-de-Luz basins on top of the Aquitaine basin (northern margin of the St-Jean-de-Luz–Mauléon basins) via the NPFT (Figure 3). The Labourd massif has been transported several kilometers northwards in the hanging wall of the Labourd thrust (>8 km according to Richard, 1986), displacing the granulitic and Palaeozoic rocks of the massif on top of the Cretaceous sediments of the Mauléon and St-Jean-de-Luz basins. They also show that the Labourd thrust crosscut the thin-skinned Arbéroue backthrust (Figure 2a), suggesting that the Labourd thrust postdates the thin-skinned deformation of the Mauléon basin accommodated northward by the NPFT. Moreover, the Labourd thrust reaches the surface along the western margin of the Labourd massif (Figure 2b) and propagates at depth eastward beneath the southern Mauléon basin and the NMD/SMD (Figures 3a and 3b). This suggests that it could correspond to a lateral ramp during the Alpine orogeny that potentially reactivated a former extensional detachment surface, which evolved westward as an NNE-SSW oriented relay ramp during rifting as observed for the SMD/NMD (Figure 2). Interestingly, very little Alpine imprint is observed throughout the massif allowing a good preservation of the Cretaceous rift architecture and the Permian basin (Figure 4). Finally, the comparison of the Mauléon - St-Jean-de-Luz basins on both cross-sections shows a western domain where the Neocomian to mid-Albian deposits are very reduced or absent (Figure 3b) in comparison to the eastern section (Figure 3a), suggesting that the Ayherre-Bardos faults (Figure 2b) might have represented the western termination of a basin during the Early Cretaceous such as proposed by Richard (1986).

3.2. St-Jean-de-Luz Basin–Northern Cinco Villas Massif

Figure 5 is an N-S cross-section across the St-Jean-de-Luz basin, north of the Cinco Villas massif, modified and simplified after Razin (1989). This cross-section runs through the Cinco Villas massif, the Sare basin, and the St-Jean-de-Luz basin up to the Ste Barbe back-thrust (Figure 2). The tectono-stratigraphic units have been delimited based on the geological maps from the BRGM (Genna, 2007). The Ustaritz 1 borehole has been used to determine the stratigraphic units at depth.

To the south of the section, the Lower Triassic sandstones are unconformably overlain by the deltaic Zugarramurdi conglomerates and sandstones (Feuillée, 1964; Prave, 1986) deposited during the Late Albian to Early Cenomanian and are affected by strong contractional deformation. On top, the Upper Cenomanian to Coniacian Sare carbonate platform and Campanian calcareous flysch are steeply dipping toward the north and form the southern flank of the Sare basin syncline, which corresponds to the eastern continuation of La Rhune massif (Figure 2). The Sare basin is bounded to the north by the north-dipping Amotz reactivated normal fault that corresponds to the southern margin of the St-Jean-de-Luz basin. Here, the fault-related Amotz breccias show clasts of Paleozoic to Mesozoic rocks. These breccias are time equivalent to the Ascain

sandstones (or St Pée sandstones; Souquet et al., 1985) and to the deep facies turbidites of the Flysch Noir (or locally "Flysch de Mixe"). As such, it suggests a Late Albian to Cenomanian age for this fault, before it was reactivated. At depth (Ustaritz borehole, interpretation of Teyssonnières, 1983), these sandstones and turbidites lie on about 50 meters of Upper Hettangian sediments. South-vergent thrust faults soling out into the Upper Triassic evaporites and reactivating paleo-normal faults (e.g., Ste Barbe thrust) have been described by Razin (1989). They are locally cross-cut and overturned by north-vergent thrust faults that used the same décollement level. Further to the north of our section, the Labenne 1 borehole displays the repetition of the Eocene deposits into the Lutetian décollement horizon (Razin, 1989). This décollement has not been recognized further south at the surface nor at depth in the Ustaritz borehole and as such, this décollement needs to be rooted deeper below the Mesozoic cover of the St-Jean-de-Luz basin (i.e., in the footwall of the NPFT).

This section highlights the allochthony of the Late Albian to Cenomanian St-Jean-de-Luz basin that was controlled by WNW-ESE and WSW-ENE normal faults associated with the westward prolongation of the Mauléon basin. In the basin, Middle Jurassic to mid-Albian sediments have not been observed and were probably never deposited as only clasts of Lower Jurassic sediments have been observed in the Upper Albian deposits (Richard, 1986). The Upper Albian deltaic facies are overlain by up to 2,000 m of syn-rift turbidite deposits. From Late Cretaceous onwards, the basin was affected by thin-skinned thrusting toward the south that reactivated normal faults (e.g., Ste Barbe fault) and by north-vergent thin-skinned thrusts that transported the Mesozoic sequence on top of Eocene deposits (Razin, 1989). The basin shows a general tilt toward the north that reflects the crustal buttress involved by the thick-skinned northward displacement of the allochthonous Cinco Villas massif on top of the Aquitaine platform along the NPFT. The amount of shortening has been estimated to 60 km by Razin (1989) based on structural considerations and basin reconstruction.

3.3. Eastern BCB–Southern Cinco Villas Massif

Figure 6 represents an N-S cross-section across the eastern BCB, south of the Cinco Villas massif. To avoid complexities raised by the Estella-Pamplona diapirs, we split the cross-sections into two segments. The northern segment runs from the Cinco Villas massif to the Aralar thrust, where previous (Bodego et al., 2015) and new field measurements (Figure 7) together with the geological map (Del Valle, Villalobos, et al., 1973) are used to constrain the upper part of the section. The line drawing and the suggestion of interpretation of the OS13 seismic line (projected, see location on Figure 2a) are used to constrain the deeper part of the section (Figures 2 and 6). The southern segment is located further to the west and runs from the Aralar thrust to the Ebro basin to the south. As such, the Aralar thrust can be used as a reference to extend the cross-section to the southwest, where seismic lines and boreholes are available. We used the RL40 and ALL2 seismic lines, Urbasa-2, Zuñiga-1, and Gastiain-1 boreholes, and subsurface data from IGME geological maps to constrain this segment (Figure 2a). Note that Cámara (2020) has recently proposed an interpretation of the seismic profiles RL40 and ALL2.

On the northern segment (Figure 6), the north-dipping Ollin thrust, located at the southern edge of the Cinco Villas massif, places the Triassic and Paleozoic rocks of the massif on top of the Mesozoic sediments of the Central Depression (DeFelipe et al., 2018, 2019). The Ollin thrust has been suggested to correspond to a former north-dipping Cretaceous extensional fault, reactivated during the Alpine orogeny by DeFelipe et al. (2018, 2019) based on thermochronological data and structural considerations. Note that the continuation of the Ollin thrust at depth has been proposed to correspond to the present-day location of aligned seismic hypocenters (Ruiz, Gallart, et al., 2006; DeFelipe et al., 2018). The Central Depression shows a thick succession of Upper Cretaceous calciturbidites on top of a very reduced Upper Triassic, Jurassic, and Albian sequences unconformably overlying Lower Triassic sandstones (Bodego et al., 2015; Iriarte, 2004). Toward the south, the Nappe des Marbres displays a thicker Aptian (Urgonian platform facies) and Albian to Cenomanian (calcareous turbidites) sequences unconformably laying on top of either very reduced Purbeck-Weald sediments or more generally on Jurassic limestones and marls (Lamare, 1936). The Mesozoic succession is underlain by the Upper Triassic evaporites, which represent the detachment horizon (e.g., DeFelipe et al., 2018; Ducoux et al., 2019). The Upper Triassic to Albian sediments of the Nappe des Marbres shows recrystallization and dypire formation related to the mid-Cretaceous HT/LP event. This metamor-

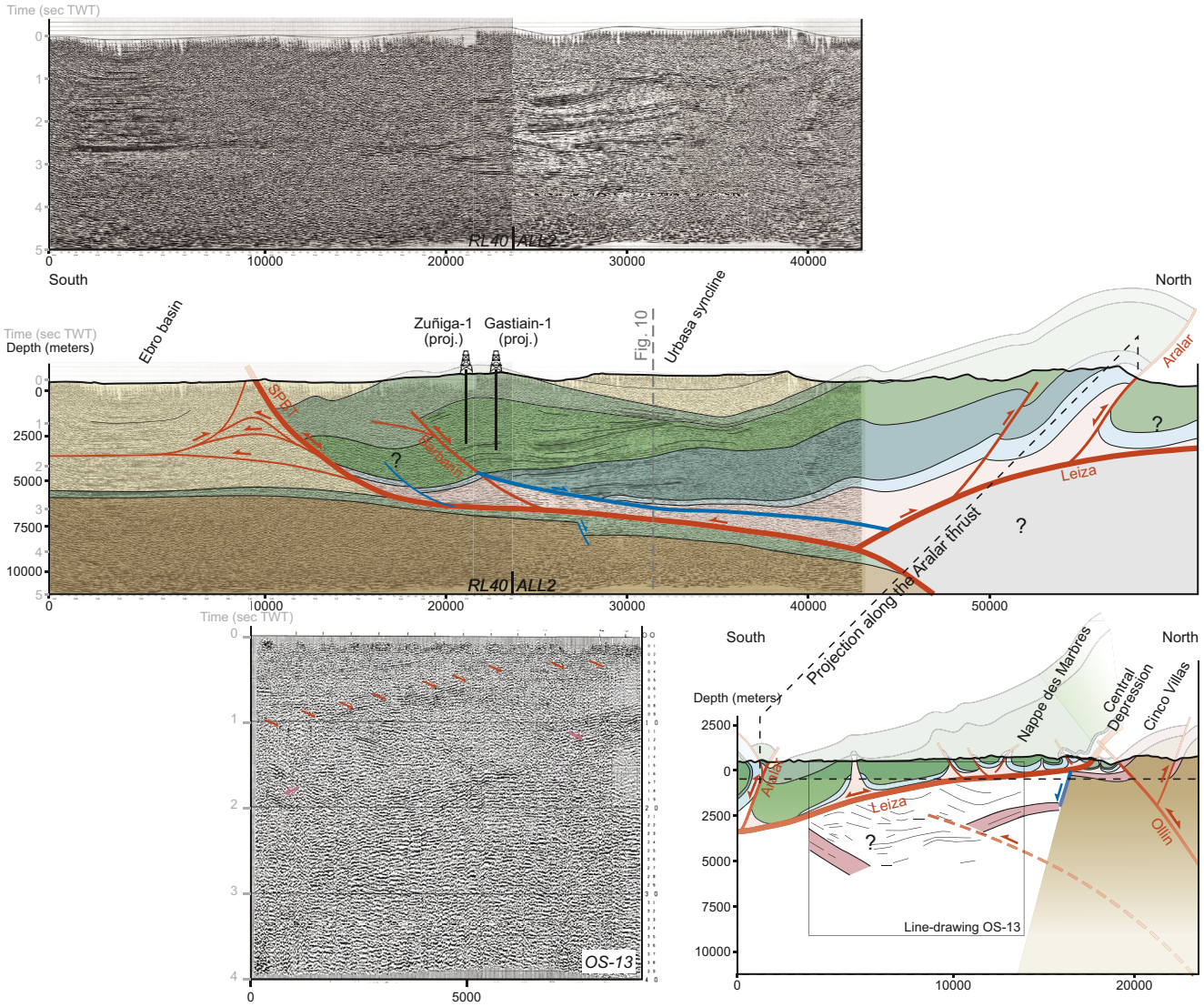

Figure 6. N-S cross-section and seismic interpretation across the BCB. Red arrows on seismic profile OS-13 point toward a continuous reflector gently dipping toward the south and interpreted as the Leiza fault, whereas pink arrows indicate the thick sub-parallel reflectors interpreted as the Lower Triassic sandstones. Location in Figure 2. See caption in Figure 3. Description of the figure is provided in the text.

phism increases toward the north (Martínez-Torres, 1992; Ducoux et al., 2019) up to the Leiza fault, where metric-scale folds and quartz-rich fluid veins are observed. Nevertheless, a significant E-W variation of the recorded metamorphic temperatures has also been observed along the hanging wall adjacent to the Leiza fault (Ducoux et al., 2019). Indeed, recorded maximum temperatures (T_{max}) show maximum values to the north of the Nappe des Marbres (up to 578°C) and decrease significantly to the west of the village of Leiza (411°C) as well as in the eastern corner of the Leiza fault (368°C). In its eastern termination, i.e., where the granulite and mantle rocks of Ziga are cropping out (Figures 2a and 9), the temperatures decrease by about 200°C in 8 km. As a result, isotherms are oblique to the basal detachment in all directions. Unfortunately, there are no data to constrain the geometry and values of the isotherms along the western border of the Alludes massif. On the OS-13 seismic line (Figure 6), we interpret a strong low-angle reflector dipping toward the south as the continuation at the depth of the Leiza fault as it rises up northwards, connecting with its trace at surface (Figures 6 and 7). This reflector lies beneath a package of sub-parallel semi-transparent reflectors (e.g., at X = 4,000 and between 0 and 1 s) that we attribute to the Mesozoic sedimentary cover detached over the Leiza fault within the evaporite décollement. Underneath, some reflectors display either north or south-dipping planar (e.g., between 1.0 and 1.2 s north of the profile) or folded packages

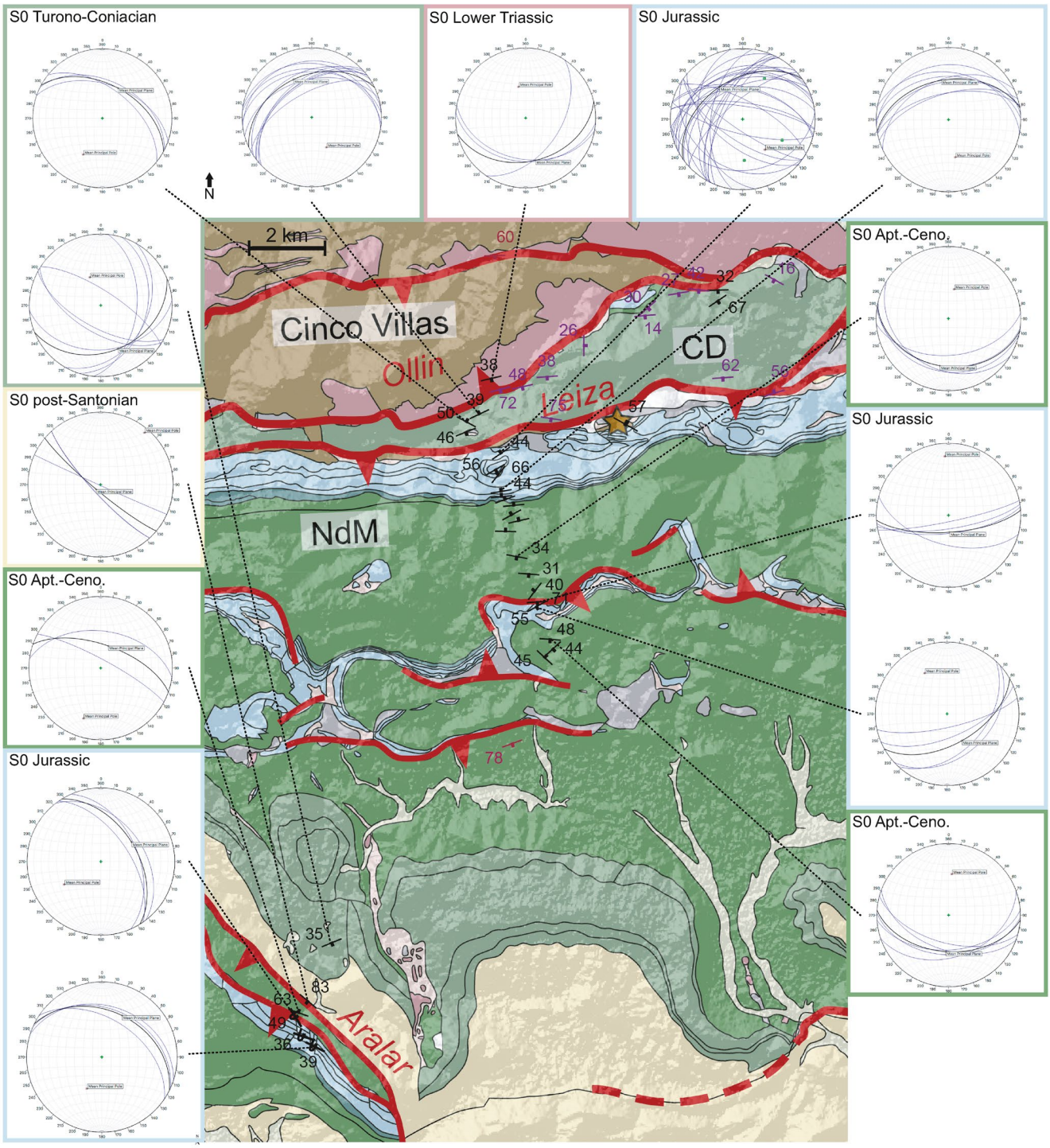

Figure 7. Geological map of the northern BCB basin and associated structural data. Black dip data are own measurements, purple are from Bodego et al. (2015) and red are from IGME 1/50,000 maps of Sumbilla (Del Valle et al., 1973) and Gulina (Carbayo et al., 1977). CD, Central Depression; NdM, Nappe des Marbres. For caption, see Figure 2.

(e.g., between 0.6 and 1.1 s at X = 7,000) that could correspond to the detached and deformed Mesozoic sedimentary cover over the south-dipping Lower Triassic sandstones. The latter is probably deformed by south-vergent thrust faults such as observed further north with the Ollin thrust. The southern boundary of the Nappe des Marbres is represented by the south-dipping Aralar thrust, which delimits a southern

domain composed of thick (>300 m) Upper Jurassic to Barremian sediments deposited in a lagoonal to lacustrine environment. On the Aralar ridge, the mid-Cretaceous rocks are mostly represented by carbonate platforms (Feuillée, 1971; Mathey, 1986), contrasting with the deep water turbidites and flysch sediments of the Nappe des Marbres.

On the southern segment, the top Neocomian is projected from the seismic line of Figure 10 and the Urbasa-2 borehole (Figure 2a). The Purbeck-Weald sequence and the Aptian-lower Cenomanian succession above show a continuous shallow south dipping panel underneath the unconformity at the bottom of the upper Cenomanian carbonates and obliquely above a strong reflector, which is interpreted as the top of the Keuper. This geometry suggests that the syn-rift packages form a salt-detached hanging wall ramp-syncline basin (Roma et al., 2018), suggesting a decoupling along the Upper Triassic evaporites during deposition. Above the Neocomian sequence, we identified the continuous reflectors of the Urgonian facies (Aptian) onto which the reflective semi-continuous horizons of the sandstones and claystones of the Upper Albian Utrillas formation (Carola i Molas, 2014) are onlapping. The Aptian to Cenomanian sequence is getting thin below the Urbasa syncline and increases again southward against the Barbarin thrust. On the southernmost part of the section, underneath the Ebro basin, strong and remarkably flat reflectors located at 2.5–2.7 s (TWT) can be assigned to Upper Albian–Upper Cretaceous sediments (Carola et al., 2013; Carola i Molas, 2014) that occur over the seismic basement characterized by a chaotic reflection pattern (Gallastegui, 2000). These reflectors can be followed underneath the SPBT and the Urbasa syncline, at least as far as the northern edge of the ALL2 seismic line (Figure 6), where the top basement (locally deformed by normal faults) is tilted toward the north. In the Ebro foreland basin, syn-convergence sediments are thickening and deformed toward the SPBT (Figure 6; Riba Arderiu, 1992; Almar et al., 2008). The hanging wall ramp-syncline geometry of the syn-rift reflectors, as well as the flat-lying reflectors underneath the Urbasa syncline in continuation with the autochthonous Upper Cretaceous succession of the Ebro foreland, imaged by the seismic data (Figure 6), not only demonstrates decoupling along the Triassic salt during the extensional deformation but also reactivation of this detachment as a south-vergent thrust during the contractional deformation. This geometry also rules out the involvement of the basement underneath the thrust front as proposed recently (DeFelipe et al., 2018). Further north, the sole thrust would involve the basement underneath the Aralar thrust. This can explain the regional southward tilting of the Mesozoic succession at the northern limb of the Urbasa syncline and the rise of the top basement observed on the northern segment of the section. This south-vergent crustal thrust can also account for the northward tilt of the Ebro basement.

The cross-section and seismic interpretation highlight a strong decoupling and an allochthony of the post-salt Mesozoic cover. Indeed, these sections show that at least 20 km of northward displacement has been accommodated by the Leiza fault in order to bring the thick metamorphic sedimentary sequence of the Nappe des Marbres above the thinned and unmetamorphosed sediments of the Central Depression (e.g., DeFelipe, 2017, 2018). Note that the strong allochthony of the Mesozoic cover contrasts with the interpretation of Ducoux et al. (2019), which assumes less horizontal displacement along the Leiza fault. Indeed, these authors suggest an abrupt transition from the Central Depression to the exhumed mantle via a single E-W trending reactivated normal fault (Leiza fault). In contrast, our interpretation proposes a more gradual transition between the unstretched crust of the Basque massifs and the hyperextended domain as suggested by the stratigraphic units cropping out in the Central Depression and the reflections interpreted in the seismic data underneath the Nappe des Marbres (OS-13 on Figure 6). Moreover, this difference of interpretation raises problems that have not been addressed before such as the eastern termination of the Leiza fault and the 3D geometry of this fault system. In Figure 8, we present a geological cross-section running from the Cinco Villas massif to the north up to the Aldudes massif to the east of the BCB, crossing the Central Depression and the north-eastern extremity of the Nappe des Marbres. This section is characterized by two low-angle faults detached in the Upper Triassic evaporites. The major structure (thick line) corresponds to the Leiza fault and juxtaposes the allochthonous metamorphic sedimentary cover of the Nappe des Marbres over the unmetamorphosed sedimentary cover of the Central Depression, whereas the minor detachment (thin line) underlies the para-autochthonous sedimentary cover of the Central Depression and is responsible for the second-order thrust imbricates and salt structures recognized in the eastern corner of the Central Depression (Figures 2a and 9). In this context it is important to note that the Leiza fault has been folded in the footwall of the Ollin thrust, as evidenced by its steeply south dipping to vertical attitude at its northern front (Figures 6, 7, and 8; see also DeFelipe et al., 2018, 2019). It has been detached into the Triassic evapo-

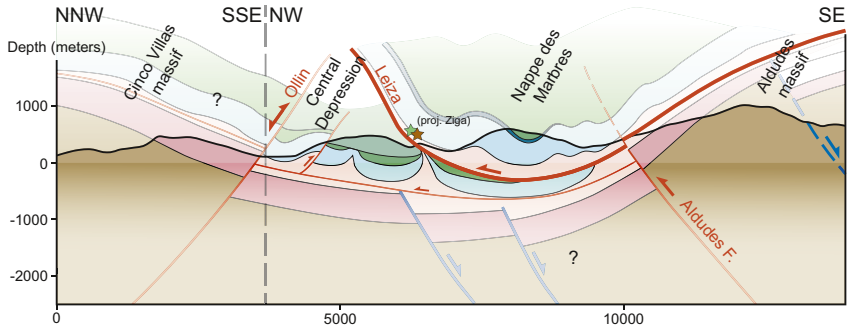

Figure 8. NW-SE geological cross-section in the north-eastern part of the BCB, from the Cinco Villas massif to the Aldudes massif. Location in Figures 2 and 9, for caption, see Figure 3. The Leiza fault brought the allochthonous sedimentary cover of the Nappe des Marbres over the Aldudes massif and the Central Depression. Mantle and granulite rocks (green and brown stars) observed at the base of the Leiza fault and described at the Ziga locality have been projected on the section. Note that both the Leiza fault and the Nappe des Marbres have been folded by the Ollin thrust and by the large anticline formed by the Aldudes massif.

rites, which include fragments of granulite and mantle rocks together with Jurassic marble clasts, particularly near the eastern edge of the east-west trace (Figures 7 and 9a) (DeFelipe et al., 2017, 2018). The Jurassic succession that continues parallel to the Leiza fault all along its trace to the south is folded into a syncline (Figure 8), which eastern termination is visible east of the village of Ziga, where the mantle rocks crop out (Figure 9a). East of this termination the Aldudes massif represents a large, west-plunging, E-W striking anticlinal in the hanging wall of the Roncesvalles thrust to the south (Lescoutre & Manatschal, 2020) and the Aldudes fault to the north-west, as evidenced by the continuous outcrop of lower Triassic sandstones along its southern, northern and western boundaries (Figure 9). On a map view, the limit between the Mesozoic cover of the Nappe des Marbres and the underlying Lower Triassic sandstones of the Aldudes massif is curved, following the limits of the large Aldudes massif anticlinal and suggesting that both the basement and the sedimentary cover have been folded during convergence and subsequently eroded (Figure 8). All these relationships suggest that the Leiza fault, and the overlying sedimentary cover of the Nappe des Marbres, do not die out into the Aldudes massif as suggested previously and as implied by the model of Ducoux et al. (2019). Thus, we propose that the Leiza fault has been folded and continues to the south following an N-S orientation and tectonically juxtaposes the metamorphic Mesozoic sediments of the Nappe des Marbres against the west-dipping Lower Triassic sandstones of the Aldudes massif (Figures 8 and 9a). This tectonic contact is always represented by the Upper Triassic evaporites and an unusual amount of ophites. Along this contact, we identified allochthonous clasts and blocks of folded Paleozoic basement embedded in the evaporites (Figures 9b–9e), attesting that this thrust has detached into a former extensional décollement level that put the denuded Paleozoic basement in tectonic contact with the base of the Nappe des Marbres. These observations are similar to what is observed in the Chaînons Béarnais in the Eastern Mauléon basin (Labaume & Teixell, 2020; Lagabrielle et al., 2010; Teixell et al., 2016). Note that this eastern part of the Leiza fault has been considered for some authors to represent a portion of the Pamplona fault that would crop out in the same area (e.g., DeFelipe et al., 2017).

Based on our interpretation, more than 35 km of displacement had to occur along the SPBT to restore back the Upper Cretaceous sediments of the hanging wall with respect to their equivalent beds in the autochthonous Ebro foreland basin (Figures 6, 10, and 11; Carola et al., 2013; Larrasoaña, Parés, Millán, et al., 2003; Martínez-Torres, 1993; Muñoz, 2019). The Aralar thrust seems to reactivate a south-dipping normal fault that defined the northern margin of a Late Jurassic-Barremian basin as evidenced by the very reduced continental deposits or even absence of deposition in its footwall (Nappe des Marbres). At the mid-Cretaceous time, the Aralar ridge probably represented a transitional domain between a shallow environment, characterized by a carbonate platform to the south, and a deeper environment toward the north characterized by turbidites (Mathey, 1986). To the south, the seismic interpretation suggests that the Barbarin thrust reactivated a north-dipping normal fault controlling the deposition of the Aptian to Cenomanian sediments (e.g., Larrasoaña, Parés, Millán, et al., 2003). Interestingly, only limited contractional internal deformation

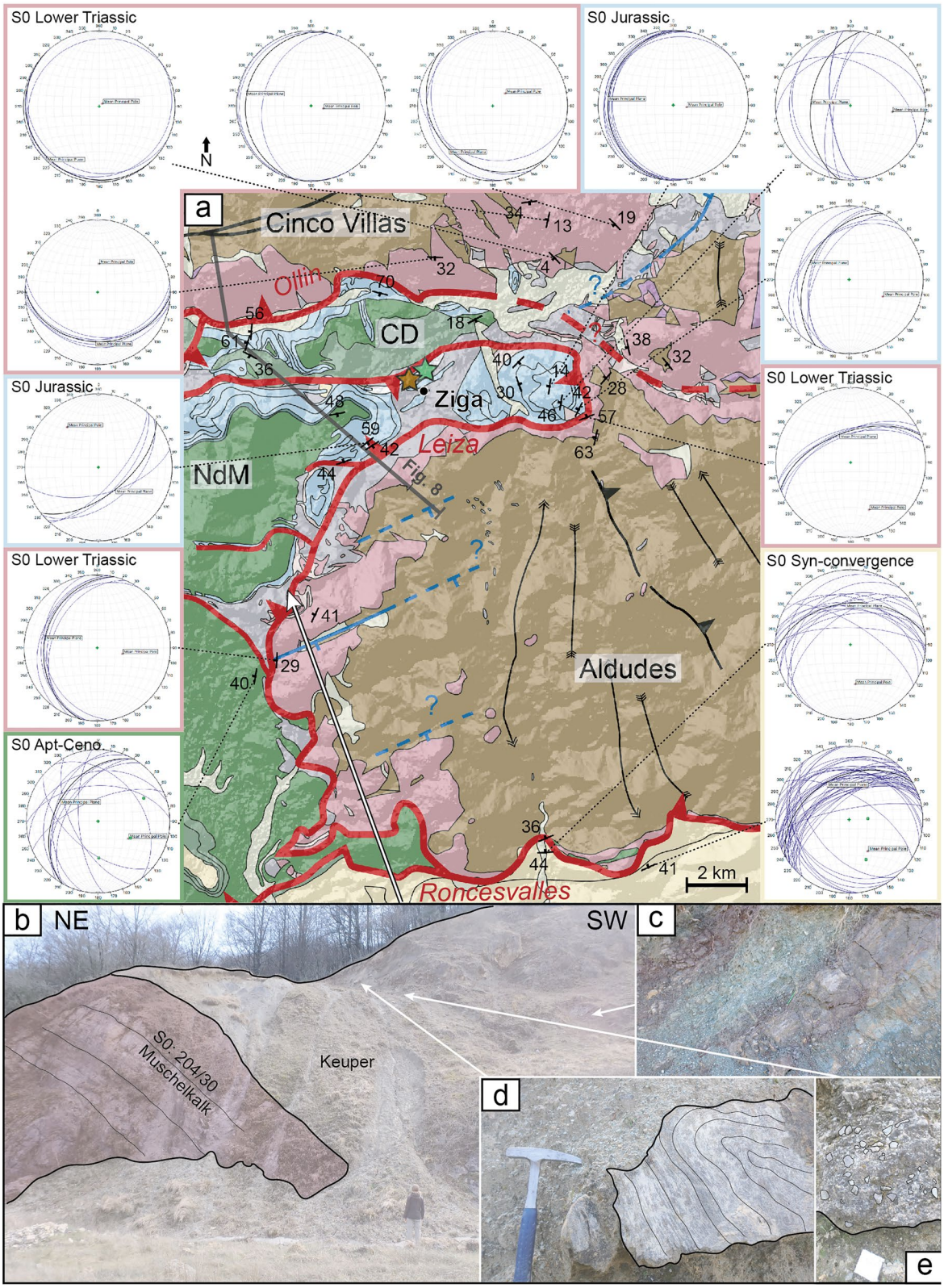
S0 Lower Triassic
S0 Jurassic
N
a
Cinco Villas
Ollín
CD
Ziga
Leiza
NdM
Fig. 8
Aldudes
Roncesvalles
2 km
S0 Jurassic
S0 Lower Triassic
S0 Lower Triassic
S0 Apt-Ceno
S0 Syn-convergence
b
NE
SW
S0: 204/30
Muschelkalk
Keuper
c
d
e

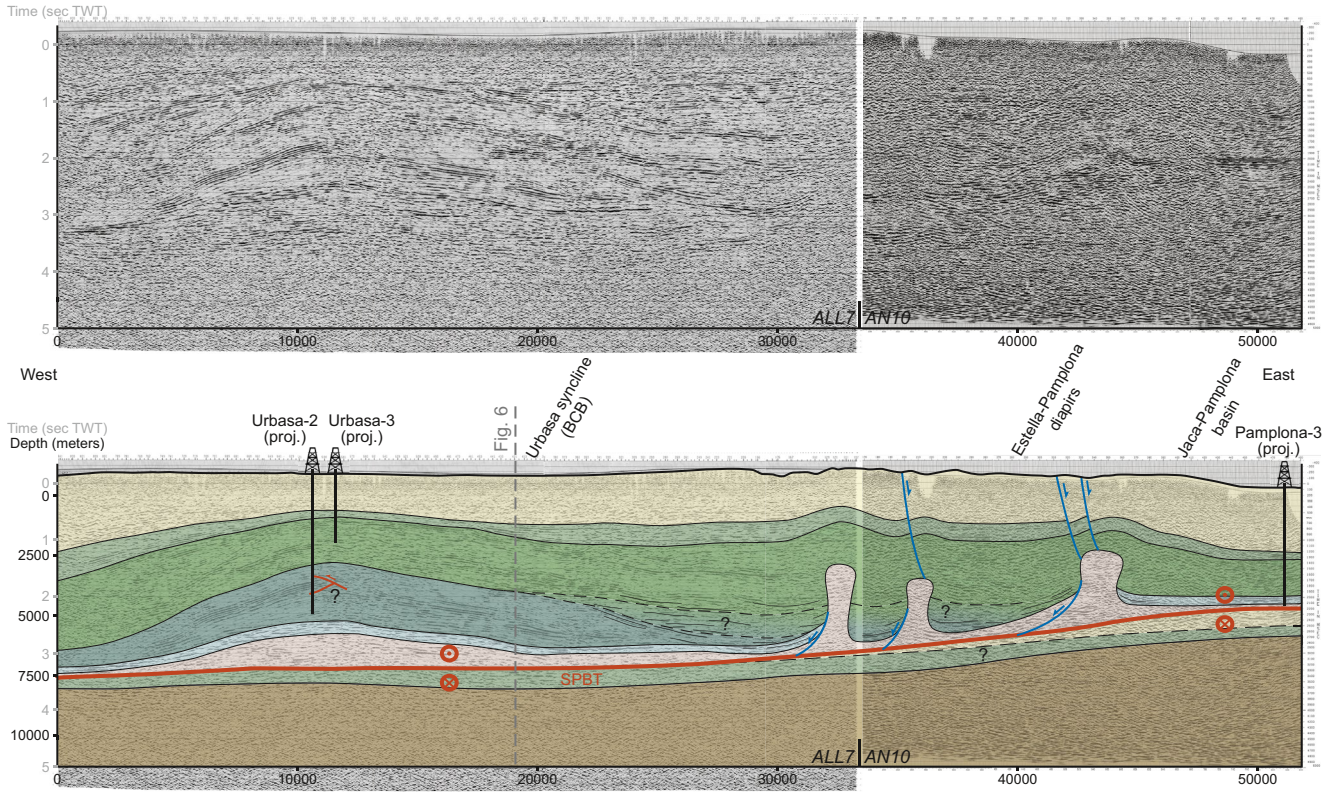

Figure 10. E-W seismic interpretation across the Estella-Pamplona diapirs. Hanging wall drop faults above the diapirs are based on Larrasoaña et al. (2003a). Location in Figure 2. See caption in Figure 3. Description of the figure is provided in the text.

is observed in this allochthonous unit of the BCB (see also Ducoux et al., 2019 for the northern part of the BCB) except along the northern margin of the Purbeck-Weald basin (Aralar thrust).

3.4. BCB–Jaca-Pamplona Basin Transition

Figure 10 is an E-W seismic interpretation across the eastern BCB and Jaca-Pamplona basin, crossing the Estella-Pamplona diapirs. We used the ALL7 and AN10 seismic lines and the Urbasa-2, Urbasa-3, and Pamplona-3 boreholes to constrain the interpretation. Note that a previous interpretation of seismic profile AN10 has been published by Vergés (2003), and Cámara (2020) has proposed an interpretation of seismic profile ALL7.

On the western part, the section shows a >10 km wide anticline composed of Jurassic to Cenomanian rocks and a core composed of Late Triassic evaporites (Figure 10). The Urbasa-2 borehole reports about 2000 m of Berriasian to Barremian sediments (5,842–3,880 m) affected by reverse faults, which are likely responsible for the disrupted reflectors observed on the seismic line at the location of the well. These Berriasian to Barremian sediments are mainly marls, claystones, and sandstones, sometimes interbedded with claystones, anhydrites, and lignite (e.g., from 4,350 to 4,100 m). Lignite has also been described within the Neocomian sediments of the Chaînons Béarnais associated with bauxites (see Section 2.1.2.2). On top of them, about 1,900 m of Aptian to Cenomanian sandstones and marls are observed, followed by Turonian to Palaeocene marls and limestones. Toward the east, the Berriasian-Barremian deposits are thinning out and terminate

Figure 9. (a) Structural data of the eastern part of the Nappe des Marbres. Note the Leiza fault delimiting the allochthonous Nappe des Marbres from the Aldudes massif and the Central Depression. CD, Central Depression; NdM, Nappe des Marbres. For caption, see Figure 3 (b) Outcrop picture of the western border of the Aldudes massif (location: 43°03′51.6″N; 1°37′04.0″W). A massive block of Muschelkalk is embedded in the Upper Triassic evaporites on top of the Lower Triassic sandstones (in the background, not visible). (c) Typical varicolored Upper Triassic evaporites. (d) Allochthonous block of folded Palaeozoic schists embedded in the evaporites. (e) Allochthonous block of Palaeozoic polymictic breccias (detached from the outcrop).

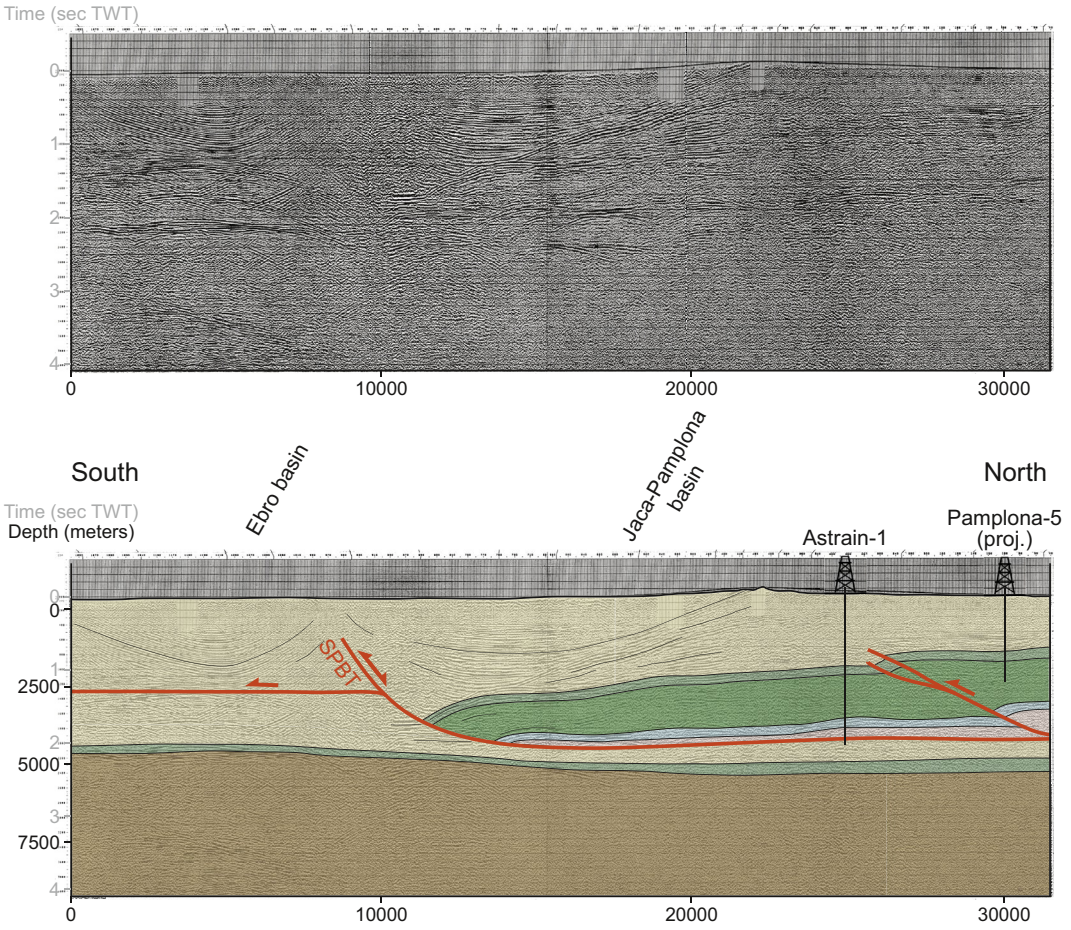

Figure 11. N-S seismic interpretation across the Jaca-Pamplona basin. Location in Figure 2. See caption in Figure 3. Description of the figure is provided in the text.

along the location of the Estella-Pamplona salt diapirs such as evidenced by the Pamplona-3 borehole. However, the Aptian to Cenomanian sediments continue to the east of the diapirs, although with a thinner succession in the Pamplona-3 borehole, but yet reaching 1,400 m of thickness and displaying a similar lithology to the western domains. All along the section, the sedimentary cover is floored by the Upper Triassic salt that lays upon the rather thin Late Cretaceous to Cenozoic rocks of the Ebro basin, which successively shallows toward the east (7,500–5,000 m).

The section displayed in Figure 10 highlights the eastern, present-day termination of the Late Jurassic to Barremian basin that corresponds to the trace of the Estella-Pamplona diapirs (Figure 2b). Indeed, Aptian to Cenomanian sediments displays similar thickness and facies on both sides of the diapirs (see Urbasa-2 and Pamplona-3 boreholes), arguing for an eastern prolongation of the BCB south of the Aldudes massif. However, Upper Jurassic to Barremian deposits, if deposited, have been eroded before Aptian east of the diapirs. As such, the change in Cretaceous sedimentary thickness on both sides of the Estella-Pamplona diapirs (see Section 2.2; Vergés, 2003) cannot be solely attributed to the Aptian-Cenomanian rifting event and might actually correspond to the eastern termination of a Late Jurassic to Barremian basin. Subsequent overburden and fault reactivation could have sustained salt mobilization, which would be responsible, together with basinward displacement above the extensional detachment, for the thickness variation and onlap geometries observed within the Aptian-Cenomanian sequence of this E-W section. Note that the large anticline on the western part of the section has been interpreted as an inverted turtle salt anticline by Cámara (2020).

In this section, the Mesozoic sedimentary cover has been transported toward the south during the contractional reactivation of the previous extensional detachment along the SBPT due to thin-skinned deformation controlled by the distribution of the Upper Triassic evaporites. Displacement was initiated within the deformed Upper Triassic horizon and resulted in the formation of a structural relief once the BCB was transported in the hanging wall of the thrust. The difference of thickness of the allochthonous unit from the Jaca-Pamplona basin to the BCB led to the formation of a "hanging wall drop fault" and to the deposition of a thick syn-convergence sequence on the eastern part of the Estella-Pamplona diapirs, such as proposed by Larrasoaña, Parés, Millán, et al. (2003).

3.5. Jaca-Pamplona Basin

Figure 11 represents an N-S seismic interpretation across the southern part of the Jaca-Pamplona basin. We used the PP17 V seismic line and the Astrain-1 and Pamplona-5 boreholes for this section.

On this section (Figure 11), the northern part shows about 1,200 m of Aptian to Cenomanian siltstones and sandstones (Astrain-1 well) laying on Jurassic marls and Upper Triassic claystones and gypsum. This Mesozoic sequence overthrust the Upper Cretaceous to Cenozoic sediments deposited on top of the Ebro basement. On top of the Aptian-Turonian succession in the hanging wall of the SPBT, the syn-convergence sediments can be divided into two sub-units. The lower unit is thinning toward the foreland and is overlain by the upper unit which appears thicker toward the south where it shows a syncline against the SBPT. In the footwall of the SPBT, the syn-convergence sediments (>4,000 m) of the Ebro basin display a syncline with strongly inclined (to overturned) beds in the northern limb, while further south the sediments are sub-horizontal and are detached from the lower autochthonous succession along Paleogene evaporites. Below, the basement of the Ebro basin slightly dips toward the north at about 5,000 m depth.

This section highlights the eastern prolongation of the Aptian-Cenomanian BCB in the Jaca–Pamplona basin with up to 1,200 m of deposits and the absence of Upper Jurassic-Barremian sediments. Here again, the Mesozoic sediments have been transported toward the south along the SPBT. The Upper Triassic salt controlled the thin-skinned deformation that carried the Aptian-Cenomanian basin above the Ebro foreland basin such as testified by the pre-convergence sedimentary pile on top of the Palaeozoic basement.

As such, the seismic interpretations across the BCB (Figure 6) and Jaca-Pamplona basins (Figures 10 and 11) show that both basins have been synchronously transported on top of the Ebro/Duero basin along the SPBT and that no strike-slip movement occurred between them during convergence. This is testified by the preservation of the rounded shape Estella-Pamplona diapirs (Figure 2; Frankovic et al., 2016) and by the absence of any strike-slip deformation along the Estella-Pamplona diapirs during convergence (Larrasoaña, Parés, Millán, et al., 2003). As a consequence, the SPBT represented the southern margin of the Aptian-Cenomanian BCB east and west of the Estella-Pamplona diapirs.

4. Discussion

4.1. Relationship Between the Leiza Fault and the Basque Massifs: A New Structural Interpretation

In this study, we show based on seismic interpretations and geological cross-sections that the Leiza fault, a former extensional detachment fault detached in the Upper Triassic evaporites, has been reactivated and was responsible for the northward transport of the Nappe des Marbres over the Mesozoic sediments of the Central Depression (Figures 6 and 8). In accordance with the interpretation of DeFelipe et al. (2018), we argue that this fault has accommodated a significant northward displacement (>20 km) of the Nappe des Marbres over the Central Depression and potentially over the Cinco Villas massif and has been subsequently deformed by the thick-skinned south-vergent Ollin thrust. Such a thick allochthonous sedimentary cover, together with any pre-to post-rift para-autochthonous sediments, transported over the Cinco Villas massif might also account for the 240–280°C burial temperatures that have been estimated on this massif during the Late Cretaceous (DeFelipe et al., 2019; see Section 2.1.2.3). Moreover, and in contrast to former studies, we argue that the Leiza fault is not terminating in outcrop along the western border of the Aldudes massif. Instead, we propose that it continues above the Aldudes massif but has been subsequently eroded.

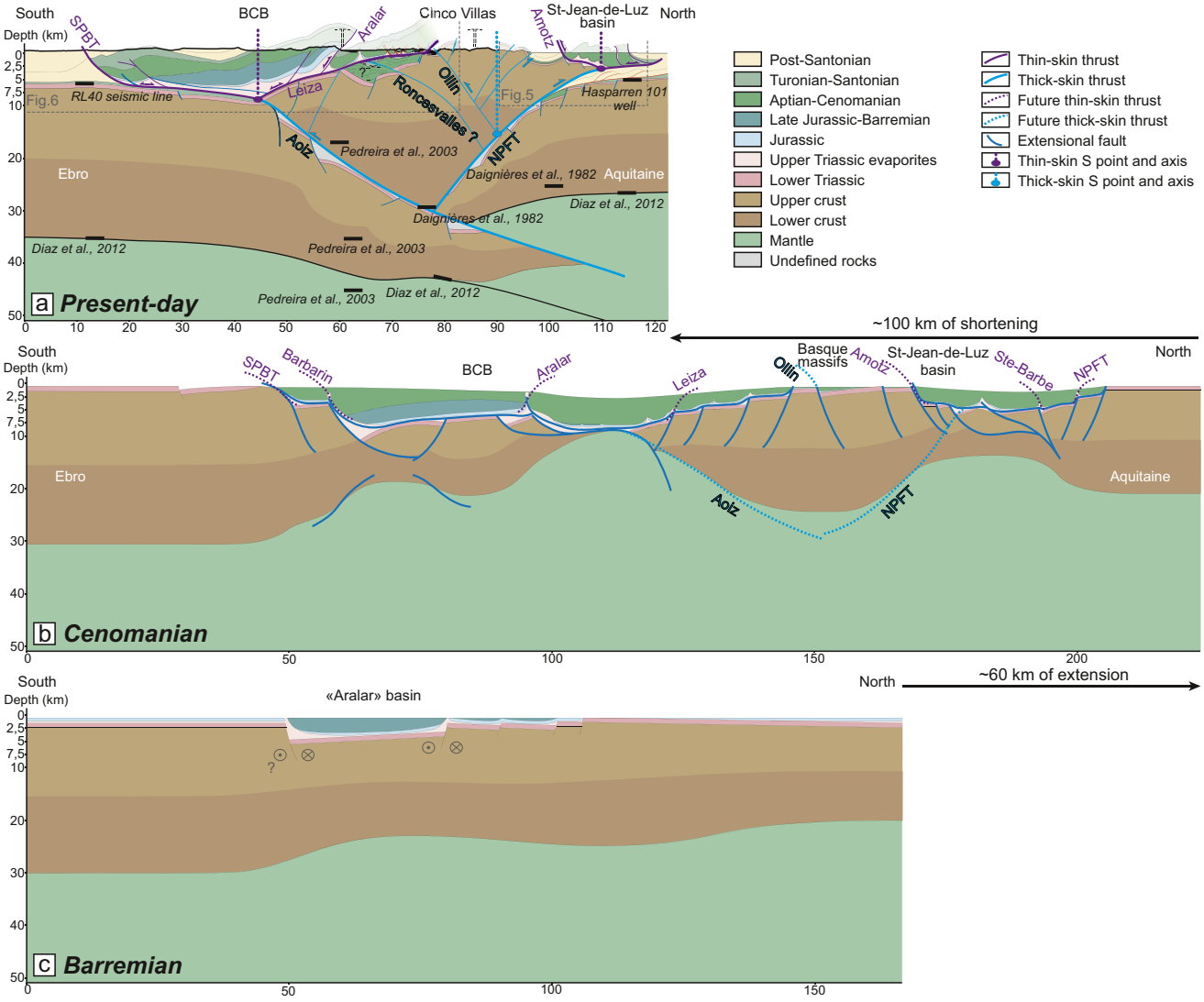

Figure 12. (a) Present-day crustal cross-section across the BCB to St-Jean-de-Luz basin (see also simplified section in Lescoutre and Manatschal [2020]). Location of cross-section in Figure 13. Note the juxtaposition of thin-skinned and thick-skinned thrusts of opposite vergence and the allochthony of the BCB and St-Jean-de-Luz basin on both sides of the crustal wedge. Moho depths are from Díaz et al. (2012) and Daignières et al. (1982), and we plot the layer segments defined on seismic reflections from profile one of Pedreira et al. (2003). The location of these geophysical profiles is presented in Figure S1. Note that, due to the lateral projection of these data onto our N-S cross-section and because of the uncertainties related to data projection in related publications, vertical offset between the different data is observed (e.g., Moho depth between the different geophysical data sets). (b) Restored cross-section at Cenomanian time depicting the architecture of the overlapping rift basins north and south of the Basque massifs. (c) Restored crustal section at Barremian time. Variation of the Moho depth from south to north is based on present-day crustal thickness.

Thus, the west-plunging attitude of the Aldudes antiform shows, in map view, a continuous outcrop of the Leiza detachment characterized by allochthonous blocks of basement embedded within the Upper Triassic evaporites (Figures 9b–9d). North of this antiform, the Nappe des Marbres and the Leiza fault have been folded into a tight syncline in between the Aldudes and Cinco Villas massifs (Figure 8). As a consequence, the restoration at Cenomanian time of such a 3D system requires to displace the Nappe des Marbres and the footwall cutoff of the Leiza fault south of the Aldudes massif, and of the Basque massifs in general (Figures 12a and 12b). This new scenario is able, for the first time, to explain the occurrence of the mantle and granulite rocks in between the Aldudes and Cinco Villas massifs, where no rift structures have been recognized to account for such amount of crustal thinning. It also discards the existence of an N-S Pamplona fault delimiting the eastern termination of the Nappe des Marbres against the thick crust of the Aldudes massif.

4.2. Role of Inheritance for the Architecture of the Pyrenean-Cantabrian Junction

The role of inherited structures in shaping the present-day architecture of the Basque-Cantabrian junction is difficult to assess. Despite NNE-SSW oriented structures are very common in the study area (Figure 2b), they cannot be linked to one particular tectonic event only. Indeed, it seems that this orientation guides the structural evolution of the Basque Pyrenees from Variscan to Alpine convergence (e.g., Variscan: García-Mondéjar et al., 1996; Permian: Lucas, 1987; Triassic: Curnelle, 1983; Late Jurassic-Barremian: Feuillée & Rat, 1971; Aptian-Cenomanian: Razin, 1989; Santonian to Miocene: Razin, 1989; see Section 2.1). This is particularly well documented by the turning of the Albo-Cenomanian SMD and NMD from a WNW-ESE to NNE-SSW orientation along the preserved NNE-SSW Bidarray Permian basin (Figure 4). Moreover, this orientation is also observed in the Alpine structures as exemplified by the Oyarzun and Labourd lateral ramps (Figure 2b), although in this case, it is more difficult to identify the nature and age of the inherited structure that is at their origin. Thus, at this stage, it is difficult to clearly define the role of inherited structures on the tectonic evolution of the Basque-Cantabrian junction. Nonetheless, we attribute an importance to inheritance in controlling the orientation and location of the Late Jurassic-Barremian basins (e.g., Delfaud, 1970; Feuillée & Rat, 1971; Razin, 1989) as observed along the Estella-Pamplona diapirs (Figure 10) or the Mena-Sedano-Poza de la Sal structure (western BCB) (e.g., Del Pozo, 1971; Feuillée & Rat, 1971), both of which depicting NNE-SSW aligned diapirs.

In this study, we identify the north-western and south-western limits of a Late Jurassic-Barremian basin in the BCB that corresponds to the reactivated Aralar thrust and SBPT/Barbarin thrust, respectively (Figure 6). This basin probably also controlled the initiation and localization of Aptian-Cenomanian hyperextended basins as indicated by the development of a thick sedimentary wedge against the former SPBT. However, the migration of the deformation into areas where no Late Jurassic-Barremian deposits are observed (i.e., Nappe des Marbres; Figures 6 and 12) shows that, apart from inheritance, the rift propagation was controlled by other processes as well.

The occurrence of thick Upper Triassic evaporites in many places affected by subsequent Late Jurassic to Cenomanian extension shows that salt tectonics has significantly controlled the style of deformation during the multiple rifting episodes and the later convergence. Indeed, throughout the study area it can be shown that the post-Triassic sedimentary cover was detached above a rather continuous and efficient decoupling level defined by the Upper Triassic evaporites, and eventually displaced above the extremely thinned continental crust and the exhumed mantle. This is well documented by the occurrence of mantle and granulite clasts embedded within the Keuper at the base of the Jurassic to Cenomanian sedimentary cover (e.g., DeFelipe et al., 2017; Jammes, Manatschal, et al., 2010; Lagabrielle et al., 2010). This décollement horizon has been reactivated during the tectonic inversion resulting in a decoupling of the sedimentary cover (thin-skinned) from the shortening of the underlying basement (thick-skinned) (Figure 12). Our work highlights the importance of inheritance on controlling the thin- and thick-skinned deformation during extension and reactivation.

4.3. Structural Evolution of the Aptian-Cenomanian Rift Basins

Based on field and seismic observations and integration of drill hole data, we propose a new model for the Aptian to Cenomanian rift architecture, which has strong implications for the paleogeographic, kinematic, and reactivation history of the Pyrenean-Cantabrian junction.

Previous interpretations suggested the occurrence of a crustal-scale NNE-SSW Pamplona fault that segmented the BCB and the Mauléon basin as either a normal fault in E-W-directed transtensional pull-apart basins or as a transfer fault in an N-S to NNE-SSW extensional direction (see Figure 1). In this study, we show that the St-Jean-de-Luz basin represents the western continuation of the Mauléon basin from Late Albian onwards, as indicated by the occurrence of more than 2000 meters of deep water turbidites in this basin (Figure 5). Similarly, we identified the prolongation of the BCB east of the Estella-Pamplona diapirs (i.e., in the Jaca-Pamplona basin; Figures 10 and 11) where up to 1,400 m of Aptian-Cenomanian sediments have been recorded. We suggest that the St-Jean-de-Luz and the western Jaca-Pamplona basins represent the western and eastern continuation of the Mauléon basin and BCB respectively (Figures 5,10, and 11). The Aptian-Cenomanian BCB likely narrows toward the east and terminates in the vicinity of the Oroz-Betelu

massif. There, post-rift Santonian carbonates unconformably overlie the Lower Triassic red beds all around the massif (Upper Triassic evaporites are lacking). Only in the NW corner of the massif, the upper Albian sandstones and conglomerates (Ciry et al., 1963) are in fault contact (NE-SW striking fault) with the Lower Triassic sediments that could be interpreted as reminiscent of extensional faults segmenting the eastern edge of the BCB (Figures 2 and 13). The Late Albian to Cenomanian St-Jean-de-Luz basin probably tipped out against the Landes high or Biscay massifs (Voort, 1964) from where the basin was fed (Razin, 1989). The extend of the Aptian-Cenomanian hyperextended basin is well shown by the distribution of the post-rift upper Cretaceous facies distribution (Figures 2 and S1), which includes the western Jaca-Pamplona and St-Jean-de-Luz basins.

In this study, we also highlight former WNW-ESE extensional faults (SPBT, SMD, NMD, NPFT, and Amotz faults) that bounded the Aptian-Cenomanian BCB, Mauléon, and St-Jean-de-Luz rift basins (Figures 2, 3, 5, and 6). The orientation of these structures corresponds to the trend of the HT/LP Albo-Cenomanian metamorphic rocks and exhumed mantle/granulite rocks in the BCB and Mauléon basins (e.g., Clerc et al., 2015). Moreover, several NNE-SSW trending second-order transfer or release faults such as the Ibarron, Saison, or St-Jean-Pied-de-Port faults have been described across the area. However, in our study area, there are not any evident major NNE-SSW transfer faults that allow for crustal segmentation along the corridor, which has been historically referred to as the Pamplona fault. Indeed, the western boundary of the Aldudes massif is here proposed to correspond to the continuation of the folded Leiza fault, corresponding to a reactivated extensional detachment. Further north, in the Labourd massif the NNE-SSW faults correspond either to Permian extensional faults related to the development of the Bidarray basin (Saspiturry, Cochelin, et al., 2019) or to the lateral termination or rotation of some of the extensional and contractional Alpine structures along the inherited NNE-SSW structural trend (Variscan to Permian in age). Note also that these N°20E oriented structures are not solely observed along this corridor but in many places within the Pyrenean-Cantabrian system, suggesting that they might have been overinterpreted because of the obvious rift segmentation in the Western Pyrenees. The only structural feature that could be referred to as the Pamplona structure corresponds to the lineament of the Estella-Pamplona diapirs, extending from the SPBT to the Aralar thrust (Figure 13b). However, it has been shown recently that these diapirs are surrounding a depocenter of the pre-Aptian sediments of the BCB that developed by salt evacuation (Cámara, 2020). The Late Jurassic-Barremian sediments do not terminate abruptly at the eastern margin of the BCB coinciding with the lineation of diapirs observed at surface. Instead, these sediments terminate by onlap above the pre-rift Jurassic carbonates and by truncation with the extensional detachment and related extensional faults and diapirs which, in detail, are not distributed along a single lineament (Figure 10). These diapirs have probably initiated over NNE-SSW striking basement-involved faults (which could be named the Pamplona fault system?) at the eastern boundary of a pre-Aptian basin, but the basin has been subsequently decoupled and transported above the Triassic evaporites both during extension and contraction.

As a consequence, we show that the Pyrenean-Cantabrian junction in the Basque Pyrenees corresponds to an accommodation zone during the mid-Cretaceous, and that the termination of the Cantabrian and Pyrenean rift segments were characterized by a V-shaped geometry south and north of the Basque massifs (previously suggested by Floquet & Mathey, 1984). The evolution of such overlapping extensional segments in analog and numerical models shows that the intermediate block, here corresponding to the Basque massifs, is able to rotate in a clockwise direction (e.g., Liao & Gerya, 2015; Tentler & Acocella, 2010). This observation is consistent with paleomagnetic data from the Permo-Triassic red beds of the Basque massifs, where significant clockwise vertical-axis rotations (~20°–37°) of these massifs between the Triassic and the Late Cretaceous have been calculated (see Oliva-Urcia et al., 2012 and references therein). However, the reliability of these paleomagnetic values is questioned by the same authors due to the scarcity of the data, the often large variability of results from site to site for the same massif, the presence of multiple magnetic components of unknown age, and the difficulty to define the reference plate model for the sampled massifs. Note moreover that such rotations, if taken into account, imply that the present-day NNE-SSW inherited Variscan-Permian structural trend was initially striking NNW-SSE. One should note that, based on analog models, hard linkage such as transfer faults have been shown to preferentially develop between offset rift axis during oblique to very oblique extension, while overlapping rift segments better develop in orthogonal settings (Acocella, 2008; Zwaan & Schreurs, 2017). The comparison with analog models provides additional credits against any major E-W transtension during Late Aptian to Cenomanian in the Pyrenean domain.

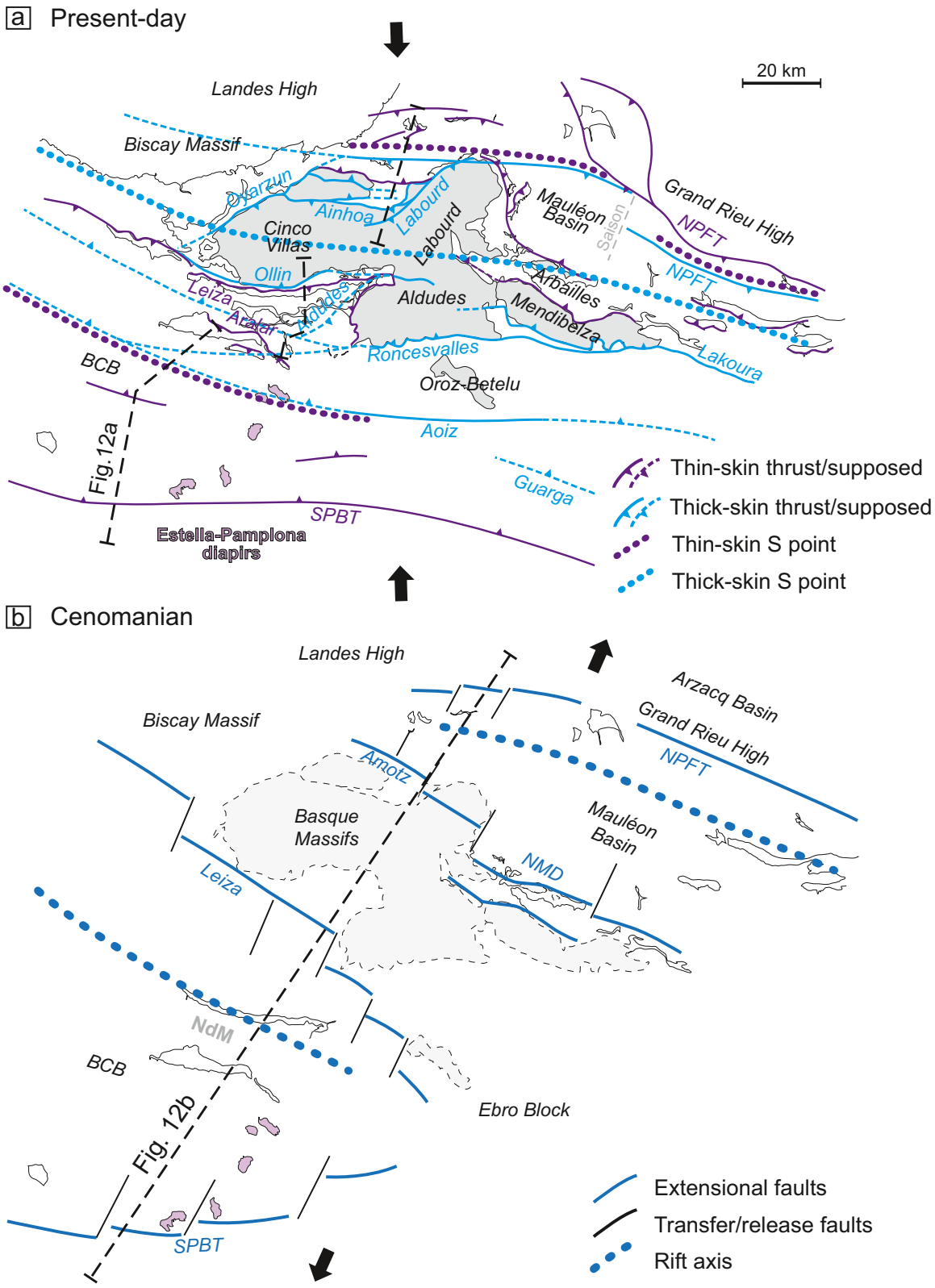

Figure 13. (a) Present-day thin-skinned and thick-skinned thrusts at the Pyrenean-Cantabrian junction. (b) Attempt of restoration of the Aptian-Cenomanian rift basin architecture at Cenomanian time. Note the overlapping rift architecture (accommodation zone) during Aptian-Cenomanian and the proposed limits and interpretation of the Leiza fault within the BCB.

Our results in general discard the existence of a major NNE-SSW striking Pamplona fault that would transfer the deformation between the Cantabrian and the Pyrenean rift segments. All these observations argue for an N-S to NNE-SSW direction of extension during Aptian to Cenomanian in the Basque Pyrenees as already suggested by Tugend et al. (2015), Tavani and Muñoz (2012), and Tavani et al. (2018). This is also in line with kinematic indicators described from the SMD and NMD (Masini et al., 2014) in the Mauléon basin.

4.4. A New Model for Inheritance and Reactivation at the Pyrenean-Cantabrian Junction

These new results, implying overlapping WNW-ESE striking rift basins north and south of the Basque massifs and rebutting crustal decoupling between the Cantabrian and Pyrenean rift segments, suggest a new initial framework for the reactivation of this domain during Pyrenean convergence. In particular, little is known about how reactivation proceeds in such a system where weak rift basins overlap in the direction of shortening.

In the following, we identify and characterize the thin-skinned (supra-salt) and thick-skinned (crustal) deformation on an N-S crustal cross-section (Figure 12a; note that a simplified version of this section has been published by Lescoutre and Manatschal [2020]) and on a map view (Figure 13a). In Figures 12 and 13, we plot the thin-skinned and thick-skinned singular points (S point; e.g., Willett et al., 1993), which correspond to the location of the basal tip of the double-wedge formed by the post-salt unit (thin-skinned) and crustal unit (thick-skinned), respectively, during contractional deformation. As such, the location of the thin-skinned S points for the Mauléon-St-Jean-de-Luz and BCB-Jaca-Pamplona basins correspond to the intersection between the NPFT and Amotz-Arbéroue thrusts, and SPBT and Leiza thrusts, respectively. The location of the thick-skinned S point corresponds to the former wedge at reactivation initiation and as such, corresponds at present-day to the axis between the north-vergent and south-vergent crustal thrusts.

In Figure 12a, we project the cross-sections of Figures 5 and 6 on a crustal-scale cross-section running from the Ebro basin to the Aquitaine basin via the BCB, the Cinco Villas massif, and the St-Jean-de-Luz basin. The top basement is defined by seismic interpretations and the Hasparren 101 borehole, while the Moho depth is constrained by the studies of Díaz et al. (2012) and Daignieres et al. (1982). We also propose a restoration of the cross-section at a late rifting stage (i.e., Cenomanian; Figures 12b) and a pre-Apto-Cenomanian stage (i.e., Late Barremian; Figure 12c) taking into account crustal "volume" preservation using the ImageJ software (https://imagej.nih.gov/ij/). In detail, this software allows, among others, to measure the surface and length of an image based on pixels, and has been used to check and update our cross-sections so that we preserve the same amount of material in both the upper and the lower crust between each time step (>95% of surface preservation), as well as the length of the top Lower Triassic (considered as a marker horizon to analyze deformation from the Cretaceous rifting to the Alpine deformation). Based on these cross-sections and our study, we propose a general map (Figure 13a) highlighting the main thin-skinned and thick-skinned structures of our study area.

Thin-skinned thrust faults south of the Basque massifs correspond to the SPBT (and the Barbarin thrust fault that is part of the splay faults), the Leiza fault, and the Aralar thrust (Figure 6). At least 35 km of southward displacement has been accommodated along the SPBT and minimum of 20 km have been estimated along the north-directed Leiza fault (Figures 6 and 12). Both reactivated Aptian-Cenomanian detachment faults and transported the supra-salt sedimentary cover above the thick crusts of the Ebro and Basque massifs, respectively. The internal part of the BCB shows only minor north-vergent thrust faults mainly reactivating inherited structures such as the Late Jurassic-Barremian Aralar paleo-normal fault or the E-W striking squeezed salt structures observed in the Nappe des Marbres (Ducoux et al., 2019). North of the Basque massifs, the frontal part of the north-vergent NPFT represents the thin-skinned reactivation of an Aptian (or Late Albian in the St-Jean-de-Luz basin) to Cenomanian extensional detachment fault (Razin, 1989). The NPFT is responsible for a significant northward transport of the Mesozoic basin as highlighted by Figures 3 and 5 where it unconformably overlies the Cenozoic deposits on top of the Aquitaine platform (>20 km of displacement according to our restored cross-section in Figure 12). Most of the thin-skinned thrusts that crop out at the surface at present-day are dipping toward the north such as the Arbéroue, Amotz, and St-Barbe thrusts, which reactivated north-dipping Aptian-Cenomanian and Late Albian–Cenomanian detachment faults. The Chaînons Béarnais display a similar architecture as observed

in the Nappe des Marbres and in the St-Jean-de-Luz basins, with E-W striking squeezed salt walls that are affected by minor south-vergent thrusts (e.g., Labaume & Teixell, 2020; Lagabrielle et al., 2010; Razin, 1989).

The thick-skinned deformation can be defined by surface geology and by deep imaging of the crust. In our study, we identified and summarized major north-vergent thick-skinned thrusts such as the Labourd, Ainhoa, and the NPFT (e.g., Razin, 1989; Teixell et al., 2016) that are located on the northern part of the Basque massifs (Figures 2 and 13a). The NPFT, which accommodated a significant amount of crustal shortening, is relayed northward from east to west across the Saison transfer fault (Masini et al., 2014) and has been identified in both the Mauléon and St-Jean-de-Luz basins. This structure can be continuous toward the west and correspond to the North Iberian/Pyrenean Front located at the south of the Landes High (e.g., Roca et al., 2011). South-vergent crustal thrusts such as the Roncesvalles, Ollin, and Lakoura thrusts are observed on the southern border of the Basque massifs (DeFelipe, 2017; Ruiz, Gallart, et al., 2006; Teixell, 1990, 1998). Note that, in contrast to our interpretation, the Ollin thrust has been proposed to reach as deep as 30 km during the formation of the orogen based on the present-day distribution of seismicity (Ruiz, Gallart, et al., 2006; DeFelipe et al., 2018). However, the focal mechanism associated with this fault shows that it has been reactivated as an extensional feature related to post-orogenic extension, which may, as such, have later propagated in the underlying crustal rocks of the European crust. Moreover, these interpretations did not consider the closure of the St-Jean-de-Luz basin to the north and the related amount of crustal shortening accommodated along the thick-skinned NPFT, which imply underthrusting of European crust beneath the Basque massifs and associated crustal thickening (Moho at ~30 km in the overriding plate). Seismic interpretation across the BCB argues for a south-vergent crustal thrust below the Urbasa syncline (see Section 4.3). Note that this thrust (Aoiz thrust on Figure 12a), that we interpret as being responsible for the underthrusting the Ebro crust beneath the Basque massifs and as such to the juxtaposition of denser lower crustal rocks over upper crustal metasedimentary rocks, may explain the velocity anomaly at mid-crustal depth observed on the velocity models of Pedreira et al. (2003); see thick black lines in Figure 12a). Based on receiver function analysis, Díaz et al. (2012) imaged a continuous north-dipping "slab" from east to west below the Basque massifs, connecting the Cantabrian and Pyrenean segments. The WSW-ENE striking orientation of the Roncesvalles thrust, which differs from the general WNW-ESE striking of contractional structures, has been suggested to represent a shortcutting structure in between the inverted Pyrenean and Cantabrian rift segments (Lescoutre & Manatschal, 2020), and may be parallel as such to the trend of the "slab" at depth. Such reorientation of the contractional structures and of the orogenic wedge in general in the Basque Pyrenees (Lescoutre & Manatschal, 2020) may explain the diffuse eastward disappearance of the mid-crustal to lower crustal velocity anomalies on the E-W velocity models of Pedreira et al. (2003) and Daignières et al. (1982), formerly attributed to the Pamplona fault (see Section 2.2; DeFelipe et al., 2018; Pedreira et al., 2003).

These observations suggest a decoupling between the thin-skinned and thick-skinned deformation at the scale of the orogen. The entire BCB-western Jaca-Pamplona basin has been transported and uplifted along the thin-skinned SPBT and Leiza faults on top of the colliding Ebro and Basque crustal blocks (Figures 8, 10, and 12) and leading to the formation of a sedimentary wedge at the front of the allochthonous Basque massifs (Figures 6 and 12). Similarly, the Mauléon and St-Jean-de-Luz basins have been transported along the thin-skinned NPFT and Arbéroue-Amotz faults during the crustal shortening that brought the Basque massifs above the Aquitaine basin (Figures 3, 5, and 12). In that aspect, it is interesting to point out that the footwalls of the NPFT and Aoiz thrusts correspond to the top of the former European and Ebro rifted crustal domains, respectively, while the hanging walls correspond to the rift basins onto which they were formerly detached (Figures 12a and 12b). Independently, the crustal deformation appears to be continuous from the Pyrenean to the Cantabrian segments. Indeed, crustal thrusts do not show a change in vergence or any major offset across the Basque Pyrenees (Figure 13a). As such, change in thrust vergences previously attributed to the Pamplona fault (see Section 2.2) actually corresponds to the present-day juxtaposition of the thin-skinned and thick-skinned deformations (Figure 13a). Moreover, on a map view (Figure 13a), the crustal faults depict a sigmoid shape across the Pyrenean to Cantabrian systems and do not argue in favor of a crustal decoupling between both systems (see also Lescoutre & Manatschal, 2020). Complexities on the cylindric reactivation pattern are brought by the Labourd and Oyarzun lateral ramps that we can eventually attribute to oblique N-S to NW-SE convergence direction (Macchiavelli et al., 2017) with respect to the

inherited NNE-SSW trend in the area. In this context, the existence of a regional scale NNE-SSW crustal fault decoupling the reactivation between the Pyrenean and the Cantabrian segments is unlikely.

Our mapping and field data evidence a good preservation from the Alpine deformation of the Labourd and the Basque massifs in general such as represented by the Bidarray Permian basin, the SMD and NMD rift structures and the distribution of the Lower Triassic sandstones. Moreover, previous authors (Masini et al., 2014; Teixell, 1998; Teixell et al., 2016) suggested that in the western Mauléon basin, a larger amount of basement was involved in the orogenic prism that formed on top of the NPFT, and along which a piece of lower crustal or subcontinental mantle was transported and responsible for the present-day positive gravity anomaly (Casas et al., 1997). This peculiar structural framework has been interpreted by Lescoutre and Manatschal (2020) as the result of the reactivation of the overlapped, weak Pyrenean and Cantabrian hyperextended rift basins and the inability to deform the intermediate crustal block formed by the Basque massifs. Indeed, hyperextended domains have been shown to localize the initiation of reactivation and the northward underthrusting of the Iberian crust (e.g., DeFelipe, 2017; Jammes et al., 2009; Lescoutre & Manatschal, 2020; Masini et al., 2014; Mouthereau et al., 2014; Quintana et al., 2015; Teixell et al., 2016, 2018; Vacherat et al., 2017). However, in this area, the western Mauléon basin and the eastern BCB rift systems might compete during reactivation. As a consequence, geophysical data reflect this structural complexity that we can barely observe in the field.

4.5. Implications for Kinematics of the Western Pyrenees

The kinematics between Iberia, Ebro, and Europe and the location of the plate boundaries have been widely debated in the Pyrenean community (see Figure 1). At a plate kinematic scale, geodynamic reconstructions involve a significant strike-slip component from Valanginian to Santonian between Iberia and Eurasia (Stampfli & Borel, 2002). At the scale of the Pyrenean-Cantabrian system, previous kinematic scenarios imply either a Late Jurassic to Late Cretaceous E-W strike-slip deformation associated with the formation of pull-apart basins or an N-S extension associated with offset rift segments along transfer faults from either Early Cretaceous or Aptian (see 2.2). However, none of these scenarios satisfy geophysical or geological observations (Barnett-Moore et al., 2016; Nirrengarten et al., 2018). Based on geological and geophysical constraints, Nirrengarten et al. (2018) propose that the Iberia and Eurasia plate kinematics can imply a more diffuse boundary with the interplay of a Landes High and an Ebro block, where transtensional deformation might be distributed between the Central Iberian rift system and the Pyrenean system.

In our study, we show that the Aquitaine and Ebro basements were connected via the Basque massifs from Aptian onward and that Aptian-Cenomanian rift systems opened along an N-S direction of extension (Figure 13b). Furthermore, we did not observe evidence for major strike-slip deformation (E-W or N-S) or rotation from Triassic onward within the Basque massifs, neither at larger scale such as suggested by the redundancy of the NNE-SSW Variscan to Triassic inherited trend on both the Aquitaine and Ebro blocks (e.g., Ebro: Feuillée & Rat, 1971; Basque massifs: Lucas, 1987; Aquitaine: Curnelle, 1983). Moreover, similar orientations of Permo-Triassic structures (e.g., Teruel fault) have been described in the south-eastern part of the Ebro basin (Arche & López-Gómez, 1996; Vargas et al., 2009, Figure 1).

As a consequence, the Ebro block can hardly be displaced and rotated by 400 km from Europe during the Jurassic and Cretaceous. In this context, the existence of the NPF, on which most of the sinistral strike-slip movement was supposedly accommodated, seems unlikely in the Western Pyrenees (e.g., Chevrot et al., 2014; Mattauer & Séguret, 1971). Furthermore, the western prolongation of the NPF across the Aldudes–Labourd massifs and at the location of the Leiza fault (e.g., Arthaud & Matte, 1977; Combes et al., 1998; Floquet & Mathey, 1984; Hall & Johnson, 1986; Martínez-Torres, 1992; Mathey et al., 1999; Mendia & Ibarguchi, 1991; Muller & Roger, 1977; Rat, 1988) is not corroborated by our study (see also Saspiturry, Cochelin, et al., 2019) and would imply an even greater offset as we need to restore back the Leiza fault south of its present-day situation. As such, questions remain about the accommodation of the sinistral strike-slip movement. Although we cannot exclude that part of the movement was accommodated along NNE-SSW transfer faults in the BCB and Mauléon basin (e.g., Canérot, 2017; Iriarte & García-Mondéjar, 2001; Tavani et al., 2018), such structures certainly do not account for the proposed 400 km of eastward displacement of Iberia with respect to Eurasia during Aptian to Albian extension.

As a consequence, we suggest that the strike-slip deformation took place, if it existed, either outside the present-day Pyrenean–Cantabrian junction or along a diffuse plate boundary, as previously proposed by Larrasoaña, Parés, Millán, et al. (2003). The lateral component had to be accommodated during the Late Jurassic to Late Barremian/Early Aptian (i.e., from about M0 to C34 magnetic anomalies) associated with the formation of sparse and confined pull-apart basins. Finally, these results suggest that affecting an Iberian or Eurasian affinity to the Palaeozoic basement on both sides of the NPF or in the Basque massifs is misleading as the Ebro block could be part of Eurasia since the Triassic (see also discussion in Larrasoaña, Parés, Millán, et al. [2003]). In any case, the Basque massifs would be a bridge connecting the European and Ebro crusts between the overlapped BCB and Mauléon hyperextended basins.

5. Conclusion

This study aimed to define the nature and the evolution of the Pyrenean-Cantabrian junction with particular emphasis on the role of structural inheritance. We used field cross-sections and seismic interpretations combined with drill hole data to describe the present-day architecture of the eastern and western terminations of the BCB and Mauléon basin, respectively, that correspond to the trace of the formerly defined Pamplona fault. Our results show that:

(1) Aptian-Cenomanian rifting took place along an NNE-SSW direction of extension controlled by WNW-ESE striking detachment faults and NNE-SSW transfer/release faults, associated with mantle exhumation and HT/LP metamorphism in WNW-ESE oriented V-shaped basins. The Late Jurassic-Barremian rift episode was potentially controlled by similar WNW-ESE and NNE-SSW structures. In our study area, we showed that Aptian-Cenomanian rifting initiated but did not propagate at the location of Late Jurassic-Barremian basins.
(2) The Aptian to Cenomanian BCB and the Mauléon basin propagated further eastward and westward respectively, than the trace of the so-called and suggested Pamplona fault. As a consequence, we discard the occurrence of any major NNE-SSW fault to transfer the deformation from the Cantabrian to the Pyrenean rift segments and the use of the transfer fault/zone terminology on which the Pamplona fault is usually related. Instead, we propose the term “Basque massifs accommodation zone” which better defines the nature and architecture of the area.
(3) No major strike-slip or rotational deformation has been observed in the Basque Pyrenees as argued by the conspicuous Variscan to Triassic inherited NNE-SSW trend across the Aquitaine and Ebro basements.
(4) Thin-skinned and thick-skinned structures display a contrasting architecture in the study area. Thin-skinned deformation reactivated and transported the former Aptian-Cenomanian rift basins while thick-skinned deformation seems to shortcut across the Basque Pyrenees, eventually responsible for the preservation of the pre-Alpine structures in the Basque massifs.

These results have major implications for the kinematics of the Basque Pyrenees and for the architecture of the Pyrenean-Cantabrian junction:

(1) The architecture of the Basque Pyrenees at Cenomanian time results in two overlapping rift segments north and south of the Basque massifs, corresponding to an accommodation zone. As such, the tectonic evolution of the Cantabrian-Pyrenean junction cannot be explained by crustal decoupling between both systems.
(2) The Ebro is proposed to be connected with the Eurasia plate along the Basque massifs zone since the Triassic and therefore undermines any important strike-slip displacement along the NPF during the Jurassic and Cretaceous.
(3) The Iberia-Eurasia plate boundary has to be located outside the study area or had to occur over a more diffuse area during the Late Jurassic to Barremian.

Data Availability Statement

Seismic lines used in this study and borehole information can be requested from the IGME website (info.igme.es/sigeof/). Field structural data presented in this manuscript are available on the 4TU.ResearchData repository (http://doi.org/10.4121/13665023). Supporting Information related to this article is included as one Figure S1 (http://doi.org/10.4121/13664936).

Acknowledgments
This study was funded by the Orogen project, a tripartite joint academic-industry research program between the CNRS, BRGM, and Total R&D Frontier Exploration program. J. A. Muñoz acknowledges the support by the projects CGL2014-54118-C2-1-R/BTE and CGL2017-85532-P of the Ministerio de Economía y Competitividad. We thank most of the numerous reviewers that provided a constructive criticism of an initial version of this manuscript. We appreciate editorial handling by John Geissman and an anonymous Associate Editor. The authors thank Petroleum Experts Limited for providing us with the Move software academic license. Patricia Cadenas and Jordi Miró are thanked for the fruitful discussions during the field excursion in the Basque Country.

References

Ábalos, B. (2016). Geologic map of the Basque-Cantabrian Basin and a new tectonic interpretation of the Basque Arc. *International Journal of Earth Sciences*, *105*, 2327–2354. https://doi.org/10.1007/s00531-016-1291-6

Ábalos, B., Alkorta, A., & Iríbar, V. (2008). Geological and isotopic constraints on the structure of the Bilbao anticlinorium (Basque-Cantabrian basin, North Spain). *Journal of Structural Geology*, *30*(11), 1354–1367. https://doi.org/10.1016/j.jsg.2008.07.008

Acocella, V. (2008). Transform faults or Overlapping Spreading Centers? Oceanic ridge interactions revealed by analogue models. *Earth and Planetary Science Letters*, *265*(3–4), 379–385. https://doi.org/10.1016/j.epsl.2007.10.025

Aguilar, C., Liesa, M., Castiñeiras, P., & Navidad, M. (2013). Late Variscan metamorphic and magmatic evolution in the eastern Pyrenees revealed by U-Pb age zircon dating. *Journal of the Geological Society*, *171*(2), 181–192. https://doi.org/10.1144/jgs2012-086

Aguilar, C., Liesa, M., Štípská, P., Schulmann, K., Muñoz, J. A., & Casas, J. M. (2015). P-T-t-d evolution of orogenic middle crust of the Roc de Frausa Massif (Eastern Pyrenees): A result of horizontal crustal flow and Carboniferous doming? *Journal of Metamorphic Geology*, *33*(3), 273–294. https://doi.org/10.1111/jmg.12120

Albarède, F., & Michard-Vitrac, A. (1978). Age and significance of the North Pyrenean metamorphism. *Earth and Planetary Science Letters*, *40*(3), 327–332. https://doi.org/10.1016/0012-821X(78)90157-7

Aller, J., & Zeyen, H. J. (1996). A 2.5-D interpretation of the Basque country magnetic anomaly (northern Spain): Geodynamical implications. *Geologische Rundschau*, *85*(2), 303–309. https://doi.org/10.1007/BF0242223610.1007/s005310050076

Allken, V., Huismans, R. S., & Thieulot, C. (2012). Factors controlling the mode of rift interaction in brittle-ductile coupled systems: A 3D numerical study. *Geochemistry, Geophysics, Geosystems*, *13*. https://doi.org/10.1029/2012GC004077

Almar, Y., Garcés, M., Beamud, E., & Muñoz, J. A. (2008). Timing and evolution of the frontal structure of the southwestern Pyrenees from paleomagnetic analysis on its foreland basin (Ebro basin). *Geotemas*, *10*, 1143–1146.

Amiot, M. (1982). El Cretácico superior de la región Navarro-Cántabra. *El Cretácico de España*, 88–111.

Angrand, P., Mouthereau, F., Masini, E., & Asti, R. (2020). A reconstruction of Iberia accounting for W-Tethys/N-Atlantic kinematics since the late Permian-Triassic. *Solid Earth Discussions*. *11*, 1313–1332. https://doi.org/10.5194/se-2020-24

Arche, A., & López-Gómez, J. (1996). Origin of the Permian-Triassic Iberian Basin, central-eastern Spain. *Tectonophysics*, *266*(1–4), 443–464. https://doi.org/10.1016/S0040-1951(96)00202-8

Arthaud, F., & Matte, P. (1975). Les decrochements tardi-hercyniens du sud-ouest de l'europe. Geometrie et essai de reconstitution des conditions de la deformation. *Tectonophysics*, *25*(1–2), 139–171. https://doi.org/10.1016/0040-1951(75)90014-1

Arthaud, F., & Matte, P. (1977). Late Paleozoic strike-slip faulting in southern Europe and northern Africa: Result of a right-lateral shear zone between the Appalachians and the Urals. *Geological Society of America Bulletin*, *88*(9), 1305–1320. https://doi.org/10.1130/0016-7606(1977)88<1305:LPSFIS>2.0.CO;2

Aurell, M., Robles, S., Bádenas, B., Rosales, I., Quesada, S., Meléndez, G., & García-Ramos, J. C. (2003). Transgressive–regressive cycles and Jurassic paleogeography of northeast Iberia. *Sedimentary Geology*, *162*(3–4), 239–271. https://doi.org/10.1016/S0037-0738(03)00154-4

Azambre, B., & Monchoux, P. (1998). Métagabbros amphiboliques et mise en place crustale des lherzolites des Pyrénées (France). *Comptes Rendus de l'Academie des Sciences - Series IIA: Earth and Planetary Science*, *327*(1), 9–15. https://doi.org/10.1016/S1251-8050(98)80012-8

Azambre, B., & Rossy, M. (1976). Le magmatisme alcalin d'age cretace, dans les Pyrenees occidentales et l'Arc basque; ses relations avec le metamorphisme et la tectonique. *Bulletin de la Societe Geologique de France*, *S7-XVIII*(6), 1725–1728. https://doi.org/10.2113/gssgfbull.S7-XVIII.6.1725

Bádenas, B. (1996). El jurásico superior de la sierra de Aralar (Guipúzcoa y Navarra): Caracterización sedimentalógica y paleogeográfica. *Estudios Geológicos*, *52*, 147–160. https://doi.org/10.3989/egeol.96523-4262

Ballèvre, M., Martínez Catalán, J. R., López-Carmona, A., Pitra, P., Abati, J., Fernández, R. D., et al. (2014). Correlation of the nappe stack in the Ibero-Armorican arc across the Bay of Biscay: A joint French-Spanish project. *Geological Society, London, Special Publications*, *405*(1), 77–113. https://doi.org/10.1144/SP405.13

Barnett-Moore, N., Müller, D. R., Williams, S., Skogseid, J., & Seton, M. (2016). A reconstruction of the North Atlantic since the earliest Jurassic. *Basin Research*, *30*, 160–185. https://doi.org/10.1111/bre.12214

Beaumont, C., Muñoz, J. A., Hamilton, J., & Fullsack, P. (2000). Factors controlling the Alpine evolution of the central Pyrenees inferred from a comparison of observations and geodynamical models. *Journal of Geophysical Research*, *105*(B4), 8121–8145. https://doi.org/10.1029/1999jb900390

Biteau, J.-J., Le Marrec, A., Le Vot, M., & Masset, J.-M. (2006). The Aquitaine Basin. *Petroleum Geoscience*, *12*(3), 247–273. https://doi.org/10.1144/1354-079305-674

Bixel, F., & Lucas, C. (1987). Approche geodynamique du Permien et du Trias des Pyrenees dans le cadre du Sud-Ouest Europeen. *Cuadernos de Geología Ibérica= Journal of Iberian Geology: An International Publication of Earth Sciences*, *11*, 57–82.

Bodego, A., & Agirrezabala, L. M. (2017). The Andatza coarse-grained turbidite system (westernmost Pyrenees): Stratigraphy, sedimentology and structural control. *Estudios Geológicos*, *73*(1), 3. https://doi.org/10.3989/egeol.42535.422

Bodego, A., Iriarte, E., Agirrezabala, L. M., García-Mondéjar, J., & López-Horgue, M. A. (2015). Synextensional mid-Cretaceous stratigraphic architecture of the eastern Basque-Cantabrian basin margin (western Pyrenees). *Cretaceous Research*, *55*(Suppl C), 229–261. https://doi.org/10.1016/j.cretres.2015.01.006

Boess, J., & Hoppe, A. (1986). Mesozoischer Vulkanismus in Nordspanien: Rifting im Keuper und Kreide-Vulkanismus auf Transform-Störungen? *Geologische Rundschau*, *75*(2), 353–369. https://doi.org/10.1007/BF01820617

Boillot, G., & Capdevila, R. (1977). The Pyrenees: Subduction and collision? *Earth and Planetary Science Letters*, *35*(1), 151–160. https://doi.org/10.1016/0012-821X(77)90038-3

BRGM. (1963). Notice explicative de la feuille Bayonne à 1/50 000(1001). Éditions Du Bureau de Recherches Géologiques et Minières, Orléans, 1–16.

Brinkmann, R., & Lögters, H. (1968). Diapirs in Western Pyrenees and Foreland, Spain. In J. Braunstein & G. D. O'Brien (Eds.), *Diapirism and Diapirs: a Symposium*, AAPG Mem, (Vol. 8, pp. 275–292).

Bubeck, A., Walker, R. J., Imber, J., Holdsworth, R. E., MacLeod, C. J., & Holwell, D. A. (2017). Extension parallel to the rift zone during segmented fault growth: Application to the evolution of the NE Atlantic. *Solid Earth*, *8*(6), 1161–1180. https://doi.org/10.5194/se-8-1161-2017

Burg, J.-P., Van Den Driessche, J., & Brun, J.-P. (1994). Syn-to post-thickening extension: Mode and consequences. *Comptes Rendus de l'Académie Des Sciences. Série 2. Sciences de La Terre et Des Planètes*, *319*(9), 1019–1032.

Cámara, P. (1997). The Basque-Cantabrian basin's Mesozoic tectono-sedimentary evolution. *Mémoires de La Société Géologique de France*, *171*, 187–191.

Cámara, P. (2020). Inverted turtle salt anticlines in the Eastern Basque-Cantabrian basin, Spain. *Marine and Petroleum Geology*, *117*, 104358. https://doi.org/10.1016/j.marpetgeo.2020.104358

Campos, J. (1979). Estudio geológico del Pirineo vasco al W del río Bidasoa. *Munibe, SC Aranzadi*, *31*(1–2), 3–139.

Campos, J., & García-Dueñas, V. (1972). Mapa geológico de España E. 1:50.000, Serie MAGNA (Hoja de San Sebastián, 64).

Campos, J., García-Dueñas, V., Lamolda, M. A., & Pujalte, V. (1972a). Mapa geológico de España E. 1:50.000, Serie MAGNA (Hoja de Irún, 41).

Campos, J., García-Dueñas, V., Lamolda, M. A., & Pujalte, V. (1972b). Mapa geológico de España E. 1:50.000, Serie MAGNA (Hoja de Jaizquibel, 40).

Canérot, J. (2017). The pull apart-type Tardets-Mauléon Basin, a key to understand the formation of the Pyrenees. *Bulletin de la Societe Geologique de France*, *188*(6), 35. https://doi.org/10.1051/bsgf/2017198

Canérot, J., Majesté-Menjoulas, C., & Ternet, Y. (1999). Le cadre stratigraphique et géodynamique des altérites et des bauxites sur la marge ibérique des Pyrénées occidentales (France). *Comptes Rendus de l'Academie des Sciences - Series IIA: Earth and Planetary Science*, *328*(7), 451–456. https://doi.org/10.1016/s1251-8050(99)80145-1

Canérot, J., Peybernes, B., & Ciszak, R. (1978). Presence d'une marge meridionale a l'emplacement de la zone des chainons bearnais (Pyrenees basco-bearnaises). *Bulletin de La Société Géologique de France*, *S7-XX*(5), 673–676. https://doi.org/10.2113/gssgfbull.S7-XX.5.673

Capote, R., Muñoz, J. A., Simón, J. L., Liesa, C. L., & Arlegui, L. E. (2002). Alpine tectonics I: The Alpine system north of the Betic Cordillera. In W. Gibbons & T. Moreno (Eds.), *The Geology of Spain*. The Geological Society of London, (pp. 367–400).

Carbayo, A., del Valle, J., León, L., & Villalobos, L. (1972). Mapa geológico de España E. 1:50.000, Serie MAGNA(Hoja de Garralda, 116).

Carbayo, A., León, L., & Villalobos, L. (1977). Mapa geológico de España E. 1:50.000, Serie MAGNA(Hoja de Gulina, 115).

Carola, E., Tavani, S., Ferrer, O., Granado, P., Quintà, A., Butillé, M., & Muñoz, J. A. (2013). Along-strike extrusion at the transition between thin- and thick-skinned domains in the Pyrenean Orogen (northern Spain). *Geological Society, London, Special Publications*, *377*(1), 119–140. https://doi.org/10.1144/SP377.3

Carola i Molas, E. (2014). The transition between thin-to-thick-skinned styles of deformation in the Western Pyrenean Belt.

Casas, A., Kearey, P., Rivero, L., & Adam, C. R. (1997). Gravity anomaly map of the Pyrenean region and a comparison of the deep geological structure of the western and eastern Pyrenees. *Earth and Planetary Science Letters*, *150*(1), 65–78. https://doi.org/10.1016/S0012-821X(97)00087-3

Casas Sainz, A. M. (1993). Oblique tectonic inversion and basement thrusting in the Cameros Massif (Northern Spain). *Geodinamica Acta*, *6*(3), 202–216. https://doi.org/10.1080/09853111.1993.11105248

Chevrot, S., Sylvander, M., Diaz, J., Martin, R., Mouthereau, F., Manatschal, G., et al. (2018). The non-cylindrical crustal architecture of the Pyrenees. *Scientific Reports*, *8*(1), 9591. https://doi.org/10.1038/s41598-018-27889-x

Chevrot, S., Villaseñor, A., Sylvander, M., Benahmed, S., Beucler, E., Cougoulat, G., et al. (2014). High-resolution imaging of the Pyrenees and Massif Central from the data of the PYROPE and IBERARRAY portable array deployments. *Journal of Geophysical Research: Solid Earth*, *119*(8), 6399–6420. https://doi.org/10.1002/2014JB010953

Choukroune, P. (1992). Tectonic evolution of the Pyrenees. *Annual Review of Earth and Planetary Sciences*, *20*(1), 143–158. https://doi.org/10.1146/annurev.ea.20.050192.001043

Choukroune, P., & Mattauer, M. (1978). Tectonique des plaques et Pyrenees; sur le fonctionnement de la faille transformante nord-pyreneenne; comparaisons avec des modeles actuels. *Bulletin de La Societe Geologique de France*, *S7-XX*(5), 689–700. https://doi.org/10.2113/gssgfbull.S7-XX.5.689

Choukroune, P., Seguret, M., & Galdeano, A. (1973). Caracteristiques et evolution structurale des Pyrenees; un modele de relations entre zone orogenique et mouvement des plaques. *Bulletin de La Societe Geologique de France*, *S7-XV*(5–6), 600–611. https://doi.org/10.2113/gssgfbull.S7-XV.5-6.600

Cincunegui, M., Mendizabal, J., & Valle, A. (1943). Mapa geológico de España 1: 50.000. Explicación de la hoja núm. 172 (Allo). IGME. Madrid.

Ciry, R., Amiot, M., & Feuillee, P. (1963). Les transgressions cretacees sur le massif d'Oroz-Betelu (Navarre espagnole). *Bulletin de La Société Géologique de France*, *S7-V*(5), 701–707. https://doi.org/10.2113/gssgfbull.s7-v.5.701

Claude, D. (1990). Etude stratigraphique, sédimentologique et structurale des dépôts mésozoïques au nord du massif du Labourd: rôle de la faille de Pamplona, Pays Basque.

Clerc, C., & Lagabrielle, Y. (2014). Thermal control on the modes of crustal thinning leading to mantle exhumation: Insights from the Cretaceous Pyrenean hot paleomargins. *Tectonics*, *33*, 1340–1359. https://doi.org/10.1002/2013TC003471

Clerc, C., Lahfid, A., Monié, P., Lagabrielle, Y., Chopin, C., Poujol, M., et al. (2015). High-temperature metamorphism during extreme thinning of the continental crust: A reappraisal of the North Pyrenean passive paleomargin. *Solid Earth*, *6*(2), 643–668. https://doi.org/10.5194/se-6-643-2015

Cochelin, B. (2016). Champ de déformation du socle paléozoïque des Pyrénées.

Combes, P.-J., Peybernès, B., & Leyreloup, A. F. (1998). Altérites et bauxites, témoins des marges européenne et ibérique des Pyrénées occidentales au Jurassique supérieur - Crétacé inférieur, à l'ouest de la vallée d'Ossau (Pyrénées-Atlantiques, France). *Comptes Rendus de l'Academie des Sciences - Series IIA: Earth and Planetary Science*, *327*(4), 271–278. https://doi.org/10.1016/S1251-8050(98)80085-2

Corre, B., Boulvais, P., Boiron, M. C., Lagabrielle, Y., Marasi, L., & Clerc, C. (2018). Fluid circulations in response to mantle exhumation at the passive margin setting in the north Pyrenean zone, France. *Mineralogy and Petrology*, *112*(5), 647–670. https://doi.org/10.1007/s00710-018-0559-x

Cuevas, J., & Tubía, J. M. (1999). The discovery of scapolite marbles in the Biscay Synclinorium (Basque-Cantabrian basin, Western Pyrenees): Geodynamic implications. *Terra Nova*, *11*(6), 259–265. https://doi.org/10.1046/j.1365-3121.1999.00255.x

Curnelle, R. (1983). Evolution structuro-sédimentaire du Trias et de l'Infra-Lias d'Aquitaine. *Bulletin des Centres de Recherches Exploration-Production Elf-Aquitaine*, *7*(1), 69–99.

Cuvillier, J., Henry, J., Ribis, R., & Villanova, M. (1964). Microfaunes cenomaniennes et santoniennes dans le 'calcaire des canons' (vallee d'Aspe, Sainte-Engrace, Basses-Pyrenees). *Bulletin de La Société Géologique de France*, *S7-VI*(2), 273–277. https://doi.org/10.2113/gssgfbull.S7-VI.2.273

Daguin, F. (1948). *L'Aquitaine occidentale* (Vol. 1050). Jouve.

Daignieres, M. (1978). Geophysique et faille nord-pyreneenne. *Bulletin de la Societe Geologique de France*, *S7-XX*(5), 677–680. https://doi.org/10.2113/gssgfbull.S7-XX.5.677

Daignieres, M., Gallart, J., Banda, E., & Hirn, A. (1982). Implications of the seismic structure for the orogenic evolution of the Pyrenean Range. *Earth and Planetary Science Letters*, *57*(1), 88–100. https://doi.org/10.1016/0012-821X(82)90175-3

Debroas, E. J (1987). Modele de bassin triangulaire a l'intersection de decrochements divergents pour le fosse albo-cenomanien de la Ballongue (zone nord-pyreneenne, France). *Bulletin de La Societe Geologique de France*, *III*(5), 887. https://doi.org/10.2113/gssgfbull.III.5.887

DeFelipe, I. (2017). *Crustal structure and alpine tectonic evolution of the eastern border of the Basque-Cantabrian Zone*. Universidad de Oviedo.

DeFelipe, I., Pedreira, D., Pulgar, J. A., Beek, P. A., Bernet, M., & Pik, R. (2019). Unraveling the Mesozoic and Cenozoic tectonothermal evolution of the Eastern Basque-Cantabrian Zone–Western Pyrenees by low-temperature thermochronology. *Tectonics*, *38*(9), 3436–3461. https://doi.org/10.1029/2019TC005532

DeFelipe, I., Pedreira, D., Pulgar, J. A., Iriarte, E., & Mendia, M. (2017). Mantle exhumation and metamorphism in the Basque-Cantabrian Basin (NSpain): Stable and clumped isotope analysis in carbonates and comparison with ophicalcites in the North-Pyrenean Zone (Urdach and Lherz). *Geochemistry, Geophysics, Geosystems*, *18*(2), 631–652. https://doi.org/10.1002/2016GC006690

DeFelipe, I., Pulgar, J. A., & Pedreira, D. (2018). Crustal structure of the Eastern Basque-Cantabrian Zone-western Pyrenees: From the Cretaceous hyperextension to the Cenozoic inversion. *Revista de la Sociedad Geologica de Espana*, *31*(2), 69–82.

Delfaud, J. (1970). Résumé d'une recherche sur la dynamique du domaine aquitano-pyrénéen durant le Jurassique et le Crétacé inférieur. Société linnéenne de Bordeaux.

Del Pozo, J. R. (1971). *Bioestratigrafia y microfacies del Jurásico y Cretácico del norte de España (región cantábrica)* (Vol. 78) Departamento de Publicaciones.

Del Valle, J. R. (1972). Mapa geológico de España E. 1:50.000, Serie MAGNA(Hoja de Pamplona, 141).

Del Valle, J. R., Adler, R. E., de Boer, H. F., Jordan, H., Klarr, K., et al. (1972). Mapa geológico de España E. 1:50.000, Serie MAGNA(Hoja de Valcarlos, 91).

Del Valle, J. R., Villalobos, L., Bornhorst, H. U., de Boer, H. F., Krausse, K., et al. (1973). Mapa geológico de España E. 1:50.000, Serie MAGNA(Hoja de Sumbilla, 90).

Delvolvé, J.-J., Vachard, D., & Souquet, P. (1998). Stratigraphic record of thrust propagation, Carboniferous foreland basin, Pyrenees, with emphasis on Pays-de-Sault (France/Spain). *Geologische Rundschau*, *87*(3), 363–372. https://doi.org/10.1007/s005310050215

Denèle, Y., Paquette, J.-L., Olivier, P., & Barbey, P. (2011). Permian granites in the Pyrenees: The Aya pluton (Basque Country). *Terra Nova*, *24*(2), 105–113. https://doi.org/10.1111/j.1365-3121.2011.01043.x

Díaz, J., Pedreira, D., Ruiz, M., Pulgar, J. A., & Gallart, J. (2012). Mapping the indentation between the Iberian and Eurasian plates beneath the Western Pyrenees/Eastern Cantabrian Mountains from receiver function analysis. *Tectonophysics*, *570–571*, 114–122. https://doi.org/10.1016/j.tecto.2012.07.005

Doré, A. G., Lundin, E. R., Jensen, L. N., Birkeland, ø., Eliassen, P. E., & Fichler, C. (1999). Principal tectonic events in the evolution of the northwest European Atlantic margin. *Paper presented at Petroleum Geology of Northwest Europe: Proceedings of the 5th Conference*, 41–61. Geological Society of London. https://doi.org/10.1144/0050041

Ducasse, L., Muller, J., & Velasque, P.-C. (1986). La chaîne pyrénéo-cantabrique: subduction hercynienne, rotation crétacée de l'Ibérie et subductions alpines différentielles. *Comptes Rendus de l'Académie Des Sciences. Série 2, Mécanique, Physique, Chimie, Sciences de l'univers, Sciences de La Terre*, *303*(5), 419–424.

Ducoux, M., Jolivet, L., Callot, J. -P., Aubourg, C., Masini, E., Lahfid, A., et al (2019). The Nappe des Marbres unit of the Basque-Cantabrian Basin: The tectono-thermal evolution of a fossil hyperextended rift basin. *Tectonics*. *38*(11), 3881–3915. https://doi.org/10.1029/2018TC005348

Engeser, T., & Schwentke, W. (1986). Toward a new concept of the tectogenesis of the Pyrenees. *Tectonophysics*, *129*(1–4), 233–242. https://doi.org/10.1016/0040-1951(86)90253-2

Fernández, O., Muñoz, J. A., Arbues, P., & Falivene, O. (2012). 3D structure and evolution of an oblique system of relaying folds: The Ainsa basin (Spanish Pyrenees). *Journal of the Geological Society*, *169*(5), 545–559.

Ferrer, O., Jackson, M. P. A., Roca, E., & Rubinat, M. (2012). Evolution of salt structures during extension and inversion of the Offshore Parentis Basin (Eastern Bay of Biscay). *Geological Society, London, Special Publications*, *363*(1), 361–380. https://doi.org/10.1144/SP363.16

Feuillée, P. (1964). Sur l'âge cénomanien des calcaires à Caprines des Pyrénées basques occidentales. *Comptes Rendus Société Géologique de France*, *2*, 90–93.

Feuillée, P. (1971). Les calcaires biogéniques de l'Albien et du Cénomanien pyrénéo-cantabrique: Problèmes d'environnement sedimentaire. *Palaeogeography, Palaeoclimatology, Palaeoecology*, *9*(4), 277–311. https://doi.org/10.1016/0031-0182(71)90004-6

Feuillée, P., & Rat, P. (1971). *Structures et paléogéographies pyrénéo-cantabriques*. Technip.

Floquet, M. (1998). Outcrop cycle stratigraphy of shallow ramp deposits: The Late Cretaceous Series on the Castillian ramp (northern Spain).

Floquet, M., & Mathey, B. (1984). Evolution sédimentologique, paléogéographique et structurale des marges ibérique et européenne dans les régions basco-cantabrique et nord-ibérique au Crétacé moyen et supérieur. *Act. Lab. Sédim. Paléont. Univ. Sabatier*, *1*, 129–136.

Floquet, M., Mathey, B., Rosse, P., & Vadot, J. P. (1988). Age cenomanien et turono-coniacien des calcaires de Sare (Pays Basque, France-Espagne); consequences paleomorphologiques et tectogenetiques pour les Pyrenees occidentales. *Bulletin de La Société Géologique de France*, *IV*(6), 1021–1027. https://doi.org/10.2113/gssgfbull.IV.6.1021

Frankovic, A., Eguiluz, L., & Martínez-Torres, L. M. (2016). Geodynamic evolution of the Salinas de Añana diapir in the Basque-Cantabrian Basin, Western Pyrenees. *Journal of Structural Geology*, *83*, 13–27. https://doi.org/10.1016/j.jsg.2015.12.001

Gabaldón, V., Hernández Samaniego, A., Ramírez del Pozo, J. J., Carbaya Olivares, A., Castiella Muruzábal, J., & Solé Sedo, J. (1984). Mapa geológico de España E. 1:50.000, Serie MAGNA(Hoja de Allo, 172).

Gabaldón, V., Hernández Samaniego, A., Ramírez del Pozo, J. J., & Ramírez del Pozo, J. (1984). Mapa geológico de España E. 1:50.000, Serie MAGNA(Hoja de Tafalla, 173).

Gabaldón, V., Hernández Samaniego, A., & Simó Marja, A. (1985). Mapa geológico de España E. 1:50.000, Serie MAGNA(Hoja de Sangüesa, 174).

Gabaldón, V., R. Merino, Ramírez del Pozo, J. J., Olivé Davo, A., Villalobos Vilches, L., León González, L., & Carbayo Olivares, A. (1984). Mapa geológico de España E. 1:50.000, Serie MAGNA(Hoja de Alsasua, 114).
Gallastegui, J. (2000). Estructura cortical de la cordillera y margen continental cantábricos: perfiles ESCI-N. *Trabajos de Geología*, *22*(22), 3–234.
Gallego, M. R., Aurell, M., Bádenas, B., Fontana, B., & Meléndez, G. (1994). Origen de las brechas de la base del Jurásico de Leitza (Cordillera Vasco–Cantábrica Oriental, Navarra). *Geogaceta*, *15*, 26–29.
García-Mondéjar, J., Agirrezabala, L., Aranburu, A., Fernández-Mendiola, P., Gómez-Pérez, I., López-Horgue, M., & Rosales, I. (1996). Aptian—Albian tectonic pattern of the Basque—Cantabrian Basin (Northern Spain). *Geological Journal*, *31*(1), 13–45.
García-Mondéjar, J., Pujalte, V., & Robles, S. (1986). Caracteristicas sedimentologicas, secuenciales y tectoestratigraficas del Triasico de Cantabria y norte de Palencia. *Cuadernos de Geologia Iberica*, *10*, 151–172.
Genna, A. (2007). Carte géologique harmonisée au 1/50 000 du département des Pyrénées-Atlantiques, (BRGM/RP-55408-FR).
Golberg, J. M., & Leyreloup, A. F. (1990). High temperature-low pressure Cretaceous metamorphism related to crustal thinning (Eastern North Pyrenean Zone, France). *Contributions to Mineralogy and Petrology*, *104*(2), 194–207. https://doi.org/10.1007/BF00306443
Gräfe, K.-U. (1999). Sedimentary cycles, burial history and foraminiferal indicators for systems tracts and sequence boundaries in the Cretaceous of the Basco-Cantabrian Basin (northern Spain). *Neues Jahrbuch Fur Geologie Und Palaontologie-Abhandlungen*, *212*(1), 85–130.
Granado, P., Ferrer, O., Muñoz, J. A., Thöny, W., & Strauss, P. (2017). Basin inversion in tectonic wedges: Insights from analogue modeling and the Alpine-Carpathian fold-and-thrust belt. *Tectonophysics*, *703–704*, 50–68. https://doi.org/10.1016/j.tecto.2017.02.022
Guitard, G., Vielzeuf, D., Martinez, F., Barnolas, A., & Chiron, J. (1996). Métamorphisme hercynien. *Synthèse Géologique et Géophysique Des Pyrénées*, *1*, 501–584.
Hall, C. A., & Johnson, J. A. (1986). Apparent western termination of the North Pyrenean Fault and tectonostratigraphic units of the western north Pyrenees, France and Spain. *Tectonics*, *5*(4), 607–627. https://doi.org/10.1029/TC005i004p00607
Hart, N. R., Stockli, D. F., & Hayman, N. W. (2016). Provenance evolution during progressive rifting and hyperextension using bedrock and detrital zircon U-Pb geochronology, Mauléon Basin, western Pyrenees. *Geosphere*, *12*(4), 1166–1186. https://doi.org/10.1130/GES01273.1
Hart, N. R., Stockli, D. F., Lavier, L. L., & Hayman, N. W. (2017). Thermal evolution of a hyperextended rift basin, Mauléon Basin, western Pyrenees. *Tectonics*, *36*(6), 1103–1128. https://doi.org/10.1002/2016TC004365
Heddebaut, C. (1973). Etudes géologiques dans les massifs paléozoïques basques.
Iriarte, E., 2004. La Depresión Intermedia entre Leiza y Elizondo (Pirineo Occidental): estratigrafía y relaciones tectónica-sedimentación durante el Cretácico (Doctoral Thesis), Univ. País Vasco, 310 p.
Iriarte, E., & García-Mondéjar, J. (2001). Flysch siliciclástico y flysch carbonatado en el relleno del graben cretácico de Latsaga ("Depresión Intermedia", Navarra). *Geogaceta*, *30*, 207–210.
Jammes, S., Huismans, R. S., & Munoz, J. A. (2014). Lateral variation in structural style of mountain building: controls of rheological and rift inheritance. *Terra Nova*, *26*(3), 201–207. https://doi.org/10.1111/ter.12087
Jammes, S., Manatschal, G., & Lavier, L. (2010). Interaction between prerift salt and detachment faulting in hyperextended rift systems: The example of the Parentis and Mauléon basins (Bay of Biscay and western Pyrenees). *AAPG Bulletin*, *94*(7), 957–975. https://doi.org/10.1306/12090909116
Jammes, S., Manatschal, G., Lavier, L., & Masini, E. (2009). Tectonosedimentary evolution related to extreme crustal thinning ahead of a propagating ocean: Example of the western Pyrenees. *Tectonics*, *28*(4). TC4012. https://doi.org/10.1029/2008TC002406
Jammes, S., Tiberi, C., & Manatschal, G. (2010). 3D architecture of a complex transcurrent rift system: The example of the Bay of Biscay–Western Pyrenees. *Tectonophysics*, *489*(1–4), 210–226. https://doi.org/10.1016/j.tecto.2010.04.023
Johnson, J. A., & Hall, C. A. (1989). The structural and sedimentary evolution of the Cretaceous North Pyrenean Basin, southern France. *The Geological Society of America Bulletin*, *101*(2), 231–247.
Juch, D., Krausse, H. F., Müller, D., Requadt, H., Schafer, D., Solé, J., & Villalobos, L. (1972). Mapa geológico de España E. 1:50.000, Serie MAGNA(Hoja de Maya de Baztán, 66).
Knausse, H. F., Müller, D., Requadt, H., Campos, J., García-Dueñas, V., Garrote, A., et al. (1972). Mapa geológico de España E. 1:50.000, Serie MAGNA(Hoja de Vera de Bidasoa, 65).
Labaume, P., & Teixell, A. (2020). Evolution of salt structures of the Pyrenean rift (Chaînons Béarnais, France): From hyper-extension to tectonic inversion. *Tectonophysics*, *785*. 228451. https://doi.org/10.1016/j.tecto.2020.228451
Lagabrielle, Y., Labaume, P., & de Saint Blanquat, M. (2010). Mantle exhumation, crustal denudation, and gravity tectonics during Cretaceous rifting in the Pyrenean realm (SW Europe): Insights from the geological setting of the lherzolite bodies. *Tectonics*, *29*(4).TC4012. https://doi.org/10.1029/2009TC002588
Lago, M., Arranz, E., Pocoví, A., Galé, C., & Gil-Imaz, A. (2004). Permian magmatism and basin dynamics in the southern Pyrenees: a record of the transition from late Variscan transtension to early Alpine extension. *Geological Society, London, Special Publications*, *223*(1), 439–464. https://doi.org/10.1144/GSL.SP.2004.223.01.19
Lamare, P. (1936). *Recherches géologiques dans les Pyrénées basques d'Espagne* (Thèse) (pp. 1896–1968). Faculté des sciences, Université de Paris, France.
Larrasoaña, J. C., Parés, J. M., del Valle, J., & Millán, H. (2003). Triassic paleomagnetism from the Western Pyrenees revisited: Implications for the Iberian–Eurasian Mesozoic plate boundary. *Paleomagnetism Applied to Tectonics. A Tribute to Rob Van Der Voo*, *362*(1), 161–182. https://doi.org/10.1016/S0040-1951(02)00636-4
Larrasoaña, J. C., Parés, J. M., Millán, H., del Valle, J., & Pueyo, E. L. (2003). Paleomagnetic, structural, and stratigraphic constraints on transverse fault kinematics during basin inversion: The Pamplona Fault (Pyrenees, north Spain). *Tectonics*, *22*(6). https://doi.org/10.1029/2002TC001446
Le Pochat, G. (1982). Reconnaissance des écailles de cristallin et de Paléozoïque dans les massifs paléozoïques basques. *Progr. Géol. Prof. Fr., Bur. Rech. Géol. Min.*, *7*, 285–287.
Lenoble, J. L. (1992). Les plates-formes carbonatées ouest-pyrénéennes du dogger à l'Albien, stratigraphie séquentielle et évolution géodynamique (Doctoral dissertation).
Lescoutre, R., & Manatschal, G. (2020). Role of rift-inheritance and segmentation for orogenic evolution: Example from the Pyrenean-Cantabrian system. *Bulletin de la Societe Geologique de France*, *191*. https://doi.org/10.1051/bsgf/2020021
Lescoutre, R., Tugend, J., Brune, S., Masini, E., & Manatschal, G. (2019). Thermal evolution of asymmetric hyperextended magma-poor rift systems: Results from numerical modelling and Pyrenean field observations. *Geochemistry, Geophysics, Geosystems*, *20*(10), 4567–4587. https://doi.org/10.1029/2019GC008600

Liao, J., & Gerya, T. (2015). From continental rifting to seafloor spreading: Insight from 3D thermo-mechanical modeling. *Gondwana Research*, *28*(4), 1329–1343. https://doi.org/10.1016/j.gr.2014.11.004

Llanos, H. (1980). Estudio geologico del borde sur del macizo de Cinco Villas, Transversal Huici-Leiza (Navarra). University of País Vasco, UPV, EHU, 75–116.

López-Gómez, J., Martín-González, F., Heredia, N., la Horra, de, R., Barrenechea, J. F., et al. (2019). New lithostratigraphy for the Cantabrian Mountains: A common tectono-stratigraphic evolution for the onset of the Alpine cycle in the W Pyrenean realm, N Spain. *Earth-Science Reviews*, *188*, 249–271. https://doi.org/10.1016/j.earscirev.2018.11.008

Lucas, C. (1987). Estratigrafia y datos Morfo-estructurales sobre el Permico y Triasico de fosas norte Pirenaicas. *Cuadernos de Geología Ibérica*, *11*, 25–40.

Macchiavelli, C., Vergés, J., Schettino, A., Fernández, M., Turco, E., Casciello, E., et al. (2017). A new southern North Atlantic isochron map: Insights into the drift of the Iberian plate since the Late Cretaceous. *Journal of Geophysical Research: Solid Earth*, *122*(12), 9603–9626. https://doi.org/10.1002/2017JB014769

Manatschal, G., & Müntener, O. (2009). A type sequence across an ancient magma-poor ocean–continent transition: The example of the western Alpine Tethys ophiolites. *Tectonophysics*, *473*(1–2), 4–19. https://doi.org/10.1016/j.tecto.2008.07.021

Martínez Catalán, J., Arenas, R., García, F. D., Cuadra, P. G., Gómez-Barreiro, J., Abati, J., et al. (2007). Space and time in the tectonic evolution of the northwestern Iberian Massif: Implications for the Variscan belt 4-D framework of continental crust (Vol. 200, pp. 403–423). Geological Society of America Memoir Boulder.

Martínez-Torres, L. (1992). El Manto de los Mármoles (Pirineo Occidental): Geología estructural y evolución geodinámica. Servicio Editorial de la Universidad del País Vasco= Argitarapen Zerbitzua. Euskal Herriko Unibertsitatea.

Martínez-Torres, L. M. (1993). Corte balanceado de la Sierra Cantabria (cabalgamiento de la Cuenca Vasco-Cantábrica sobre la Cuenca del Ebro). *Geogaceta*, *14*, 113–115.

Masini, E., Manatschal, G., Tugend, J., Mohn, G., & Flament, J.-M. (2014). The tectono-sedimentary evolution of a hyper-extended rift basin: The example of the Arzacq–Mauléon rift system (Western Pyrenees, SW France). *International Journal of Earth Sciences*, *103*(6), 1569–1596. https://doi.org/10.1007/s00531-014-1023-8

Mathey, B. (1986). Les flyschs crétacé supérieur des Pyrénées basques : âge, anatomie, origine du matériel, milieu de dépôt et relations avec l'ouverture du Golfe de Gascogne.

Mathey, B., Floquet, M., & Miguel Martînez-Torres, L. (1999). The Leiza palaeo-fault: Role and importance in the Upper Cretaceous sedimentation and paleogeography of the Basque Pyrenees (Spain). *Comptes Rendus de l'Academie des Sciences - Series IIA: Earth and Planetary Science*, *328*(6), 393–399. https://doi.org/10.1016/S1251-8050(99)80105-0

Mattauer, M. (1968). Les traits structuraux essentiels de la chaîne pyrénéenne. *Revue de Geologie Dynamique et de Geographie Physique*, *10*(1), 3–11.

Mattauer, M., & Séguret, M. (1971). Les relations entre la chaîne des Pyrénées et le golfe de Gascogne. *J. Debyser, X. Le Pichon, and L. Montadert. Technip, Paris*, 1–24.

Matte, P. (2002). Les plis hercyniens kilométriques couchés vers l'ouest-sud-ouest dans la région du pic du Midi d'Ossau–col du Somport (zone axiale des Pyrénées occidentales). *Comptes Rendus Geoscience*, *334*(10), 773–779.

McClay, K., Muñoz, J. A., & García-Senz, J. (2004). Extensional salt tectonics in a contractional orogen: A newly identified tectonic event in the Spanish Pyrenees. *Geology*, *32*(9), 737. https://doi.org/10.1130/G20565.1

Mendia, M. S., & Ibarguchi, J. I. G. (1991). High-grade metamorphic rocks and peridotites along the Leiza Fault (Western Pyrenees, Spain). *Geologische Rundschau*, *80*(1), 93–107. https://doi.org/10.1007/BF01828769

Merino, R. J. J., Olivé Davo, A., Carballo Olivares, A., Villalobos Vilches, L., & León González, L. (1984). Mapa geológico de España E. 1:50.000, Serie MAGNA (Hoja de Estella, 140).

Mohr, K., & Pilger, A. (1965). Das Nord-Süd-streichende Lineament von Elizondo in den westlichen Pyrenäen. *Geologische Rundschau*, *54*(2), 1044–1060. https://doi.org/10.1007/BF01820771

Montigny, R., Azambre, B., Rossy, M., & Thuizat, R. (1986). K-Ar Study of cretaceous magmatism and metamorphism in the pyrenees: Age and length of rotation of the Iiberian Peninsula. *The Geological Evolution of the Pyrenees*, *129*(1), 257–273. https://doi.org/10.1016/0040-1951(86)90255-6

Mouthereau, F., Filleaudeau, P.-Y., Vacherat, A., Pik, R., Lacombe, O., Fellin, M. G., et al. (2014). Placing limits to shortening evolution in the Pyrenees: Role of margin architecture and implications for the Iberia/Europe convergence. *Tectonics*, *33*(12). 2014TC003663. https://doi.org/10.1002/2014TC003663

Muller, J., & Roger, P. (1977). L'Evolution structurale des Pyrénées (Domaine central et occidental) Le segment hercynien, la chaîne de fond alpine. *Geologie Alpine*, *53*(2), 149–191.

Muñoz, J. A. (1992). Evolution of a continental collision belt: ECORS-Pyrenees crustal balanced cross-section. *Thrust Tectonics*, 235–246.

Muñoz, J. A. (2019). Alpine Orogeny: Deformation and structure in the Northern Iberian Margin (Pyrenees s.l.). In C. Quesada, & J. Oliveira (Eds.), *The geology of Iberia: A geodynamic approach*. Regional Geology Reviews. Springer. https://doi.org/10.1007/978-3-030-11295-0_9

Muñoz, J. A., Beamud, E., Fernández, O., Arbués, P., Dinarès-Turell, J., & Poblet, J. (2013). The Ainsa fold and thrust oblique zone of the central Pyrenees: Kinematics of a curved contractional system from paleomagnetic and structural data. *Tectonics*, *32*, 1–34. https://doi.org/10.1002/tect.20070

Nirrengarten, M., Manatschal, G., Tugend, J., Kusznir, N., & Sauter, D. (2018). Kinematic evolution of the southern North Atlantic: Implications for the formation of hyperextended rift systems: Kinematic of hyperextended rift systems. *Tectonics*, *37*(1), 89–118. https://doi.org/10.1002/2017TC004495

Odlum, M. L., & Stockli, D. F. (2019). Thermotectonic evolution of the North Pyrenean Agly Massif during early Cretaceous hyperextension using multi-mineral U-Pb thermochronometry. *Tectonics*. *38*(5), 1509–1531. https://doi.org/10.1029/2018TC005298

Oliva-Urcia, B., Pueyo, E. L., Larrasoaña, J. C., Casas, A. M., Román-Berdiel, T., Van der Voo, R., & Scholger, R. (2012). New and revisited paleomagnetic data from Permian–Triassic red beds: Two kinematic domains in the west-central Pyrenees. *Tectonophysics*, *522*, 158–175.

Oliva-Urcia, B., Román-Berdiel, T., Casas, A. M., Pueyo, E. L., & Osácar, C. (2010). Tertiary compressional overprint on Aptian–Albian extensional magnetic fabrics, North-Pyrenean Zone. *Journal of Structural Geology*, *32*(3), 362–376. https://doi.org/10.1016/j.jsg.2010.01.009

Olivet, J. (1996). Kinematics of the Iberian plate. *Bulletin des Centres de Recherches Exploration-Production Elf-Aquitaine*, *20*(1), 131–195.

Pedreira, D., Pulgar, J. A., Gallart, J., & Díaz, J. (2003). Seismic evidence of Alpine crustal thickening and wedging from the western Pyrenees to the Cantabrian Mountains (north Iberia). *Journal of Geophysical Research: Solid Earth*, *108*(B4), 2204. https://doi.org/10.1029/2001JB001667

Péron-Pinvidic, G., Manatschal, G., Masini, E., Sutra, E., Flament, J. M., Haupert, I., & Unternehr, P. (2017). Unravelling the along-strike variability of the Angola–Gabon rifted margin: a mapping approach. *Geological Society, London, Special Publications*, *438*(1), 49–76.

Peybernes, B. (1978). Dans les Pyrenees la paleogeographie antecenomanienne infirme la theorie d'un coulissement senestre de plusieurs centaines de kilometres le long de la "faille nord-pyreneenne" des auteurs. *Bulletin de La Société Géologique de France*, *S7-XX*(5), 701–709. https://doi.org/10.2113/gssgfbull.S7-XX.5.701

Peybernès, B. (1982). Création puis évolution de la marge nord-ibérique des Pyrénées au Crétacé inférieur. *Cuadernos de Geología Ibérica, Madrid*, *8*, 983–1000.

Peybernès, B., & Souquet, P. (1984). Basement blocks and tecto-sedimentary evolution in the Pyrenees during Mesozoic times. *Geological Magazine*, *121*(05), 397. https://doi.org/10.1017/S0016756800029927

Pflug, R., & Schöll, W. (1976). Un bloque de material jurásico metamorfizado en el Keuper del Diapiro de Estella (Navarra). *Munibe*, *4*, 349–353.

Prave, A. R. (1986). *An interpretation of late Cretaceous sedimentation and tectonics and the nature of pyrenean deformation in the Northwestern Basque Pyrenees: A thesis in geology*. Pennsylvania State University.

Pueyo-Anchuela, Ó., Garrido, H. M., Juan, A. P., & Gil-Imaz, A. (2007). Zona de transferencia en el sector occidental del Pirineo Central, ejemplo de la falla de Oroz-Betelu-Unzué. Zona surpirenaica. *Navarra Geogaceta*, *42*, 19–22.

Puigdefábregas, C., Rojas Tapia, B., Sánchez Carpintero, I., & del Valle, J. (1976). Mapa geológico de España E. 1:50.000, Serie MAGNA(Hoja de Aoiz, 142).

Puigdefàbregas, C., & Souquet, P. (1986). Tecto-sedimentary cycles and depositional sequences of the Mesozoic and Tertiary from the Pyrenees. *The Geological Evolution of the Pyrenees*, *129*(1), 173–203. https://doi.org/10.1016/0040-1951(86)90251-9

Pujalte, V. (1977). El complejo Purbeck-Weald de Santander: estratigrafía y sedimentación (Unpublished Ph. D. Thesis). Univ. de Bilbao, 202.

Quintana, L., Pulgar, J. A., & Alonso, J. L. (2015). Displacement transfer from borders to interior of a plate: A crustal transect of Iberia. *Tectonophysics*, *663*, 378–398. https://doi.org/10.1016/j.tecto.2015.08.046

Ramírez, J. I., Olivé, A., Aguilar, M. J., Ramírez, J., Meléndez, A., Pujalte, V., et al. (1986). Mapa geológico de España E. 1:50.000, Serie MAGNA(Hoja de Tolosa, 89).

Rat, P. (1959). Les Pays Crétacés: Basco-Cantabriques (Espagne) (Vol. 18)). Presses Universitaires de France.

Rat, P. (1988). The Basque-Cantabrian basin between the Iberian and European plates: Some facts but still many problems. *Revista de La Sociedad Geológica de España*, *1*(3–4), 327–348.

Razin, P. (1989). Evolution tecto-sédimentaire alpine des Pyrénées Basques à l'Ouest de la transformante de Pamplona (province du Labourd).

Riba Arderiu, O. (1992). Las secuencias oblicuas en el borde Norte de la Depresión del Ebro en Navarra y la Discordancia de Barbarín. *Acta Geológica Hispánica*, *27*(1–2), 55–68.

Ribeiro, M. L., Reche, J., López-Carmona, A., Aguilar, C., Bento dos Santos, T., Chichorro, M., et al. (2019). Variscan metamorphism The geology of Iberia: A geodynamic approach (Vol. 39, pp. 431–495). Springer International Publishing. https://doi.org/10.1007/978-3-030-10519-8_12

Richard, P. (1986). Structure et évolution alpine des massifs paléozoïques du Labourd (Pays Basque francais). Éditions du Bureau de recherches géologiques et minières.

Roca, E., Muñoz, J. A., Ferrer, O., & Ellouz, N. (2011). The role of the Bay of Biscay Mesozoic extensional structure in the configuration of the Pyrenean orogen: Constraints from the MARCONI deep seismic reflection survey. *Tectonics*, *30*(2). https://doi.org/10.1029/2010TC002735

Roma, M., Vidal-Royo, O., McClay, K., Ferrer, O., & Muñoz, J. A. (2018). Tectonic inversion of salt-detached ramp-syncline basins as illustrated by analog modeling and kinematic restoration. *Interpretation*, *6*(1), T127–T144. https://doi.org/10.1190/INT-2017-0073.1

Roure, F., Choukroune, P., Berastegui, X., Munoz, J. A., Villien, A., Matheron, P., et al. (1989). Ecors deep seismic data and balanced cross sections: Geometric constraints on the evolution of the Pyrenees. *Tectonics*, *8*(1), 41–50. https://doi.org/10.1029/TC008i001p00041

Ruiz, M., Díaz, J., Gallart, J., Pulgar, J. A., González-Cortina, J. M., & López, C. (2006). Seismotectonic constraints at the western edge of the Pyrenees: Aftershock series monitoring of the 2002 February 21, 4.1 Lg earthquake. *Geophysical Journal International*, *166*(1), 238–252.

Ruiz, M., Gallart, J., Díaz, J., Olivera, C., Pedreira, D., López, C., et al. (2006). Seismic activity at the western Pyrenean edge. *Tectonophysics*, *412*(3–4), 217–235. https://doi.org/10.1016/j.tecto.2005.10.034

Salomon, J.-N., Rat, P., Ros, A. P., Amiot, M., Floquet, M., & Mathey, B. (1982). Évolution de la marge cantabrique et de son arrière-pays ibérique au Crétacé. *Cuadernos de Geología Ibérica= Journal of Iberian Geology: An International Publication of Earth Sciences*, *8*, 37–64.

Saspiturry, N., Cochelin, B., Razin, P., Leleu, S., Lemirre, B., Bouscary, C., et al. (2019). Tectono-sedimentary evolution of a rift system controlled by Permian post-orogenic extension and metamorphic core complex formation (Bidarray Basin and Ursuya dome, Western Pyrenees). *Tectonophysics*, *768*. https://doi.org/10.1016/j.tecto.2019.228180

Saspiturry, N., Razin, P., Baudin, T., Serrano, O., Issautier, B., Lasseur, E., et al. (2019). Symmetry vs. asymmetry of a hyper-thinned rift: Example of the Mauléon Basin (Western Pyrenees, France). *Marine and Petroleum Geology*. *104*, 86–105. https://doi.org/10.1016/j.marpetgeo.2019.03.031

Schoeffler, J. (1982). Les transversales basco-landaises. *Bulletin Des Centre de Recherches ELF-Aquitaine*, *6*, 257–263.

Schott, J. J., & Peres, A. (1988). Paleomagnetism of Permo-Triassic red beds in the western Pyrenees: Evidence for strong clockwise rotations of the Paleozoic units. *Tectonophysics*, *156*(1–2), 75–88. https://doi.org/10.1016/0040-1951(88)90284-3

Scotese, C. R., & Schettino, A. (2017). Late Permian-Early Jurassic paleogeography of western Tethys and the world. In *Permo-triassic salt provinces of Europe, North Africa and the Atlantic margins* (pp. 57–95). Elsevier. https://doi.org/10.1016/B978-0-12-809417-4.00004-5

Seguret, M. (1972). Étude tectonique des nappes et séries décollées de la partie centrale du versant sud des Pyrénées. *Pub. Estela, Ser Geol. Struct.*, *2*, 1–155.

Serrano, O., Delmas, J., Hanot, F., Vially, R., Herbin, J. P., Houel, P., & Tourlière, B. (2006). Le Bassin d'Aquitaine: Valorisation des données sismiques, cartographie structurale et potentiel pétrolier. *BRGM*. https://doi.org/10.13140/2.1.1304.2241

Soler, R. (1971). El Jurásico Marino de la Sierra de Aralar (Cuenca Cantábrica occidental): los problemas poskinméricos. *Cuadernos de Geología Ibérica= Journal of Iberian Geology: An International Publication of Earth Sciences*(2), 509–532.

Soto, J. I., Flinch, J. F., & Tari, G. (2017). Permo-Triassic basins and tectonics in Europe, North Africa and the Atlantic Margins: A synthesis. In J. I. Soto, J. F. Flinch, & G. Tari (Eds.), *Permo-triassic salt provinces of Europe, North Africa and the Atlantic margins tectonics and hydrocarbon potential* (p. 604). Elsevier. https://doi.org/10.1016/B978-0-12-809417-4.00038-0

Soula, J.-C., Lucas, C., & Bessiere, G. (1979). Genesis and evolution of Permian and Triassic basins in the Pyrenees by regional simple shear acting on older Variscan structures: Field evidence and experimental models. *Tectonophysics*, *58*(3–4), T1–T9. https://doi.org/10.1016/0040-1951(79)90307-X

Souquet, P., Debroas, E.-J., Boirie, J.-M., Pons, P., Fixari, G., Roux, J.-C., et al. (1985). Le groupe du Flysch noir (albo-cénomanien) dans les Pyrénées. *Bull Cent. Rech Exlpo-Prod Elf-Aquitaine Pau*, *9*, 183–252.

Souquet, P., Peybernes, B., Bilotte, M., & Debroas, E.-J. (1977). La chaine alpine des Pyrenees. *Geol. alp. (Grenoble)*, *53*(2), 193–216.

Stampfli, G. M., & Borel, G. D. (2002). A plate tectonic model for the Paleozoic and Mesozoic constrained by dynamic plate boundaries and restored synthetic oceanic isochrons. *Earth and Planetary Science Letters*, *196*(1), 17–33. https://doi.org/10.1016/S0012-821X(01)00588-X

Stevaux, J., & Winnock, E. (1974). Les bassins du Trias et du Lias inferieur d'Aquitaine et leurs episodes evaporitiques. *Bulletin de la Societe Geologique de France*, *S7-XVI*(6), 679–695. https://doi.org/10.2113/gssgfbull.S7-XVI.6.679

Sussman, A. J., Butler, R. F., Dinarès-Turell, J., & Vergés, J. (2004). Vertical-axis rotation of a foreland fold and implications for orogenic curvature: An example from the Southern Pyrenees, Spain. *Earth and Planetary Science Letters*, *218*(3–4), 435–449. https://doi.org/10.1016/S0012-821X(03)00644-7

Tavani, S., Bertok, C., Granado, P., Piana, F., Salas, R., Vigna, B., & Muñoz, J. A. (2018). The Iberia-Eurasia plate boundary east of the Pyrenees. *Earth-Science Reviews*, *187*, 314–337. https://doi.org/10.1016/j.earscirev.2018.10.008

Tavani, S., Carola, E., Granado, P., Quintà, A., & Muñoz, J. A. (2013). Transpressive inversion of a Mesozoic extensional forced fold system with an intermediate décollement level in the Basque-Cantabrian Basin (Spain): Inversion of extensional forced folds. *Tectonics*, *32*(2), 146–158. https://doi.org/10.1002/tect.20019

Tavani, S., & Muñoz, J. A. (2012). Mesozoic rifting in the Basque-Cantabrian Basin (Spain): Inherited faults, transversal structures and stress perturbation: Mesozoic rifting in the Basque-Cantabrian Basin. *Terra Nova*, *24*(1), 70–76. https://doi.org/10.1111/j.1365-3121.2011.01040.x

Teixell, A. (1990). Alpine thrusts at the western termination of the Pyrenean axial zone. *Bulletin de la Societe Geologique de France*, *VI*(2), 241. https://doi.org/10.2113/gssgfbull.VI.2.241

Teixell, A. (1993). Coupe géologique du massif d'Igountze: implications sur l'évolution structurale de la bordure sud de la zone nord-pyrénéenne occidentale. *Comptes Rendus de l'Académie Des Sciences. Série 2, Mécanique, Physique, Chimie, Sciences de l'univers, Sciences de La Terre*, *316*(12), 1789–1796.

Teixell, A. (1998). Crustal structure and orogenic material budget in the west central Pyrenees. *Tectonics*, *17*(3), 395–406. https://doi.org/10.1029/98TC00561

Teixell, A., Labaume, P., Ayarza, P., Espurt, N., de Saint Blanquat, M., & Lagabrielle, Y. (2018). Crustal structure and evolution of the Pyrenean-Cantabrian belt: A review and new interpretations from recent concepts and data. *Tectonophysics*, *724–725*, 146–170. https://doi.org/10.1016/j.tecto.2018.01.009

Teixell, A., Labaume, P., & Lagabrielle, Y. (2016). The crustal evolution of the west-central Pyrenees revisited: Inferences from a new kinematic scenario. *Comptes Rendus Geoscience*, *348*(3–4), 257–267. https://doi.org/10.1016/j.crte.2015.10.010

Tentler, T., & Acocella, V. (2010). How does the initial configuration of oceanic ridge segments affect their interaction? Insights from analogue models. *Journal of Geophysical Research: Solid Earth*, *115*(B1). https://doi.org/10.1029/2008JB006269

Ternet, Y., Barrère, P., & Canérot, J. (2004). Geological Map of Laruns-somport (1/50 000). BRGM, Orléans, France.

Teyssonnières, M. (1983). Approche analytique du Flysch crétacé supérieur des Pyrénées-Atlantiques, 222.

Thinon, I., Fidalgo-González, L., Réhault, J.-P., & Olivet, J.-L. (2001). Déformations pyrénéennes dans le golfe de Gascogne. *Comptes Rendus de l'Academie des Sciences - Series IIA: Earth and Planetary Science*, *332*(9), 561–568. https://doi.org/10.1016/S1251-8050(01)01576-2

Tugend, J., Manatschal, G., & Kusznir, N. J. (2015). Spatial and temporal evolution of hyperextended rift systems: Implication for the nature, kinematics, and timing of the Iberian-European plate boundary. *Geology*, *43*(1), 15–18. https://doi.org/10.1130/G36072.1

Tugend, J., Manatschal, G., Kusznir, N. J., Masini, E., Mohn, G., & Thinon, I. (2014). Formation and deformation of hyperextended rift systems: Insights from rift domain mapping in the Bay of Biscay-Pyrenees. *Tectonics*, *33*(7). 2014TC003529. https://doi.org/10.1002/2014TC003529

Turner, J. P. (1996). Switches in subduction direction and the lateral termination of mountain belts: Pyrenees-Cantabrian transition, Spain. *Journal of the Geological Society*, *153*(4), 563–571. https://doi.org/10.1144/gsjgs.153.4.0563

Vacherat, A., Mouthereau, F., Pik, R., Huyghe, D., Paquette, J.-L., Christophoul, F., et al. (2017). Rift-to-collision sediment routing in the Pyrenees: A synthesis from sedimentological, geochronological and kinematic constraints. *Earth-Science Reviews*, *172*, 43–74. https://doi.org/10.1016/j.earscirev.2017.07.004

Vargas, H., Gaspar-Escribano, J. M., López-Gómez, J., Van Wees, J.-D., Cloetingh, S., de La Horra, R., & Arche, A. (2009). A comparison of the Iberian and Ebro Basins during the Permian and Triassic, eastern Spain: A quantitative subsidence modelling approach. *Tectonophysics*, *474*(1–2), 160–183. https://doi.org/10.1016/j.tecto.2008.06.005

Vergés, J. (2003). Evolución de los sistemas de rampas oblicuas de los Pirineos meridionales: fallas del Segre y Pamplona. *Boletin Geologico y Minero*, *114*(1), 87–101.

Vielzeuf, D. (1984). *Relations de phases dans le faciès granulite et implications géodynamiques: l'exemple des granulites des Pyrénées* (PhD thesis). University of Clermont-Ferrand II.

Vissers, R. L. M. (1992). Variscan extension in the Pyrenees. *Tectonics*, *11*(6), 1369–1384. https://doi.org/10.1029/92TC00823

Voort, H. B. (1964). Zum Flyschproblem in den Westpyrenäen. *Geologische Rundschau*, *53*(1), 220–233. https://doi.org/10.1007/BF02040748

Wang, Y., Chevrot, S., Monteiller, V., Komatitsch, D., Mouthereau, F., Manatschal, G., et al. (2016). The deep roots of the western Pyrenees revealed by full waveform inversion of teleseismic P waves. *Geology*, *44*(6), 475–478. https://doi.org/10.1130/G37812.1

Willett, S., Beaumont, C., & Fullsack, P. (1993). Mechanical model for the tectonics of doubly vergent compressional orogens. *Geology*, *21*(4), 371. https://doi.org/10.1130/0091-7613(1993)021<0371:MMFTTO>2.3.CO;2

Zolnaï, G. (1971). Le front nord des Pyrénées occidentales. Histoire Structural Du Golfe de Gascogne. *Technip*, 1–10.

Zwaan, F., & Schreurs, G. (2017). How oblique extension and structural inheritance influence rift segment interaction: Insights from 4D analog models. *Interpretation*, *5*(1), SD119–SD138. https://doi.org/10.1190/INT-2016-0063.1

Zwaan, F., Schreurs, G., Naliboff, J., & Buiter, S. J. H. (2016). Insights into the effects of oblique extension on continental rift interaction from 3D analogue and numerical models. *Tectonophysics*, *693*, 239–260. https://doi.org/10.1016/j.tecto.2016.02.036